Design and Implementation of Oversampled Modulated Filter Banks

by

Bradley Douglas Riel
B.A.Sc. University of Regina. 2001
Certificate Software Systems Engineering University of Regina. 2001

A Thesis Submitted in Partial Fulfillment of the Requirements
for the Degree of

MASTER OF APPLIED SCIENCE

in the Department of Electrical and Computer Engineering

We accept this thesis as conforming
to the required standard

University of Victoria

Supervisors: Dr. Andreas Antoniou, Dr. Dale Shpak

ABSTRACT

A method for the design and implementation of practical and efficient oversampled filter banks (OFB) is proposed. Specifically, a technique for designing perfect reconstruction (PR) oversampled cosine modulated (CM) and discrete Fourier transform modulated (DFT-M) filter banks (FB) of either odd- or even-stacking type that can be implemented using lifting-based structures is proposed.

A generalized, efficient factorization of the polyphase transfer matrices for oversampled modulated filter banks (O-MFB) is proposed that can be applied to the factorization of transfer matrices resulting from discrete Fourier transform (DFT) or cosine modulation, of either odd- or even-stacking type. This factorization is derived by directly associating the prototype filter coefficients with the modulation matrix coefficients and exploiting redundancies in the modulation transform. By applying the well-known DFT and cosine modulation matrices to this factorization, the general conditions imposed on the resulting factorization matrices are derived for both DFT and cosine modulated filter banks (CMFB) with either odd- or even-stacking type. By exploiting the paraunitary (PU) property of zero-padded square PU matrices, rectangular PU matrices are generated and shown to correspond to PU OFBs. A PU factorization of square matrices is then applied in order to derive a PU factorization of the transfer matrices generated from O-MFBs.

Next, a lifting-based factorization of the rectangular transfer matrices is proposed. This lifting-based factorization extends a lifting-based factorization for square transfer matrices to the case of rectangular transfer matrices. A specific PU lifting-based factorization of square matrices is then applied to the zero-padded square PU matrices related to the rectangular PU transfer matrices corresponding to O-MFBs. This results in a generalized lifting-based structure for the implementation of PR O-MFBs. By applying the DFT and cosine modulation matrices, the specific conditions on the lifting-based factorization matrices are derived. These conditions are associated with the design limitations of the FB, such as the length and phase of the analysis and synthesis prototype filters and the relationship between the number of channels M and the subsampling factor N, for each type of modulated filter bank (MFB).

Finally, a design method is proposed for the design of O-MFBs implemented using a lifting-based structure. It is shown that this method provides optimal solutions and results in subband filters having acceptable stopband attenuation. Furthermore, it is shown that FBs with linear phase subband filters can be designed.

Examiners:

Table of Contents

Abstract ii

Table of Contents iv

List of Tables and Figures vi

List of Abbreviations viii

Acknowledgements ix

1 Introduction 1

1.1 Background 1

1.2 Contributions and Outline of Thesis 5

2 Multirate Filter Banks – Fundamental Building Blocks 9

2.1 Upsampler 10

2.2 Downsampler 12

2.3 Upsampler–Downsampler Cascade 14

2.4 Downsampler–Upsampler Cascade 14

2.5 Upsampler–Filter Cascade 16

2.6 Filter–Downsampler Cascade 17

2.7 Noble Identities 17

2.8 Polyphase Representation 18

2.9 Summary and Conclusions 20

3 Oversampled Filter Banks 21

3.1 Representation in the Frequency Domain 22

3.2 Representation in the Polyphase Domain 25

3.3 FIR Factorization 27

3.4 Perfect Reconstruction 30

3.5 Biorthogonality, Paraunitariness, and Overcomplete Expansions 33

3.6 Summary and Conclusions 36

4 Oversampled Modulated Filter Banks **38**
4.1 Generalized Factorization 39
4.2 DFT Modulation 47
4.3 Cosine Modulation 50
4.4 Summary and Conclusions 54

5 Lifting-Based Implementation **55**
5.1 Fundamental Structure 56
5.2 Factorization of Modulated Filter Bank Transfer Matrices 64
5.3 Summary and Conclusions 69

6 Filter Bank Design **70**
6.1 Lifting-Based Design Method 72
6.2 Lifting-Based Design Examples 73
6.3 Summary and Conclusions 76

7 Conclusions and Future Research **77**
7.1 Lifting-Based Factorization 77
7.2 Design Method 78
7.3 Future Research 79

Bibliography **81**

Appendix A Proofs **87**
A.1 General Conditions for PR 87
A.2 PR Conditions for Oversampled Even-Stacked Cosine-Modulated Filter Banks 89

List of Tables and Figures

Table 1. Lifting-based factorization parameters for oversampled DFT-modulated filter banks 65

Table 2. Lifting-based factorization parameters for oversampled cosine-modulated filter banks 66

Figure 1. N-fold upsampler. 10

Figure 2. Time-domain effect of an upsampling operation with an upsampling factor of $N = 2$. (a) Input sequence. (b) Output sequence. 11

Figure 3. Frequency-domain effect of an upsampling operation with an upsampling factor of $N = 2$. (a) Input spectrum. (b) Output spectrum 11

Figure 4. N-fold downsampler. 12

Figure 5. Time-domain effect of a downsampling operation with a downsampling factor of $N = 2$. (a) Input sequence. (b) Output sequence. 13

Figure 6. Frequency-domain effect of a downsampling operation with a downsampling factor of $N = 2$. (a) Input spectrum. (b) Output spectrum 13

Figure 7. N-fold upsampler followed by an N-fold downsampler 14

Figure 8. N-fold downsampler followed by an N-fold upsampler 14

Figure 9. Time-domain effect of a downsampling operation followed by an upsampling operation with subsampling factors of $N = 2$. (a) Input sequence. (b) Output sequence. 15

Figure 10. Frequency-domain effect of a downsampling operation followed by an upsampling operation with subsampling factors of $N = 2$. (a) Input spectrum. (b) Output spectrum. 16

Figure 11. N-fold upsampler followed by an anti-imaging filter with impulse response $f[n]$. 16

Figure 12. N-fold downsampler preceded by an anti-aliasing filter with impulse response $h[n]$ 17

Figure 13. Noble Identity #1. 18

Figure 14. Noble Identity #2. 18

Figure 15. Frequency-domain representation of an M-channel filter bank with subsampling factor N. 23

Figure 16. Polyphase-domain representation of an M-channel filter bank with subsampling factor N. 26

Figure 17. Polyphase-domain representation of an M-channel modulated filter bank with subsampling factor N. 39

Figure 18. Amplitude response of the subband filters in an M-channel DFT-modulated filter bank. (a) Odd-stacked case. (b) Even-stacked case. 48

Figure 19. Amplitude response of the subband filters in an M-channel odd-stacked cosine-modulated filter bank. 50

Figure 20. Amplitude response of the two banks of subband filters in a $2M$-channel even-stacked cosine-modulated filter bank. 52

Figure 21. Lifting-based implementation applying filtering operations between channels i and j. (a) Analysis bank. (b) Synthesis bank. 63

Figure 22. Association of $\mathbf{E}_i(z)$ to $p[n]$ for a $2M$-spaced polyphase decomposition of $p[n]$ with $L_p = 24$ and $M = 6$ 67

Figure 23. Effect of multiplying $\mathbf{E}_8(z)$ and $\mathbf{E}_9(z)$ by z^{-1}. 68

Figure 24. Association of $\mathbf{E}_i(z)$ with $p[n]$ following multiplication of $\mathbf{E}_8(z)$ and $\mathbf{E}_9(z)$ by z^{-1}. 68

Figure 25. Amplitude response of the subband filters in an odd-stacked oversampled DFT-modulated filter bank with $M = 6$, $N = 4$, and $L_p = 28$. 74

Figure 26. Amplitude response of the subband filters in an even-stacked oversampled cosine-modulated filter bank with $2M = 12$, $2N = 4$, and $L_p = 24$. (a) First bank. (b) Second bank. 76

List of Abbreviations

CM	Cosine modulated
CMFB	Cosine modulated filter bank
DCT	Discrete cosine transform
DFT	Discrete Fourier transform
DFT-M	Discrete Fourier transform modulated
DST	Discrete sine transform
FB	Filter bank
FFT	Fast Fourier transform
FIR	Finite-duration impulse response
IIR	Infinite-duration impulse response
IDFT	Inverse discrete Fourier transform
LP	Linear phase
MFB	Modulated filter bank
O-CMFB	Oversampled cosine modulated filter bank
O-MFB	Oversampled modulated filter bank
OFB	Oversampled filter bank
PR	Perfect reconstruction
PRFB	Perfect reconstruction filter bank
PU	Paraunitary
PUFB	Paraunitary filter bank
QCLS	Quadratically-constrained least squares
QMFB	Quadrature mirror filter bank

Acknowledgements

I would like to express my sincerest gratitude towards my supervisor Dr. Andreas Antoniou for teaching me the value of independent research, showing me how to express my ideas clearly and concisely, and providing the means for this work to be performed. Thanks also go to my co-supervisor Dr. Dale Shpak for the numerous papers he reviewed, helping me broaden my perspective on graduate school, and providing the means for this work to be performed.

I would also like to thank Dr. Wu-Sheng Lu for the numerous discussions on filter banks that helped expand my scope of thought, and Dr. Dale Olesky for helping to provide reference and direction with respect to the mathematical analysis of filter bank theory.

Finally, I would like to thank the student members of the DSP group for providing an excellent atmosphere for spending most of my time. Special thanks go to a couple of my closest friends, Rajeev Nongpiur and Stuart Bergen, for their numerous discussions on both DSP-related and life-related topics, and for being great role models as dedicated, focused, and responsible students with clear direction and goals.

Dedication

I dedicate this thesis to my parents.

Chapter 1

Introduction

The theory of multirate filter banks (FBs) has experienced aggressive development over the last two decades as the advantages offered by processing digital signals at different sampling rates throughout a system are exploitable in many practical applications. Initial work on multirate FBs included studying the adverse effects of modifying the sampling rate at various points throughout a digital system and developing an understanding of the fundamental relationships necessary to reduce or eliminate these effects. More recently, focus has been directed towards deriving techniques to implement these systems as practical digital systems. In the design of practical systems, we must consider the minimization or elimination of errors in the reconstructed signal due to the quantization of filter coefficients, truncation of intermediate results, and processing of overflows during intermediate operations. Finally, in an effort to develop efficient FB realizations, research has been performed on deriving implementations wherein integer mathematics can be exploited or multiplierless processors can be used.

This thesis deals specifically with the design and efficient implementation of practical oversampled filter banks (OFBs). Chapter 1 begins with a comprehensive background of FB theories published to date, focusing on motivations and advantages of particular research directions. This background concludes with the motivation for performing the research described in this thesis. Subsequent to this, an outline to the remainder of the thesis is presented that identifies the specific contributions made by the author.

1.1 Background

Most of multirate FB research to date has focused on critically-sampled FBs, wherein the subsampling factor in each channel is equal to the total number of channels. Initially, 2-channel FBs were introduced into the literature as quadrature mirror filter banks (QMFBs) in the mid-seventies by Croisier *et al.* [1]. These 2-channel FBs completely eliminated aliasing distortion due to subsampling operations, however,

amplitude and phase distortion from non-ideal subband filtering still remained. Subsequently, these FBs were extended to the M-channel case in [2], [3] and [4]. However, it was not until 1984 that Smith and Barnwell [5] derived what was later to be referred to as the paraunitary (PU) property, resulting in the 2-channel perfect reconstruction (PR) QMFB. 2-channel FBs employing PR were soon extended to the M-channel case by several authors, including Vetterli [6] and Vaidyanathan [7], among others.

In classical FB design, it is necessary to independently design each analysis and synthesis subband filter, which results in optimization problems with a large number of independent variables. Hence, a subclass of FBs referred to as modulated filter banks (MFBs), wherein the subband filter transfer functions are generated by multiplying a prototype filter transfer function with a modulation transform, were subsequently developed. Two of the most common types of MFBs are the discrete Fourier transform modulated (DFT-M) and cosine modulated (CM) FBs. MFB designs are very attractive to the digital filter bank designer since only the prototype filter coefficients need to be optimized and fast transforms, such as the Fast Fourier Transform (FFT) or the discrete cosine transform (DCT), can be applied. MFBs were first derived by Masson [2], Nussbaumer [3], and Rothweiler [4]. These FBs were efficient in the sense of requiring only a prototype filter to be designed; however, they did not result in PR. The first MFBs that did result in PR were developed by Ramstad [8], Koilipillai [9], and Malvar [10]. The drawback with these designs was that they were quite restrictive in the sense that fixed subband filter lengths of $2JM$ and signal reconstruction delays of $2JM - 1$ were imposed, where J is an arbitrary positive integer and M is the number of channels in the FB. In many real-time applications where feedback is involved, it is important to control and minimize the reconstruction delay. This motivated the desire to explore PR biorthogonal FBs [11][12] and PR biorthogonal MFBs [13][14], where the reconstruction delay could be controlled independently of the subband filter length. Although the MFBs derived to this point offered PR, the subband filters lacked one important property for image processing applications: linear phase (LP). Hence, in 1995, Lin and Vaidyanathan [15] derived the $2M$-channel PR cosine modulated filter bank (CMFB) with subband filters having linear phase. Following this, several authors generalized and summarized the various classes of MFBs, notably deriving PR conditions for biorthogonal MFBs, associating the original CM scheme to the DCT IV modulation transform, and associating the $2M$-channel LP CMFBs to the DCT II modulation transform [16][17]. CMFBs incorporating DCT II and DCT IV modulation transforms have since been referred to as odd- and even-stacked CMFBs, respectively, by Gopinath in [17][18].

The PU property that Smith and Barnwell unknowingly explored in [5] was more thoroughly introduced for M-channel FBs in [6], [7] and [19] and M-channel MFBs in [8], [9] and [10]. Paraunitary filter banks (PUFB) are quite desirable since the PU property facilitates simple design of the synthesis bank for a given analysis bank, guaranteed subband filter stability, and optimization formulations that tend to

exhibit fast convergence. Recently, more complete and thorough studies on M-channel FBs have been performed by Vaidyanathan [20], Malvar [21], Vetterli [22], and Strang [23], among others that demonstrate the PU case to simply be a specific case of biorthogonal FBs.

In practical implementations of multirate FBs, it is necessary to quantize the filter coefficients since they are stored in hardware with finite-length registers. FB implementations utilizing direct structures are subjected to non-linear distortion caused by coefficient quantization, the truncation of intermediate results, and the processing of overflows during intermediate operations. In order to maintain PR in practical implementations it is therefore of considerable interest to develop structures wherein PR is inherent in the structure. Hence, subsequent to the development of PUFBs was the development of lattice-structure FB implementations. Lattices provide a structure for implementing PUFBs while inducing many important properties, including that of PR. In [20], Vaidyanathan showed that every PUFB can be represented by a lattice-structure. He first applied this structure to the design of 2-channel PR PU QMFBs in [24], and subsequently extended it to the design of M-channel PR PUFBs in [25]. Lattice structures have since been derived for LP PR PUFBs [26][27] and MFBs [9][18]. In addition to guaranteeing PR over the entire class of PUFBs even when the coefficients are quantized, lattice structures also facilitate FBs to be designed with modular components and the overall system delay to be minimized during implementation.

The drawback with FBs implemented using arbitrary lattice structures is that they are not resilient to the non-linear distortion introduced when intermediate results are quantized or overflows are processed during intermediate operations. In addition to this, lattice structures can only be applied to the design of PUFBs. Hence, a special type of lattice-structure known as the lifting-based (or ladder) structure was developed. Whereas lattice structures are realized using a cascade of low-order PU building blocks, lifting-based structures are realized using a cascade of structures that perform particular elementary matrix operations. Lifting-based structures were first introduced in the FB literature by Breukers in [28] and have subsequently been applied to generate approximations of the DCT [29][30], design biorthogonal wavelets [31][32], biorthogonal FBs [30][33], biorthogonal MFBs [34][35], and LP FBs [36][37].

A natural extension of FBs with structurally-inherent PR, such as those implemented using lattice or ladder-based structures, are integer- or dyadic-coefficient FBs. Since structurally-inherent perfect reconstruction filter banks (PRFB) maintain PR regardless of coefficient quantization, the filter coefficients can be quantized arbitrarily while still retaining the PR property. In integer-coefficient FBs, the filter coefficients are quantized to integer values. In dyadic-coefficient FBs, the filter coefficients are quantized to values of $k/2^m$, where k and m are positive integers. Integer-coefficient FBs offer the advantage that integer mathematics can be computed much faster in hardware, whereas dyadic-coefficient FBs offer the advantage that the filter banks can be implemented using only shift and add operations rather than

computationally complex multipliers. 2-channel integer- and dyadic-coefficient LP biorthogonal and PUFBs were first studied by Antononi [38] and Horng [39], respectively, with M-channel extensions subsequently derived by Karp [40] and Chan [41]. Integer-modulated PRFBs, wherein both the prototype filter coefficients and the modulation transform coefficients are represented by integer approximations, were then studied by Bi [42] and Mertins [43].

OFBs are a generalization of critically-sampled FBs characterized by the subsampling factor in each channel being less than the total number of channels. At the expense of increased computational complexity due to the redundant number of samples in each subband, OFBs offer increased design freedom, reduced reconstruction noise, and higher subband signal redundancy when compared to critically-sampled FBs. In order to reduce the computational complexity inherent in OFBs, oversampled modulated filter banks (O-MFB) such as DFT-MFBs [44][45], odd-stacked CMFBs [46][47], even-stacked CMFBs [48], and generalized CMFBs [49] have been explored. Subsequent to this, a thorough study of OFBs was performed in the context of frame theory [50][51] as links can be established between the subband filters and a frame, where a frame is defined by a family of uniformly shifted filters. Through these relationships, conditions were determined for the analysis and synthesis bank transfer matrices to generate PRFBs for finite-duration impulse response (FIR) subband filters. In addition to this, a parameterization was derived for all possible PR synthesis banks for a given analysis bank employing FIR subband filters.

Further reductions in the computational complexity of OFBs can be obtained by exploiting the structural PR property of lattice and ladder-based structures. In this case, efficient realizations can be derived when the coefficients are quantized to integer or dyadic values, facilitating multiplierless implementations. Lattice structures for OFBs have only recently been considered by Labeau *et al.* who proposed a lattice-structure for oversampled PR-LP-PUFBs in [52]. For O-MFBs, lattice structures for odd- and even-stacked oversampled cosine modulated filter banks (O-CMFB) have been proposed by Bolcskei in [49][50]. Ladder structures for OFBs, on the other hand, have received little attention in the literature. A 'pseudo' ladder structure wherein only a portion of the FB is parameterized using a ladder structure was proposed by Gan in [53]. Further to this, it has been the work of this author to derive ladder structures for OFBs. A fairly restrictive ladder structure was proposed for biorthogonal oversampled odd-stacked CMFBs in [54], and a much less restrictive ladder structure for oversampled PU MFBs (odd- and even-stacked, DFT-M and CMFBs) has been more recently proposed in [55].

Maximally-decimated FBs tend to be very effective in applications where it is desired to minimize the amount of information being processed. This is typical in applications such as the subband coding of speech and image signals [56][57]. In these applications, the subband energy content can be exploited in order to appropriately allocate bits for samples in each subband and hence minimize the number of coded

bits required to represent the original signal. Other typical applications include communication systems (analog voice privacy systems [58] and digital transmultiplexers [59]), antenna systems (beamforming), and radar. OFBs tend to be very effective in applications where storage and processing requirements are not at a premium, and where increased design freedom, reduced reconstruction noise, and redundancy in the subband signals are desirable. This is typical in applications such as subband adaptive filtering [60] (applied to echo cancellation [61], noise reduction [62], beamforming [62], line enhancement [63]), communication systems [64] (enhanced resilience to erasures in lossy channels [65]), and various denoising applications [66]. Relationships between OFBs and multiple description coding [67] and independent component analysis [68] have also been derived.

1.2 Contributions

The contributions of this thesis begin in section 4.1. In this section, a factorization of O-MFB transfer matrices that was originally proposed by Weiss and Stewart in [69] is extended to include a multiplication of the polyphase transfer matrices with a subband filter delay matrix. Whereas the factorization derived in [69] is for O-MFB transfer matrices generated using discrete Fourier transform (DFT) modulation, the factorization derived in section 4.1 generalizes this factorization to include both O-MFB transfer matrices generated using DFT modulation and O-MFB transfer matrices generated using cosine modulation, of either odd- or even-stacking type. The generalized factorization involves multiplying the original factorization of the analysis and synthesis transfer matrices with a subband filter delay matrix. The subband filter delay matrix in the Z-domain comprises elements z^{-k} with appropriate values of k located on the diagonal, wherein the value of k can be associated with the additional amount of delay k in the time domain required for implementation of O-CMFBs realizing PR. The necessity of such a delay matrix is specifically recognized for *even-stacked* O-CMFB transfer matrix factorizations.

In section 4.1, a factorization of the generalized analysis and synthesis polyphase transfer matrices is also presented wherein the analysis and synthesis polyphase transfer matrices are factorized into a product of permutation matrices $\mathbf{P}$ and $\mathbf{Q}$, a plurality of advance and delay matrices $\mathbf{M}_l(z)$ and $\mathbf{N}_l(z)$, and a plurality of rectangular matrices $\mathbf{S}_l(z)$. This factorization is based on the factorization presented by Cvetković in [44]. In [44], a factorization is derived for O-MFB transfer matrices generated using DFT modulation. The factorization derived in section 4.1 shows how a similar factorization can be applied to O-MFB transfer matrices generated using both DFT modulation and cosine modulation.

Section 4.1 concludes with a PU factorization of the generalized analysis and synthesis polyphase transfer matrices. This PU factorization applies the generalized factorization of a degree-C square matrix

into a product of degree-1 PU building blocks and Householder matrices as derived by Vaidyanathan in [20]. It is shown that the plurality of rectangular matrices $\mathbf{S}_i(z)$ can be embedded into zero padded square matrices $\mathbf{G}(z)$. It is then further shown that forcing $\mathbf{G}(z)$ to be PU (i.e. by applying a PU factorization of square matrices such as that presented by Vaidyanathan) the embedded rectangular matrix $\mathbf{S}_i(z)$ will then also be PU. This results in a PU factorization of generalized O-MFBs transfer matrices.

In section 4.2, the generalized factorization of O-DFT-MFB transfer matrices is given. By applying the well-known DFT modulation matrices to the generalized factorization of O-MFB transfer matrices derived in section 4.1, the conditions on the factorization matrices for the specific factorization of O-DFT-MFB transfer matrices are determined. The conditions imposed on the modulation matrix $\mathbf{T}$ and the factorization matrices $\mathbf{L}_2$, $\mathbf{A}_k$, and $\mathbf{E}(z)$ are given for both odd-stacked and even-stacked oversampled DFT-MFBs. In addition to this, the forms that $\mathbf{E}(z)$ must assume and the condition on the length of the prototype filter impulse response, L_p, for each form of $\mathbf{E}(z)$, are also given. Furthermore, the conditions imposed on the analysis and synthesis prototype filter impulse responses in order to generate PU solutions are reviewed for completeness by following the derivation by Eneman in [70].

In section 4.3, the generalized factorization of O-CMFB transfer matrices is given. By applying the well-known CM matrices to the generalized factorization of O-MFB transfer matrices derived in section 4.1, the conditions on the factorization matrices for the specific factorization of O-CMFB transfer matrices are determined. The conditions imposed on the modulation matrix $\mathbf{T}$ and the factorization matrices $\mathbf{L}_2$, $\mathbf{A}_k$, and $\mathbf{E}(z)$ are given for both odd-stacked and even-stacked O-CMFBs, as well as the forms that $\mathbf{E}(z)$ must assume and the condition on the length of the prototype filter impulse response, L_p, for each form of $\mathbf{E}(z)$. Furthermore, the conditions imposed on the analysis and synthesis filter impulse responses in order to generate PU solutions as derived by Kliewer in [47] are related to the forms that $\mathbf{E}(z)$ may assume. This relationship is essential for realizing that Form 1 factorizations of $\mathbf{E}(z)$ are necessary for ensuring that PR Condition #1 is satisfied for O-CMFBs.

In section 5.1, the lifting-based factorization of square matrices derived by Chen and Amaratunga in [30] is applied to generate a lifting-based factorization of rectangular matrices. A lifting-based factorization of square matrices is then applied to the Smith form decomposition of rectangular polynomial matrices, resulting in a generalized lifting-based factorization of rectangular matrices. This factorization is associated with the factorization of rectangular matrices representing OFB transfer matrices. Following this, the lifting-based factorization for a subset of rectangular matrices that satisfy the PU property is presented. This factorization is based on the application of the aforementioned lifting-based factorization to a subset of left-inverse solutions, wherein a PU rectangular matrix is generated by zero-padding a PU

square matrix. Section 5.1 concludes with a filter bank analysis that deals with the association between the channels in a multirate filter bank and the lifting-based factorization of square and rectangular matrices.

In section 5.2, the lifting-based factorization of PU matrices as derived in section 5.1 is applied to the generalized factorization of the PU transfer matrices for oversampled DFT-MFBs and O-CMFBs as derived in section 4.1. This results in a lifting-based factorization for O-MFB transfer matrices with arbitrary modulation and stacking types. For the lifting-based factorization, the parameters for odd-stacked and even-stacked O-MFBs are provided that result in PUFBs and PR. The new parameters derived in section 5.2 include the number, dimensions, and order of factorization matrices $\mathbf{S}_i(z)$, as well as the number of parameters required for optimization, for each form that $\mathbf{E}(z)$ may assume.

In chapter 6, a method for designing PU O-MFBs, as well as both odd- and even-stacked DFT-MFBs and CMFBs that can be realized using a lifting-based structure is presented. This method comprises the steps of selecting the FB properties such as the number of channels and the subsampling factor; deriving the appropriate analysis polyphase transfer matrix for the desired modulation and stacking type; manipulating the transfer matrix into submatrices that are conducive to PU factorization; applying Vaidyanathan's well-known PU factorization to generate rectangular PU transfer matrices; and applying a lifting-based factorization of square PU matrices to generate a lifting-based factorization of rectangular PU transfer matrices.

In Appendix A.1, the general conditions for obtaining PR in OFBs are explicitly derived. While many references such as [18][44][47] and [50] provide the PR conditions for OFBs, the generalized PR conditions on the analysis and synthesis polyphase transfer matrices for OFBs with arbitrary system delay do not appear to have been reported in the literature. Therefore, a succinct and straight-forward derivation following the logic used in the critically-sampled case provided by Vaidyanathan in [20] is given. In this derivation, the input-output transfer function of an OFB is first derived in the Z-domain. Recognizing the necessity to set the aliasing terms caused by the downsampling operations to zero, a matrix representation is then presented wherein the necessary conditions for PR result in the product $\mathbf{P}(z) = \mathbf{R}(z)\mathbf{E}(z)$ being a right pseudo-circulant matrix. In order to induce PR, specific relationships between the elements of $\mathbf{P}(z)$ are identified. Ensuring that these relationships are met results in the relationship of $\mathbf{R}(z)$ to $\mathbf{E}(z)$ that is necessary for a PRFB to be obtained.

In Appendix A.2, the general conditions for obtaining PR in even-stacked O-CMFBs are explicitly derived. Gopinath has provided a derivation of the PR conditions for even-stacked O-CMFBs in [17] that considers analysis subband filter impulse responses given by

$$h_i(n) = h_i h(n) \cos\left(\frac{\pi}{M} i\left(n - \frac{\alpha}{2}\right)\right)$$

The derivation for the general conditions necessary for obtaining PR as provided in Appendix A.2 are derived for even-stacked O-CMFBs with analysis subband filter impulse responses given by

$$h_k[n] = \rho_k p[n] \cos\left[\frac{\pi}{M} k\left(n - \frac{L_p - 1 + M}{2}\right)\right]$$

Gopinath's PR conditions apply to CMFBs with arbitrary system delay α. The PR conditions derived in Appendix A.2 apply to CMFBs with system delay $L_p - 1 + M$. It is this form with a fixed system delay that is considered throughout this thesis. It is shown that the PR conditions derived for the specific case considered in the context of this paper are equivalent to those derived for the more general case derived by Gopinath.

Chapter 2

Multirate Filter Banks – Fundamental Building Blocks

Multirate FBs consist of a parallel implementation of analysis and synthesis subband filters in series with appropriate subsampling operations such as the downsampling and upsampling operations. Multirate systems, as compared to singlerate systems, modify the sampling rate of an input signal as the signal propagates throughout the system. By modifying the sampling rate and manipulating the order of the cascades of subband filters and subsampling operations, efficiencies can be obtained in the form of relaxed requirements on the subband filters, subband filters operating at a reduced sampling rate, and processing of subband signals at reduced sampling rates. To perform an analysis on the effects of separating an input signal into multiple subbands and subsequently recombining these subbands in order to reconstruct the input signal, it is necessary to understand the effects of the independent multirate operations such as the upsampling and downsampling operations.

In this chapter, the fundamental building blocks of multirate FBs are introduced. In sections 2.1 and 2.2, the upsampling and downsampling operations are discussed. Since cascades of upsamplers and downsamplers are often found in multirate FBs, the effects that these cascades induce on a signal are discussed in sections 2.3 and 2.4. Downsampling operations tend to be destructive in nature, introducing aliasing effects, whereas upsampling operations tend to introduce images of the original signal. Manipulations of the sampling rate in multirate systems must therefore be performed very carefully. Appropriate filtering operations such as the employment of anti-imaging and anti-aliasing filters typically precede or follow the subsampling operations in order to reduce or eliminate the aliasing and imaging effects caused by subsampling. The effects due to cascading anti-imaging and anti-aliasing filters with upsamplers and downsamplers are discussed in sections 2.5 and 2.6. Furthermore, the cascading of subsamplers with anti-imaging or anti-aliasing filters can be performed extraordinarily efficiently by

application of the Noble identities, which are introduced in section 2.7, and the polyphase representation, which is discussed in section 2.8.

2.1 Upsampler

One of the fundamental building blocks in multirate systems is the upsampler[1] which is illustrated in figure 1. The response of an upsampler to an input sequence $x[n]$ is given by

$$y(n) = \begin{cases} x\left(\frac{n}{N}\right) & \text{if } n = 0, \pm N, \pm 2N, \ldots \\ 0 & \text{otherwise} \end{cases} \tag{2.1}$$

where N is an integer.

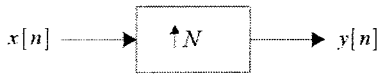

Figure 1. *N-fold upsampler.*

The upsampling operation increases the sampling rate of a discrete-time sequence by inserting $N - 1$ zero valued new samples between successive samples of $x[n]$. To illustrate this property in the time domain, consider the input sequence $x[n]$ shown in figure 2(a). Applying this sequence to an upsampler with an upsampling factor of $N = 2$ results in the output sequence illustrated in figure 2(b). The Z-transform of the input-output relationship shown in equation (2.1) is given by

$$Y(z) = \sum_{n=-\infty}^{\infty} y(n) z^{-n} = \sum_{n=-\infty}^{\infty} y(nN) z^{-nN} = \sum_{n=-\infty}^{\infty} x(n) z^{-nN} = X\left(z^N\right) \tag{2.2}$$

Consequently, if we assume a normalized sampling period of 1 s[2], the Z-transform evaluated over the unit circle results in the frequency-domain relationship

$$Y\left(e^{j\omega}\right) = X\left(e^{jN\omega}\right) \tag{2.3}$$

---

[1] Also commonly referred to as an interpolator or an expander.

[2] A normalized sampling period $T = 1$ which corresponds to a sampling frequency of 2π rad/s will be assumed throughout the thesis.

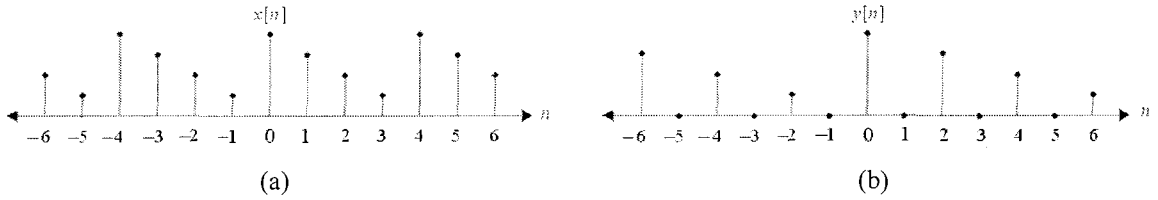

Figure 2. *Time-domain effect of an upsampling operation with an upsampling factor of N = 2. (a) Input sequence. (b) Output sequence.*

As is evident from equation (2.3), an N-fold upsampling operation essentially increases the sampling frequency by a factor of N. Since common convention is to normalize the sampling frequency to 2π before and after upsampling, the original spectrum appears to be compressed by a factor of N. This results in multiple compressed copies of the baseband spectrum appearing centered around $\omega = \pm 2\pi k/N$, for $k = 1, 2, \ldots, N-1$, which are referred to as images. To illustrate this property in the frequency domain, consider the input spectrum $X(e^{j\omega})$ shown in figure 3(a). Applying this signal to an upsampler with an upsampling factor of $N = 2$ results in the output spectrum illustrated in figure 3(b). The output spectrum appears to be a compressed copy of the original spectrum with images at $\omega = \pm\pi$ and $\omega = \pm 2\pi$. Noting that the baseband of the output spectrum is identical in shape to that of the input spectrum, the original signal can always be extracted from the output signal following appropriate anti-imaging filtering.

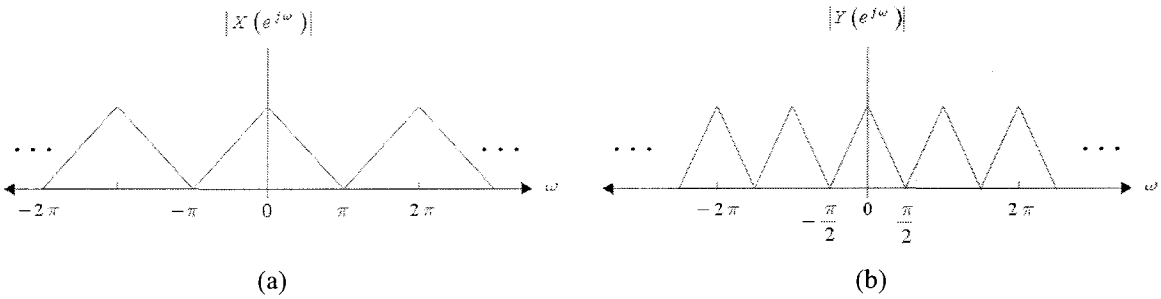

Figure 3. *Frequency-domain effect of upsampling operation with an upsampling factor of N = 2. (a) Input spectrum. (b) Output spectrum.*

2.2 Downsampler

Another fundamental building block in multirate systems is the downsampler[1] which is illustrated in figure 4. The response of a downsampler to an input sequence $x[n]$ is given by

$$y[n] = x[nN] \tag{2.4}$$

where N is an integer.

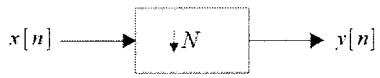

Figure 4. *N-fold downsampler.*

The downsampling operation decreases the sampling rate of a discrete-time sequence by removing $N-1$ samples between successive samples of $x[n]$. To illustrate this property in the time domain, consider the input sequence $x[n]$ shown in figure 5(a). Applying this sequence to the input of a downsampler with a downsampling factor of $N = 2$ results in the output sequence illustrated in figure 5(b). The Z-transform of the input-output relationship shown in equation (2.4) is given by

$$Y(z) = \frac{1}{N}\sum_{k=0}^{N-1} X\left(z^{1/N} W_N^k\right) \tag{2.5}$$

where $W_N = e^{-j2\pi/N}$. Consequently, the frequency-domain relationship between the input and output can be expressed as

$$Y\left(e^{j\omega}\right) = \frac{1}{N}\sum_{k=0}^{N-1} X\left(e^{j(\omega-2\pi k)/N}\right) \tag{2.6}$$

[1] Also commonly referred to as a decimator or compressor.

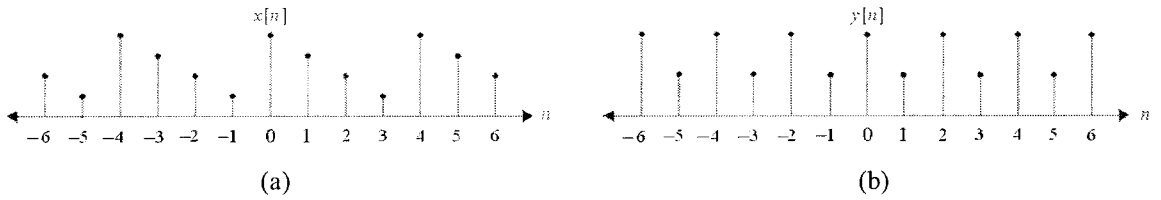

Figure 5. *Time-domain effect of a downsampling operation with a downsampling factor of N = 2. (a) Input sequence. (b) Output sequence.*

As is evident from equation (2.6), an N-fold downsampling operation essentially decreases the sampling frequency by a factor of N. Since common convention is to normalize the frequency axis, the original spectrum appears to be expanded by a factor of N, and then repeated at intervals of $\omega = \pm 2\pi k/N$, for $k = 1, 2, ..., N - 1$. The expanded baseband spectrum itself is not periodic; however, after summing the multiple copies of the expanded baseband spectrum, the result is periodic with a period of 2π. As will become evident in the following example, if the original signal is not appropriately bandlimited the expanded copies of the baseband spectrum will overlap resulting in what is known as aliasing. To illustrate this property in the frequency domain, consider the input spectrum $X(e^{j\omega})$ shown in figure 6(a). Applying this signal to a downsampler with a downsampling factor of $N = 2$ results in the output spectrum shown in figure 6(b). The output spectrum is simply an expanded copy of the original spectrum, with aliasing illustrated by the shaded areas. At any frequency component where aliasing occurs it is generally not possible to extract the original signal. However, aliasing can be avoided and the original signal can be extracted from the output signal if the input signal is appropriately bandlimited prior to downsampling.

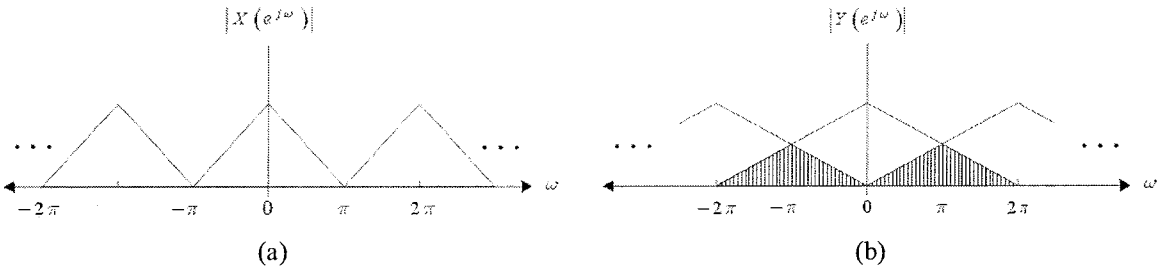

Figure 6. *Frequency-domain effect of a downsampling operation with a downsampling factor of N = 2. (a) Input spectrum. (b) Output spectrum.*

2.3 Upsampler–Downsampler Cascade

Since in multirate systems the fundamental building blocks discussed in sections 2.1 and 2.2 are frequently cascaded, it is important to understand the operation of such cascades. One example of such a cascade is the upsampler–downsampler cascade wherein an N-fold upsampler is followed by an N-fold downsampler, as illustrated in figure 7. The response of an upsampler with an integer upsampling factor of N followed by a downsampler with an integer downsampling factor of N to an input sequence $x[n]$ is

$$y[n] = x[n] \tag{2.7}$$

As is evident by equation (2.7), the upsampler–downsampler cascade has no effect on the input sequence; therefore, no further evaluation is performed.

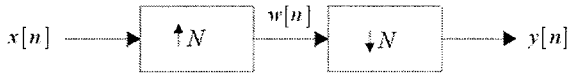

Figure 7. *N-fold upsampler followed by an N-fold downsampler.*

2.4 Downsampler–Upsampler Cascade

Another example of a cascade is the downsampler–upsampler cascade wherein an N-fold downsampler is followed by an N-fold upsampler, as illustrated in figure 8. The response of a downsampler with an integer downsampling factor of N followed by an upsampler with an integer upsampling factor of N to an input sequence $x[n]$ is

$$y[n] = \begin{cases} x[n] & \text{if } n = 0, \pm N, \pm 2N, \ldots \\ 0 & \text{otherwise} \end{cases} \tag{2.8}$$

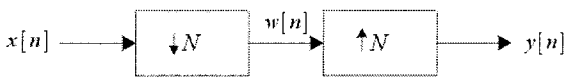

Figure 8. *N-fold downsampler followed by an N-fold upsampler.*

A downsampler-upsampler cascade removes $N-1$ samples between successive samples of $x[n]$ and then inserts $N-1$ zeros into these locations. To illustrate this property in the time domain, consider the input sequence shown in figure 9(a). Applying this sequence to a downsampler with a downsampling factor of $N = 2$ followed by an upsampler with an upsampling factor of $N = 2$ produces the sequence illustrated in figure 9(b). The Z-transform of the input-output relationship shown in equation (2.8) is given by

$$Y(z) = \frac{1}{N}\sum_{k=0}^{N-1} X\left(zW_N^k\right) \tag{2.9}$$

Consequently, the frequency-domain relationship can be expressed as

$$Y\left(e^{j\omega}\right) = \frac{1}{N}\sum_{k=0}^{N-1} X\left(e^{j(\omega-2\pi k/N)}\right) \tag{2.10}$$

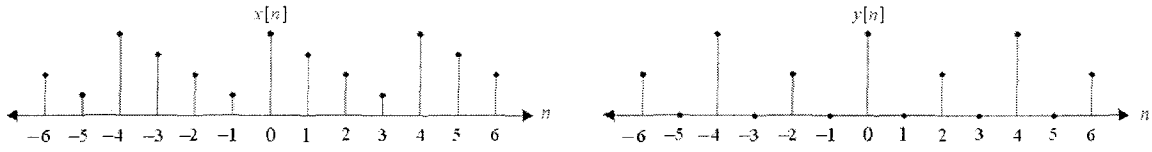

(a) (b)

Figure 9. *Time-domain effect of a downsampling operation followed by an upsampling operation with subsampling factors of $N = 2$. (a) Input sequence. (b) Output sequence.*

As is evident from equation (2.10), the downsampling–upsampling cascade first creates N-fold expanded copies of the original baseband spectrum located at intervals of $\omega = \pm 2\pi k/N$, for $k = 1, 2, \ldots, N-1$. As will become evident in the following example, if the original signal is not appropriately bandlimited the expanded copies of the baseband spectrum will overlap, resulting in aliasing. To illustrate this property in the frequency domain, consider the input spectrum $X(e^{j\omega})$ shown in figure 10(a). Applying this signal to a downsampler with a downsampling factor of $N = 2$ followed by an upsampler with an upsampling factor of $N = 2$ produces the spectrum illustrated in figure 10(b). Thus, the spectrum at the output of the downsampler is an expanded copy of the original spectrum with aliasing illustrated by the shaded areas. Applying this signal to an upsampler results in the entire spectrum being compressed by a factor of N. At any frequency component where aliasing occurs it is generally not possible to extract the original signal. However, aliasing can be avoided and the original signal can be extracted from the output signal if the input signal is appropriately bandlimited prior to downsampling.

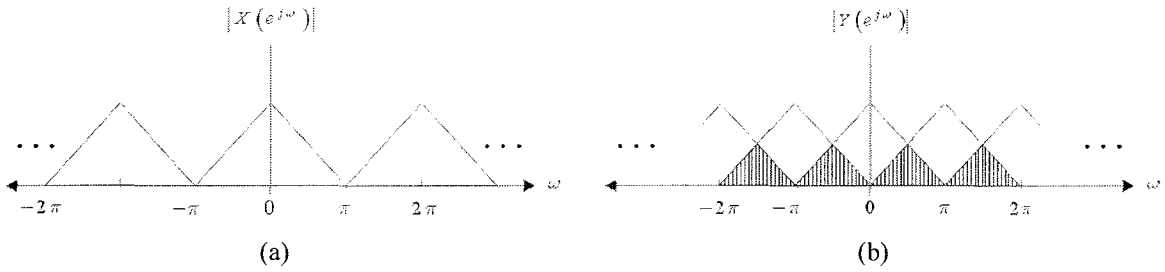

Figure 10. *Frequency-domain effect of a downsampling operation followed by an upsampling operation with subsampling factors of N = 2. (a) Input spectrum. (b) Output spectrum.*

2.5 Upsampler–Filter Cascade

Since the upsampling operation creates multiple images of the compressed baseband spectrum, it is necessary to attenuate or eliminate these images in order to properly recover the original signal. The upsampler is therefore followed by an anti-imaging filter with an impulse response given by $f[n]$, as illustrated in figure 11. The anti-imaging filter is typically a lowpass filter that has the idealized frequency response

$$F\left(e^{j\omega}\right) = \begin{cases} N & \text{if } |\omega| \le \pi/N \\ 0 & \text{otherwise} \end{cases} \tag{2.11}$$

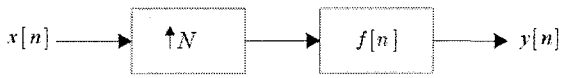

Figure 11. *N-fold upsampler followed by an anti-imaging filter with impulse response f[n].*

It has been shown in [20] that the anti-aliasing filter requires a gain of N in order to properly reconstruct the original signal $x[n]$. The input-output relationship of the upsampler–filter cascade in the Z-domain is given by

$$Y(z) = X\left(z^N\right)F(z) \tag{2.12}$$

If the anti-imaging filter provides sufficient attenuation, the images of the baseband signal located at $\omega = \pm 2\pi k/N$ will effectively be removed. The upsampler–filter cascade can therefore be seen as an operation that results in an output signal with a spectrum that is an N-fold compressed version of the input signal.

2.6 Filter–Downsampler Cascade

Since the downsampling operation creates multiple expanded replicas of the original spectrum, it is necessary to bandlimit the original signal in order to ensure that the expanded replicas do not overlap with the original spectrum. The downsampler is therefore preceded by an anti-aliasing filter with an impulse response given by $h[n]$, as illustrated in figure 12. The anti-aliasing filter is typically a lowpass filter that has the idealized frequency response

$$H\left(e^{j\omega}\right)=\begin{cases}1 & \text{if } |\omega| \le \pi/N \\ 0 & \text{otherwise}\end{cases} \tag{2.13}$$

The input-output relationship of the filter–downsampling cascade in the Z-domain is given by

$$Y(z)=\frac{1}{N}\sum_{k=0}^{N-1} H\left(z^{1/N}W_N^k\right)X\left(z^{1/N}W_N^k\right) \tag{2.14}$$

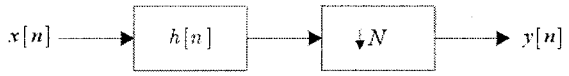

Figure 12. *N-fold downsampler preceded by an anti-aliasing filter with impulse response h[n].*

If the anti-aliasing filter provides sufficient attenuation, the aliasing distortion caused by overlapping of the input signal spectrum at $\omega = \pm 2\pi k/N$ can effectively be eliminated. The filter–downsampler cascade can therefore be seen as an operation whereby an input signal can be appropriately bandlimited in order to avoid aliasing distortion caused by downsampling operations.

2.7 Noble Identities

Downsampler–filter cascades and filter–upsampler cascades are often found in multirate systems. Using what are referred to as the Noble identities[1], it is possible to switch the order of the cascade; i.e., a downsampler–filter cascade can be transformed into a filter–downsampler cascade, and a filter–upsampler

[1]Note that these identities are only applicable if $F(z)$ and $H(z)$ are rational functions, i.e., ratios of polynomials in z or z^{-1}.

cascade can be transformed into an upsampler–filter cascade. There are two main reasons for wishing to do this; firstly, increased computational efficiency can be obtained if the filter operation is performed on the side of the upsampler (or downsampler) with the lower sampling rate, and secondly, the cascaded filters can be transformed into a form appropriate for a polyphase decomposition, as will be discussed in section 2.8. The two Noble identities are as follows:

Noble Identity #1

Given a downsampler–filter cascade with a downsampling factor of N, a filter–downsampler cascade can be substituted if the new filter is upsampled by a factor of N. This relationship is illustrated in figure 13.

Figure 13. *Noble Identity #1.*

Noble Identity #2

Given a filter–upsampler cascade with an upsampling factor of N, an upsampling–filter cascade can be substituted if the new filter is upsampled by a factor of N. This relationship is illustrated in figure 14.

Figure 14. *Noble Identity #2.*

2.8 Polyphase Representation

The polyphase representation of digital filters is widely used in the study of multirate systems. There are two main reasons for this; firstly, the polyphase representation facilitates simplification of the mathematical analysis of FBs, and secondly, the polyphase representation often leads to efficient implementation of multirate FBs following application of the Noble identities. To describe the polyphase representation, consider a digital filter with the transfer function

$$H(z) = \sum_{n=-\infty}^{\infty} h[n] z^{-n} \tag{2.15}$$

It is possible to represent this transfer function as a sum of its multiple K-spaced phases. The simplest to consider is the K-spaced Type-1 polyphase representation that is expressed as

$$H(z) = \sum_{l=0}^{K-1} z^{-l} E_l\left(z^K\right) \tag{2.16}$$

where

$$E_l(z) = \sum_{n=-\infty}^{\infty} h[Kn + l] z^{-n}$$

The K-spaced polyphase representation splits the original sequence $h[n]$ into a sum of K sequences multiplied by appropriate powers of z, where each new sequence has a Z-transform denoted by $E_l(z)$. The coefficients of each $E_l(z)$ are equal to $h[Kn + l]$ where K is the desired spacing. For example, consider the digital filter transfer function

$$P(z) = \sum_{l=0}^{11} p[l] z^{-l} \tag{2.17}$$

where $p[l]$ are the values of the digital filter impulse response. The 3-spaced Type-1 polyphase representation is expressed as

$$P(z) = E_0\left(z^3\right) + z^{-1} E_1\left(z^3\right) + z^{-2} E_2\left(z^3\right) \tag{2.18}$$

where

$$\begin{aligned} E_0(z) &= p[0] + z^{-1} p[3] + z^{-2} p[6] + z^{-3} p[9] \\ E_1(z) &= p[1] + z^{-1} p[4] + z^{-2} p[7] + z^{-3} p[10] \\ E_2(z) &= p[2] + z^{-1} p[5] + z^{-2} p[8] + z^{-3} p[11] \end{aligned} \tag{2.19}$$

Another commonly used polyphase representation is the K-spaced Type-2 polyphase representation. The Type-2 polyphase components are permutations of the Type-1 polyphase components and for the transfer function in equation (2.15) are given by

$$H(z) = \sum_{l=0}^{K-1} z^{(K-1-l)} R_l\left(z^K\right) \tag{2.20}$$

where

$$R_l(z) = E_{K-1-l}(z)$$

Since multirate FBs typically tend to incorporate cascades of filters and subsamplers, it is often desirable to perform the filtering on the side of the subsampler with the lowest sampling rate. Application of the Noble identities allows one to switch the order of the cascade on the condition that the subband filters have Z-domain transfer functions in z^M. Typically, these filters do not have transfer functions in z^M and efficient processing cannot be performed. However, representing each subband filter transfer function $H_k(z)$ and $F_k(z)$ in their polyphase form results in transfer functions in z^M thereby facilitating efficient cascades of filters and subsamplers.

2.9 Summary and Conclusions

The well-known fundamental building blocks of multirate systems were presented. In sections 2.1 and 2.2, the upsampling and downsampling operations were presented in the time, Z, and frequency domains. It was discussed how the upsampling and downsampling operations induce multiple images and aliasing components into the original signal spectrum, respectively.

In sections 2.3 and 2.4, the transfer functions of upsampler–downsampler cascades and downsampler–upsampler cascades were derived by application of the upsampler and downsampler input-output relationships. It was discussed how upsampler–downsampler cascades do not result in modifications to an input signal, whereas downsampler–upsampler cascades to introduce imaging and aliasing distortion if the input signal is not appropriately bandlimited.

In sections 2.5 and 2.6, upsampler–filter cascades and filter–downsampler cascades were taken into consideration. It was discussed how the application of ideal filtering results in the removal of imaging and aliasing components caused by the upsampling and downsampling operations, respectively.

In sections 2.7 and 2.8, the Noble identities and polyphase representation were introduced. It was shown that the application of the Noble identities in conjunction with the polyphase representation offers efficient implementations of multirate filtering.

Chapter 3

Oversampled Filter Banks

An FB is a collection of digital filters that operate in parallel with a common input or a common output. In the case of a common input, the collection of digital filters with transfer functions in the Z-domain denoted by $H_k(z)$ is referred to as an analysis bank, whereas in the case of a common output, the collection of digital filters with transfer functions denoted by $F_k(z)$ is referred to as a synthesis bank. In the analysis bank the subband filters are usually followed by downsamplers with a downsampling factor of $N = M$. Similarly, in the synthesis bank the subband filters are usually preceded by upsamplers with an upsampling factor of $N = M$. The signals at the output of the downsamplers have transfer functions denoted by $U_k(z)$ as illustrated in figure 15 and are referred to as the subband signals. Subband processing is often performed on the subband signals and is dependent on the specific application.

The analysis bank performs the process of splitting an input signal into M subbands, whereas the synthesis bank performs the process of reconstructing the input signal from the M subband signals. The frequency responses of the analysis and synthesis subband filters are either non-overlapping, slightly-overlapping, or extremely-overlapping, depending on the application. In addition to this, the analysis filters have either uniform or non-uniform frequency bands, again depending on the specific application. In this thesis, only uniform FBs with slightly-overlapping frequency responses are considered.

Multirate FBs are classified as being either finite-duration impulse response (FIR) or infinite-duration impulse response (IIR) FBs. Most research has focused on FIR FBs wherein each subband filter impulse response is restricted to be FIR and hence guaranteed to be stable. In IIR FBs, the subband filters have IIR impulse responses that often result in subband filters offering higher stopband attenuation while requiring fewer resources. However, these filters must meet strict requirements in order to maintain stability. In this thesis, only FIR FBs are considered.

The downsampling operations in the analysis bank allow the subband signals to be processed at a reduced sampling rate, whereas the upsampling operations in the synthesis bank facilitate the process of

reconstructing the input signal. If the subsampling factor N is set equal to the number of channels M, then the FB is referred to as a critically-sampled[1] FB. In this case, the sampling rate at each subband processor will be equal to $1/M$ times the sampling rate at the input of the FB. If the subsampling factor N is greater than the number of channels M then the FB is referred to as an oversampled filter bank OFB. In this case, the sampling rate at the subband processor will be greater than $1/M$ times the sampling rate at the input of the FB, resulting in an increased number of samples in each subband at the subband processor relative to critically-sampled FBs.

In section 3.1, the fundamental building blocks of multirate FBs presented in chapter 2 are used to determine the input-output relationship of OFBs in the frequency domain. Following this, in section 3.2 the Noble identities and polyphase representation presented in sections 2.7 and 2.8, respectively, are applied to derive an efficient polyphase representation of OFBs. In section 3.3, an FIR factorization of the analysis bank transfer matrix is proposed that parameterizes all OFBs. This factorization is essential for determining factorizations representing structural implementations. As outlined in chapter 1, multirate operations tend to introduce errors such as aliasing and imaging. An analysis into the removal of these errors as well as the removal of errors caused by non-ideal subband filtering is presented in section 3.4 for both the frequency-domain and polyphase-domain. Chapter 3 concludes with a discussion on biorthogonality, paraunitariness, and overcomplete expansions.

3.1 Representation in the Frequency Domain

Following an analysis similar to that presented by Vaidyanathan in [20] for critically-sampled FBs, the transfer function of an OFB can be derived by application of the fundamental building block transfer functions presented in chapter 2. Recalling the filter–downsampler cascade Z-domain transfer function presented in section 2.6, the output of each downsampler in figure 15 can be expressed as

$$U_k(z) = \frac{1}{N}\sum_{l=0}^{N-1} H_k\left(z^{1/N}W_N^l\right)X\left(z^{1/N}W_N^l\right)$$

To determine the output of each channel cascaded with an upsampler, the transfer function of an upsampler as given by equation (2.2) is applied, resulting in

---

[1] Also commonly referred to as maximally-decimated.

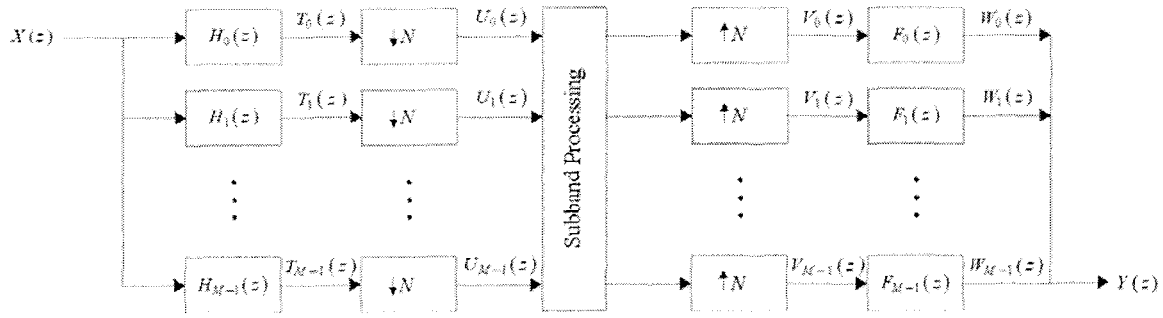

Figure 15. *Frequency-domain representation of an M-channel filter bank with subsampling factor N.*

$$V_k(z) = \frac{1}{N}\sum_{l=0}^{N-1} H_k\left(zW_N^l\right)X\left(zW_N^l\right)$$

Finally, the input-output relationship of the OFB is obtained by multiplying the transfer function of each synthesis subband filter, denoted $F_k(z)$, with each $V_k(z)$, and summing the results. This gives the OFB input-output relationship

$$Y(z) = \frac{1}{N}\sum_{k=0}^{M-1}\sum_{l=0}^{N-1} F_k(z)H_k\left(zW_N^l\right)X\left(zW_N^l\right) \tag{3.1}$$

If the subband filters have different passbands, it is evident that $Y(z)$ consists of a sum of distorted, frequency-shifted versions of the input signal $X(z)$. The frequency-shifted versions of $X(z)$ are given by $X\left(zW_N^l\right)$, where $l = 0, 1, \ldots, N-1$. Multiple types of errors are induced onto $Y(z)$, including aliasing and imaging distortion caused by the downsampling and upsampling operations, respectively, and amplitude and phase distortion caused by the non-ideal frequency responses of the subband filters. Upon inspection of equation (3.1) it is noted that the analysis and synthesis bank transfer functions can be represented using the matrix notation

$$\mathbf{H}(z) = \begin{bmatrix} H_0(z) & H_0(zW) & \cdots & H_0\left(zW_N^{N-1}\right) \\ H_1(z) & H_1(zW) & \cdots & H_1\left(zW_N^{N-1}\right) \\ \vdots & \vdots & \ddots & \vdots \\ H_{M-1}(z) & H_{M-1}(zW) & \cdots & H_{M-1}\left(zW_N^{N-1}\right) \end{bmatrix} \tag{3.2}$$

and

$$\mathbf{f}(z)=\begin{bmatrix} F_0(z) \\ F_1(z) \\ \vdots \\ F_{M-1}(z) \end{bmatrix} \tag{3.3}$$

The input-output relationship of an OFB can therefore also be expressed as

$$Y(z)=\frac{1}{N}\mathbf{f}^T(z)\mathbf{H}(z)\mathbf{x}(z) \tag{3.4}$$

where

$$\mathbf{x}(z)=\begin{bmatrix} X(z) & X(zW_N) & \cdots & X(zW_N^{N-1}) \end{bmatrix}^T$$

and $\mathbf{H}(z)$ is referred to as the analysis bank transfer matrix. The input-output relationship shown in equation (3.1) is for the special case of $X(zW_N^m)$ where $m = 0$. If we consider the general case of the frequency-shifted input $X(zW_M^m)$ for $m = 0, 1, \ldots, N-1$, we obtain after simplification the OFB input-output relationship

$$Y(zW_N^m)=\frac{1}{N}\sum_{k=0}^{M-1}\sum_{l=0}^{N-1}F_k(zW_N^m)H_k(zW_N^l)X(zW_N^l) \tag{3.5}$$

Applying the analysis bank transfer function $\mathbf{H}(z)$ from equation (3.2) and the synthesis bank transfer function $\mathbf{F}(z)$ defined by

$$\mathbf{F}(z)=\frac{1}{\sqrt{N}}\begin{bmatrix} F_0(z) & F_1(z) & \cdots & F_{M-1}(z) \\ F_0(zW) & F_1(zW) & \cdots & F_{M-1}(zW) \\ \vdots & \vdots & \ddots & \vdots \\ F_0(zW_N^{N-1}) & F_1(zW_N^{N-1}) & \cdots & F_{M-1}(zW_N^{N-1}) \end{bmatrix} \tag{3.6}$$

the generalized input-output relationship of an OFB can be expressed as

$$\mathbf{y}(z)=\mathbf{F}(z)\mathbf{H}(z)\mathbf{x}(z) \tag{3.7}$$

where

$$\mathbf{y}(z)=\begin{bmatrix} Y(z) & Y(zW_N) & \cdots & Y(zW_N^{N-1}) \end{bmatrix}^T$$

3.2 Representation in the Polyphase Domain

Although the M-channel FB illustrated in figure 15 is intuitively appealing, it is not particularly computationally efficient. As described in section 2.7, a more efficient implementation of the subband filters arises if the filtering operations are performed on the side of the subsampler with the lowest sampling rate. This motivates the desire to obtain the polyphase representation of an OFB.

By applying the Noble identities introduced in section 2.7, it is possible to represent the M-channel OFB in a polyphase form, as illustrated in figure 16. The analysis and synthesis subband filters can be represented by vectors $\mathbf{h}(z)$ and $\mathbf{f}(z)$ defined as

$$\mathbf{h}(z) = \begin{bmatrix} H_0(z) \\ H_1(z) \\ \vdots \\ H_{M-1}(z) \end{bmatrix} \tag{3.8}$$

and

$$\mathbf{f}(z) = \begin{bmatrix} F_0(z) \\ F_1(z) \\ \vdots \\ F_{M-1}(z) \end{bmatrix} \tag{3.9}$$

respectively. The transfer function for each analysis and synthesis subband filter must then assume the form of the K-spaced Type-1 and Type-2 polyphase representations, respectively, with $K = N$, resulting in

$$H_k(z) = \sum_{l=0}^{N-1} z^{-1} E_{k,l}\left(z^N\right) \tag{3.10}$$

and

$$F_k(z) = \sum_{l=0}^{N-1} z^{-(N-1-l)} R_{k,l}\left(z^N\right) \tag{3.11}$$

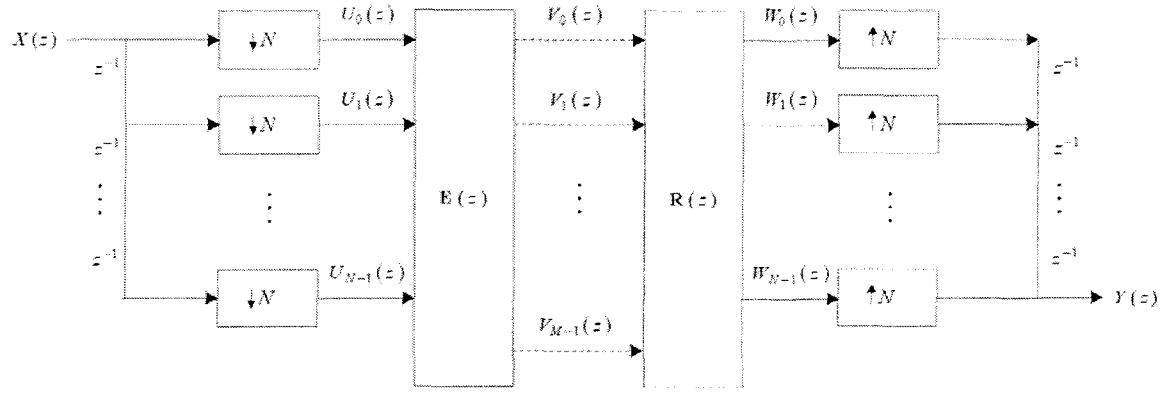

Figure 16. *Polyphase-domain representation of an M-channel filter bank with subsampling factor N.*

The analysis bank transfer function can then be expressed in its N-spaced Type-1 polyphase form, i.e.,

$$\begin{aligned}\mathbf{h}(z) &= \begin{bmatrix} E_{0,0}(z^N) & E_{0,1}(z^N) & \cdots & E_{0,N-1}(z^N) \\ E_{1,0}(z^N) & E_{1,1}(z^N) & \cdots & E_{1,N-1}(z^N) \\ \vdots & \vdots & \ddots & \vdots \\ E_{M-1,0}(z^N) & E_{M-1,1}(z^N) & \cdots & E_{M-1,N-1}(z^N) \end{bmatrix} \begin{bmatrix} 1 \\ z^{-1} \\ \vdots \\ z^{-(N-1)} \end{bmatrix} \\ &= \mathbf{E}(z^N)\mathbf{e}(z)\end{aligned} \tag{3.12}$$

where

$$\mathbf{e}(z) = \begin{bmatrix} 1 & z^{-1} & \cdots & z^{-(N-1)} \end{bmatrix}^T$$

Similarly, the synthesis bank transfer function can be expressed in its N-spaced Type-2 polyphase form, i.e.,

$$\begin{aligned}\mathbf{f}(z) &= \begin{bmatrix} z^{-(N-1)} \\ z^{-(N-2)} \\ \vdots \\ 1 \end{bmatrix}^T \begin{bmatrix} R_{0,0}(z^N) & R_{0,1}(z^N) & \cdots & R_{0,M-1}(z^N) \\ R_{1,0}(z^N) & R_{1,1}(z^N) & \cdots & R_{1,M-1}(z^N) \\ \vdots & \vdots & \ddots & \vdots \\ R_{N-1,0}(z^N) & R_{N-1,1}(z^N) & \cdots & R_{N-1,M-1}(z^N) \end{bmatrix} \\ &= z^{-(N-1)}\tilde{\mathbf{e}}(z)\mathbf{R}(z^N)\end{aligned} \tag{3.13}$$

where $\tilde{\mathbf{e}}(z)$ denotes the paraconjugate[1] of $\mathbf{e}(z)$. Finally, since the polyphase matrices $\mathbf{E}(z^N)$ and $\mathbf{R}(z^N)$ contain powers of z equal to that of the subsamplers, their order of operation can be swapped with the appropriate subsamplers by application of the Noble identities presented in section 2.7. This results in analysis and synthesis banks as illustrated in figure 16 with transfer functions given by

$$\mathbf{h}(z) = \mathbf{E}(z)\mathbf{e}(z) \tag{3.14}$$

and

$$\mathbf{f}(z) = z^{-(N-1)}\tilde{\mathbf{e}}(z)\mathbf{R}(z) \tag{3.15}$$

respectively, where $\mathbf{E}(z)$ and $\mathbf{R}(z)$ are referred to as the analysis and synthesis bank polyphase transfer matrices, respectively.

3.3 FIR Factorization

FIR FBs represent an important class of FBs since they are easy to design and implement in practical applications, can offer subband filters with linear phase, and are guaranteed to be stable. The subband filters in FIR FBs are represented by a class of Laurent polynomials where each subband filter transfer function is given by

$$H_k(z) = \sum_{i=0}^{m} h_i z^i \tag{3.16}$$

Here, m is an arbitrary positive integer and the h_i are arbitrary real-valued coefficients. A complete parameterization of FIR OFBs follows from the Smith form decomposition of rectangular polynomial matrices, which is described in [20]. The Smith form decomposition states that an $M \times N$ ($M \geq$ N) polynomial matrix $\mathbf{H}(z)$ with rank N can be factorized as

$$\mathbf{H}(z) = \mathbf{P}(z)\mathbf{D}(z)\mathbf{Q}(z) \tag{3.17}$$

---

[1] The paraconjugate of a polynomial vector $\mathbf{e}(z)$ is defined as $\tilde{\mathbf{e}}(z) = \mathbf{e}^{*T}(z^{-1})$

where $\mathbf{P}(z)$ and $\mathbf{Q}(z)$ are unimodular[1] polynomial matrices of dimensions $M \times M$ and $N \times N$, respectively. $\mathbf{D}(z)$ is referred to as the Smith form of $\mathbf{H}(z)$ and is given by

$$\mathbf{D}(z) = \begin{bmatrix} \mathbf{D}_1(z) \\ \mathbf{0}_{(M-N)\times N} \end{bmatrix} = \begin{bmatrix} D_0(z) & 0 & \cdots & 0 \\ 0 & D_1(z) & & \vdots \\ \vdots & & \ddots & 0 \\ 0 & \cdots & 0 & D_{N-1}(z) \\ & & \mathbf{0}_{(M-N)\times N} & \end{bmatrix} \tag{3.18}$$

where $D_i(z)$ are arbitrary Laurent polynomials. Furthermore, $\mathbf{P}(z)$ and $\mathbf{Q}(z)$ can be chosen such that each $D_i(z)$ is monic[2] and each $D_i(z)$ is a factor of $D_{i+1}(z)$.

Matrices $\mathbf{P}(z)$ and $\mathbf{Q}(z)$ can be generated by applying a product of a finite number of elementary row and column operation matrices, respectively, denoted by $\mathbf{P}_k(z)$ and $\mathbf{Q}_k(z)$, i.e.,

$$\mathbf{P}(z) = \mathbf{P}_0(z) \cdot \mathbf{P}_1(z) \cdot \ldots \cdot \mathbf{P}_{r-1}(z) \tag{3.19}$$

and

$$\mathbf{Q}(z) = \mathbf{Q}_0(z) \cdot \mathbf{Q}_1(z) \cdot \ldots \cdot \mathbf{Q}_{s-1}(z) \tag{3.20}$$

where r and s have integer values greater than zero. To manipulate the elements of a square matrix, such as $\mathbf{P}(z)$ or $\mathbf{Q}(z)$, four elementary matrix operations exist, namely, Type-1, Type-2, Type-3a, and Type-3b as follows:

---

[1] A square polynomial matrix with a constant, nonzero determinant.

[2] Coefficient of the highest power of z is equal to 1.

Type-1. *Interchange two rows/columns*:

$$\begin{bmatrix} 1 & & & & & & & & \\ & \ddots & & & & & & & \\ & & 1 & & & & & & \\ & & & 0 & & 1_{i,i+m} & & & \\ & & & & \ddots & & & & \\ & & & 1_{i+m,i} & & 0 & & & \\ & & & & & & 1 & & \\ & & & & & & & \ddots & \\ & & & & & & & & 1 \end{bmatrix}$$

If a Type-1 operation is applied to the left of a square $M \times M$ matrix $\mathbf{P}(z)$, the ith and $(i+m)$th rows of $\mathbf{P}(z)$ are interchanged. If a Type-1 operation is applied to the right of a square $M \times M$ matrix $\mathbf{P}(z)$, the ith and (i+m)th columns of $\mathbf{P}(z)$ are interchanged.

Type-2. *Multiply a row/column by a nonzero constant, c*:

$$\begin{bmatrix} 1 & & & & & & \\ & \ddots & & & & & \\ & & 1 & & & & \\ & & & c_{i,j} & & & \\ & & & & 1 & & \\ & & & & & \ddots & \\ & & & & & & 1 \end{bmatrix}$$

If a Type-2 operation is applied to the left of a square $M \times M$ matrix $\mathbf{P}(z)$, the ith row of $\mathbf{P}(z)$ is multiplied by an arbitrary nonzero constant c. If a Type-2 operation is applied to the right of a square $M \times M$ matrix $\mathbf{P}(z)$, the jth column of $\mathbf{P}(z)$ is multiplied by an arbitrary nonzero constant c.

Type-3a. *Add a polynomial multiple of one row to another row*:

$$\begin{bmatrix} 1 & & & & \\ & 1 & & A(z)_{i,j} & \\ & & \ddots & & \\ & & & 1 & \\ & & & & 1 \end{bmatrix}$$

If a Type-3a operation is applied to the left of a square $M \times M$ matrix $\mathbf{P}(z)$, the jth row of $\mathbf{P}(z)$ multiplied by an arbitrary Laurent polynomial $A(z)$ is added to the ith row of $\mathbf{P}(z)$.

Type-3b. *Add a polynomial multiple of one column to another column*:

$$\begin{bmatrix} 1 & & & & \\ & 1 & & & \\ & & \ddots & & \\ & B(z)_{i,j} & & 1 & \\ & & & & 1 \end{bmatrix}$$

If a Type-3b operation is applied to the right of a square $M \times M$ matrix $\mathbf{P}(z)$, the jth column of $\mathbf{P}(z)$ multiplied by an arbitrary Laurent polynomial $B(z)$ is added to the ith column of $\mathbf{P}(z)$.

Bölcskei showed in [50] that a complete parameterization of FIR OFBs is given by the Smith form decomposition if and only if the polynomials on the diagonal of $\mathbf{D}_1(z)$ have no zeros on the unit circle. Furthermore, he also showed that it is necessary and sufficient for the polynomials on the diagonal of $\mathbf{D}_1(z)$ to be monomials in order to obtain PR with FIR analysis and synthesis subband filters.

3.4 Perfect Reconstruction

An FB is referred to as a perfect reconstruction filter bank (PRFB) if and only if $y[n] = cx[n - n_0]$, where $x[n]$ is the original input sequence, $y[n]$ is the reconstructed output sequence, n_0 is an arbitrary integer greater than or equal to zero, and c is an arbitrary real-valued constant greater than zero. This means that the output sequence is an exact replica of the input sequence, possibly scaled by c and delayed by n_0 samples. In practice, there are eight types of distortion that $y[n]$ may suffer from:

Linear Distortion

- Aliasing (due to downsampling)
- Imaging (due to upsampling)
- Amplitude and phase (due to non-ideal filtering)

Non-linear Distortion

- Coefficient quantization (due to quantization of subband filter coefficients)
- Intermediate results truncation (due to the truncation of each subband filter output)
- Overflow distortion (due to the processing of overflows during intermediate operations)
- Coding (due to processing/coding of the subband signals by the subband processor)

- Transmission channel (due to non-idealities in the transmission network)

Coding and transmission channel distortion cannot be corrected for in FB designs (although they can be reduced by the employment of linear-phase subband filters as discussed in [20]), and hence will not be considered further. Non-linear distortion due to coefficient quantization, intermediate results truncation, and the processing of overflows, can be eliminated if particular structures are chosen for the FB implementation. Aliasing, imaging, amplitude and phase distortion can be fully or partially eliminated if the subband filters are judiciously chosen.

Frequency-Domain Linear Distortion PR Conditions

In order to determine the conditions that $H_k(z)$ and $F_k(z)$ must meet in order to eliminate errors due to linear distortion, it is possible to analyze the frequency-domain representation of an FB as shown in figure 15. One method to reduce aliasing distortion is to appropriately bandlimit the subband signals represented by the transfer function $T_k(z)$ prior to the downsampling operations. Imaging distortion can be reduced by the employment of anti-imaging filters following the upsamplers in the synthesis bank. Amplitude and phase distortion can be minimized by using sufficiently high-order linear phase analysis and synthesis subband filters. However, these measures tend to only minimize the linear distortion, but not remove it entirely. As will be shown, it is possible to choose the subband filters in such a fashion that all of the aforementioned types of linear distortion are entirely canceled.

The OFB input-output transfer function given in equation (3.1) shows that $Y(z)$ is equal to a sum of frequency-shifted copies of $X(z)$ multiplied by $F_k(z)$ and $H_k(z)$. The aliasing terms are given by the frequency-shifted versions of $X\left(zW_N^l\right)$, i.e., those for which $l \neq 0$. In order to completely eliminate aliasing it is therefore necessary to force each of these shifted versions of $X(z)$ to zero, i.e.,

$$\frac{1}{N}\sum_{k=0}^{M-1}\sum_{l=1}^{N-1}F_k(z)H_k\left(zW_N^l\right) \doteq 0$$

Although forcing these conditions will eliminate aliasing errors it is still necessary to eliminate amplitude and phase distortion if PR is desired. Following cancellation of aliasing, the resulting input-output transfer function of an OFB is given by

$$Y(z) = \sum_{l=0}^{N-1} T(z)X\left(zW_N^l\right) \tag{3.21}$$

where

$$T(z) \triangleq \frac{1}{N}\sum_{k=0}^{M-1} F_k(z)H_k(z)$$

In order to eliminate amplitude distortion it is necessary to ensure that $|T(z)|$ is a constant. In order to eliminate phase distortion it is necessary to ensure that $\angle T(z)$ is linear.

Equivalently, for the generalized OFB input-output relationship given in equation (3.5), as is evident from equation (3.7) the generalized PR condition can be written as

$$\mathbf{F}(z)\mathbf{H}(z) = cz^{-n_0}\mathbf{I}_N \tag{3.22}$$

where c is an arbitrary real-valued number greater than zero and n_0 is an arbitrary integer greater than or equal to zero. The value of n_0 results in an overall system delay of $D = Mn_0 + M - 1$ samples. In critically-sampled FBs, $\mathbf{F}(z)$ and $\mathbf{H}(z)$ are $M \times M$ square matrices. The only matrix that results in PR is therefore given by $\mathbf{F}(z) = cz^{-n_0}\mathbf{H}^{-1}(z)$. In oversampled FBs, $\mathbf{F}(z)$ and $\mathbf{H}(z)$ are both rectangular matrices of size $N \times M$ and $M \times N$, respectively. In this case, any left inverse of $\mathbf{H}(z)$ is a possible solution to equation (3.22). If the Smith form decomposition as described in section 3.3 is applied to $\mathbf{H}(z)$, it can be shown [70] that the left inverse of $\mathbf{H}(z)$ is given by

$$\mathbf{F}(z) = \mathbf{Q}^{-1}(z)\left(\left[\mathbf{D}_1^{-1}(z) \quad \mathbf{0}_{N\times(M-N)}\right] + \left[\mathbf{0}_{N\times N} \quad \mathbf{X}(z)\right]\right)\mathbf{P}^{-1}(z) \tag{3.23}$$

where $\mathbf{P}(z)$ and $\mathbf{Q}(z)$ are unimodular polynomial matrices of dimensions $M \times M$ and $N \times N$, respectively, $\mathbf{X}(z)$ is an arbitrary $N \times (M-N)$ polynomial matrix, and $\mathbf{D}_1(z)$ is extracted from the Smith form of $\mathbf{H}(z)$, denoted by $\mathbf{D}(z)$, as shown in equation (3.18).

Polyphase-Domain PR Conditions

It is possible to determine the conditions for PR in the polyphase domain by performing an analysis of the polyphase-domain representation of an FB illustrated in figure 16. The input-output relationship of the analysis bank is given by

$$\mathbf{V}(z) = \mathbf{E}(z)\mathbf{U}(z) \tag{3.24}$$

where $\mathbf{E}(z)$ is as defined in equation (3.14), $\mathbf{U}(z) = [U_0(z) \;\; U_1(z) \;\; \cdots \;\; U_{M-1}(z)]^T$, and $\mathbf{V}(z) = [V_0(z) \;\; V_1(z) \;\; \cdots \;\; V_{M-1}(z)]^T$. Similarly, the input-output relationship of the synthesis bank is given by

$$\mathbf{W}(z) = \mathbf{R}(z)\mathbf{V}(z) \tag{3.25}$$

where $\mathbf{R}(z)$ is as defined in equation (3.15) and $\mathbf{W}(z) = [W_0(z) \;\; W_1(z) \;\; \cdots \;\; W_{M-1}(z)]^T$. In order to obtain PR it can be seen from equations (3.24) and (3.25) that it is necessary to ensure that

$$\mathbf{R}(z)\mathbf{E}(z) = cz^{-n_0}\mathbf{I}_N \tag{3.26}$$

The value of n_0 results in an overall system delay of $D = Mn_0 + M - 1$ samples. Furthermore, the PR property can be generalized to an arbitrary delay of $D = Mn_0 + r + M - 1$ samples by satisfying

$$\mathbf{R}(z)\mathbf{E}(z) = cz^{-n_0}\begin{bmatrix} \mathbf{0}_{(N-r)\times r} & \mathbf{I}_{N-r} \\ z^{-1}\mathbf{I}_r & \mathbf{0}_{r\times(N-r)} \end{bmatrix} \tag{3.27}$$

for some $r = 0, 1, \ldots, N-1$, as shown in Appendix A.1. In critically-sampled FBs, $\mathbf{R}(z)$ and $\mathbf{E}(z)$ are $M \times M$ square matrices; therefore, the only matrix that results in PR is $\mathbf{R}(z) = cz^{-n_0}\mathbf{E}^{-1}(z)$. In oversampled FBs, $\mathbf{R}(z)$ and $\mathbf{E}(z)$ are both rectangular matrices of size $N \times M$ and $M \times N$, respectively. In this case any left inverse of $\mathbf{E}(z)$ is also a possible solution of equation (3.26). If the Smith form decomposition as described in section 3.3 is applied to $\mathbf{E}(z)$ it can be shown [70] that any left inverse of $\mathbf{E}(z)$ is given by

$$\mathbf{R}(z) = \mathbf{Q}^{-1}(z)\left(\left[\mathbf{D}_1^{-1}(z) \;\; \mathbf{0}_{N\times(M-N)}\right] + \left[\mathbf{0}_{N\times N} \;\; \mathbf{X}(z)\right]\right)\mathbf{P}^{-1}(z) \tag{3.28}$$

where $\mathbf{P}(z)$ and $\mathbf{Q}(z)$ are unimodular polynomial matrices of dimensions $M \times M$ and $N \times N$, respectively, $\mathbf{X}(z)$ is an arbitrary $N \times (M-N)$ polynomial matrix, and $\mathbf{D}_1(z)$ is extracted from the Smith form of $\mathbf{E}(z)$, denoted by $\mathbf{D}(z)$, as shown in equation (3.18).

3.5 Biorthogonality, Paraunitariness, and Overcomplete Expansions

Biorthogonality

In critically-sampled FBs the minimal number of samples exist in the subbands following decimation while still allowing for PR. The most general class of critically-sampled PRFB's is referred to as biorthogonal

FBs and has been studied extensively in FB literature [11][12][13][14]. The biorthogonal condition states that the synthesis bank transfer matrix is an unrestricted inverse of the analysis bank transfer matrix. For example, the synthesis bank transfer matrix resulting in PR for the analysis bank transfer matrix given in equation (3.2) with $M = N$ is given by $\mathbf{F}(z) = cz^{-n_0}\mathbf{H}^{-1}(z)$, where $\mathbf{F}(z)$ and $\mathbf{H}^{-1}(z)$ are M x M matrices. Similarly, in the polyphase domain, the biorthogonality condition infers that $\mathbf{R}(z) = cz^{-n_0}\mathbf{E}^{-1}(z)$.

The relative freedom to choose a PR synthesis bank in biorthogonal systems facilitates one primary advantage: the design of low-delay FBs. In low-delay FBs the overall system delay can be defined independently of the order of the prototype filter, which is typically used in MFBs. This facilitates a filter bank designer to trade off overall system delay with the stopband attenuation of the subband filters; a desirable flexibility for real-time applications.

Paraunitariness

An important subclass of biorthogonal PRFBs is described as paraunitary (PU) (or orthogonal) FBs. Critically-sampled M-channel FBs are said to be PU if

$$\tilde{\mathbf{H}}(z)\mathbf{H}(z) = cz^{-n_0}\mathbf{I}_M$$

where $\tilde{\mathbf{H}}(z)$ denotes the paraconjugate[1] of $\mathbf{H}(z)$. A factorization that parameterizes all $M \times M$ PU matrices $\mathbf{H}(z)$ was proposed by Vaidyanathan in [20] and is given by

$$\mathbf{H}(z) = \mathbf{V}_C(z)\mathbf{V}_{C-1}(z)\ldots\mathbf{V}_1(z)\mathbf{R} \tag{3.29}$$

for a degree-C $\mathbf{H}(z)$ and where each $\mathbf{V}_i(z)$ is referred to as the degree-1 PU building block that can further be expressed in the Z-domain as

$$\mathbf{V}_i(z) = \mathbf{I} - \mathbf{v}_i\mathbf{v}_i^{\dagger} + z^{-1}\mathbf{v}_i\mathbf{v}_i^{\dagger} \tag{3.30}$$

Each $\mathbf{v}_i$ is an $M \times 1$ vector with unit norm[2] and $\mathbf{R}$ is a unitary[1] matrix that can further be factorized as a product of Householder matrices, i.e.,

---

[1] The paraconjugate of a polynomial matrix $\mathbf{H}(z)$ is defined as $\tilde{\mathbf{H}}(z) = \mathbf{H}^{*T}(z^{-1})$

[2] A vector $\mathbf{v}_m$ is defined to have unit norm if $\mathbf{v}_m^{\dagger} \cdot \mathbf{v}_m = 1$ where $\mathbf{v}_m^{\dagger}$ is defined as the transpose-conjugate of $\mathbf{v}_m$.

$$\mathbf{R} = \mathbf{H}_S \mathbf{H}_{S-1} \ldots \mathbf{H}_1 \tag{3.31}$$

Furthermore, each $\mathbf{H}_j$ is a Householder matrix given by

$$\mathbf{H}_j = \mathbf{I} - 2\mathbf{u}_j \mathbf{u}_j^{\dagger} \tag{3.32}$$

where $\mathbf{u}_j$ is an $M \times 1$ vector with unit norm.

PUFBs offer the following advantages compared to biorthogonal FBs;

- PR is guaranteed, which typically reduces the complexity of the optimization procedures inherent to FB design.
- The synthesis bank subband filters are guaranteed to be stable if the analysis bank subband filters are stable.
- The synthesis bank subband filters are easily determined from the analysis bank subband filters.

Overcomplete Expansions

The most general FBs are described as OFBs, which are not fully characterized by the biorthogonality condition. As seen in section 3.4, multiple solutions to the left-inverse of the analysis transfer matrix $\mathbf{H}(z)$ exist, which result in what is referred to as an overcomplete expansion. These FBs are often referred to as pseudo-biorthogonal FBs, and in addition to the possibility of generating FBs with low overall system delay, also offer the following advantages:

- Reduced reconstruction noise which results in reduced intra-band aliasing that is exploitable in subband adaptive filtering applications.
- Subband signal redundancy which can be used to enhance resilience to erasures in communications systems.
- Existence of non-unique PR synthesis banks which facilitates a PR synthesis bank to be chosen to most appropriately suit the needs of an application.

The drawback of OFBs is an increase in computational complexity since the sampling rate in each subband is increased compared to that of critically-sampled FBs. In contrast to pseudo-biorthogonal FBs,

---

[1] A matrix $\mathbf{R}$ is said to be unitary if $\mathbf{R}^T\mathbf{R} = c\mathbf{I}$.

M-channel oversampled PUFBs with subsampling factor N exist as well and are characterized by OFB analysis transfer matrices having the property $\tilde{\mathbf{H}}(z)\mathbf{H}(z) = cz^{-n_0}\mathbf{I}_N$, or equivalently in the polyphase domain, $\tilde{\mathbf{E}}(z)\mathbf{E}(z) = cz^{-n_0}\mathbf{I}_N$. Applying the Smith form decomposition to $\mathbf{H}(z)$ results in the synthesis bank transfer matrix factorization

$$\mathbf{F}(z) = \tilde{\mathbf{H}}(z) = \tilde{\mathbf{Q}}(z)\tilde{\mathbf{D}}(z)\tilde{\mathbf{P}}(z) \tag{3.33}$$

where $\tilde{\mathbf{P}}(z)$ and $\tilde{\mathbf{Q}}(z)$ are unimodular polynomial matrices of dimensions $M \times M$ and $N \times N$, respectively, and $\tilde{\mathbf{D}}(z)$ is given by

$$\tilde{\mathbf{D}}(z) = \left[\tilde{\mathbf{D}}_1(z) \quad \mathbf{0}_{N\times(M-N)}\right] = \begin{bmatrix} D_0^*\left(z^{-1}\right) & 0 & \cdots & 0 & \\ 0 & D_1^*\left(z^{-1}\right) & & \vdots & \mathbf{0}_{N\times(M-N)} \\ \vdots & & \ddots & 0 & \\ 0 & \cdots & 0 & D_{N-1}^*\left(z^{-1}\right) & \end{bmatrix} \tag{3.34}$$

This class of OFB is referred to as a pseudo-orthogonal FB and offers all of the advantages and disadvantages of imposing the PU condition as well as the advantages and disadvantages of introducing oversampling in an FB.

3.6 Summary and Conclusions

OFBs were studied. In section 3.1, the transfer functions of the fundamental building blocks of multirate FBs were used to derive the input-output transfer functions of OFBs in the frequency domain.

In section 3.2, the polyphase decomposition and Noble identities were presented. The Noble identities were then applied to the analysis and synthesis polyphase transfer matrices to derive input-output transfer functions of OFBs in the polyphase domain.

In section 3.3, the Smith form decomposition was presented. This decomposition was used to parameterize all FIR OFBs. It was shown that OFB transfer matrices can be factorized into products of elementary matrix operations and a diagonal matrix.

In section 3.4, the conditions for PR on the analysis and synthesis transfer matrices were derived in both the frequency-domain and polyphase-domain. It was shown that multiple synthesis banks which result in PR exist for a given analysis bank.

In section 3.5, a discussion on biorthogonality, paraunitariness, and overcomplete expansions was given. In the critically-sampled case, it was shown that PUFBs are a subset of biorthogonal FBs. In the oversampled case, it was shown that PU OFBs exist and are a subset of pseudo-biorthogonal FBs.

Chapter 4

Oversampled Modulated Filter Banks

OFBs typically have subsampling rates with values less than the total number of channels, which results in redundancy of the input signal within each subband. This subband signal redundancy increases the computational cost associated with the FB, motivating the interest for efficient implementations of OFBs. One class of FBs that offers efficient implementations is that of MFBs. In MFBs, the analysis and synthesis bank subband filter transfer functions are derived by multiplying an analysis and a synthesis prototype filter transfer function, respectively, with a specified modulation transform. The analysis and synthesis prototype filters can be independently defined but are often identical in order to meet requirements for PR. There are three extraordinary advantages MFBs offer:

- The implementation cost of each analysis and synthesis FB is only equal to that of its respective prototype filter and the modulation transform used, rather than the sum of independent filter operations.
- During the design phase a relatively small number of parameters need to be optimized since it is only necessary to consider the prototype filter coefficients rather than the coefficients of all subband filters.
- The modulation transform can often be implemented using well-known fast realizations of the DFT and DCT.

In section 4.1, a generalized factorization for arbitrary O-MFB transfer matrices is reviewed, including a factorization encompassing oversampled PU MFB transfer matrices. Subsequent to this, the application of this factorization to odd- and even-stacked DFT-M and CMFB transfer matrices as well as odd- and even-stacked PU DFT-M and CMFB transfer matrices is outlined in sections 4.2 and 4.3.

4.1 Generalized Factorization

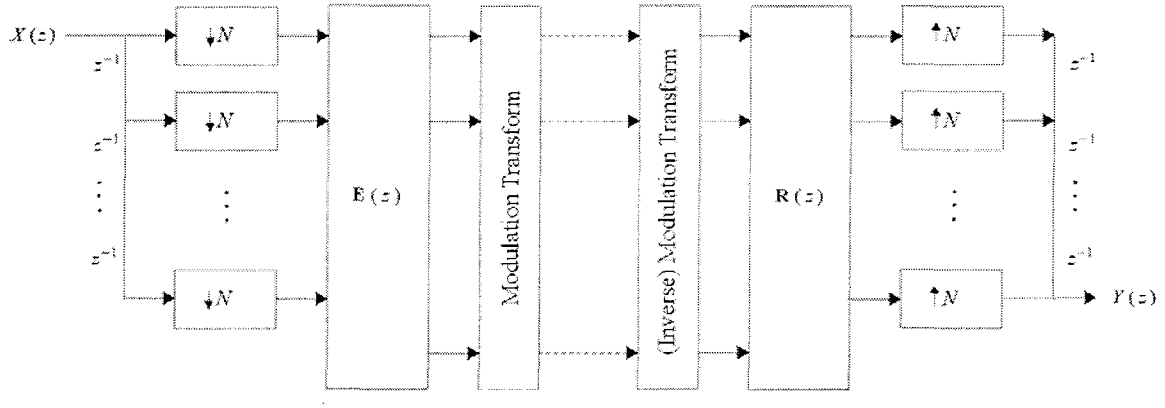

Figure 17. *Polyphase-domain representation of an M-channel modulated filter bank with subsampling factor N.*

A polyphase-domain representation of an M-channel modulated filter bank with subsampling factor N is illustrated in figure 17. A generalized factorization of the O-MFB transfer matrices $\mathbf{E}(z)$ and $\mathbf{R}(z)$ is derived by directly relating the modulation matrix to the prototype filter coefficients as described in [69]. Following slight manipulations, this factorization can then be applied to DFT-M and CMFB transfer matrices with modulations of either even- or odd-stacking types. In addition to this, factorizations are further derived for PU DFT-M and CMFB transfer matrices.

In MFBs, the analysis subband filter impulse responses $h_k[n]$ are generated by multiplying the analysis prototype filter impulse response $p[n]$ with a modulation transform. If we define the *prototype filter coefficient matrix* as

$$\mathbf{P} = \begin{bmatrix} p[0] & & & \\ & p[1] & & \\ & & \ddots & \\ & & & p[L_p - 1] \end{bmatrix} \tag{4.1}$$

where $p[i]$ are the ith coefficients of a length L_p prototype filter impulse response, and further define the *modulation vector* as

$$\mathbf{t}_k = \begin{bmatrix} t_k[0] & t_k[1] & \cdots & t_k[L_p - 1] \end{bmatrix} \tag{4.2}$$

where $t_k[i]$ represent the ith coefficients for the kth channel of the modulation transform, then the impulse response of the kth analysis filter is given by $h_k[n] = \mathbf{t}_k\mathbf{P}$. Redundancies in modulation transforms are often

experienced based on the number of channels M. These redundancies can be exploited by considering only the first K *unique* modulation coefficients, hence the *efficient modulation vector* is given by

$$\tilde{\mathbf{t}}_k = [t_k[0] \quad t_k[1] \quad \cdots \quad t_k[K-1]]^T \tag{4.3}$$

where $t_k[i]$, for $i = 0, 1, \ldots i-1$, represent the first K unique modulation coefficients extracted from $\mathbf{t}_k$. In order to use the efficient modulation vector to derive the subband filter impulse responses, it is necessary to multiply $\tilde{\mathbf{t}}_k$ by a matrix representing the redundancy pattern. This matrix is referred to as the *redundancy matrix* and is defined as

$$\mathbf{L}_2 = \begin{bmatrix} \mathbf{A}_K & \mathbf{A}_K & \cdots & \mathbf{A}_K & \mathbf{A}_S \\ & & & & \mathbf{0}_{(K-S)\times S} \end{bmatrix} \tag{4.4}$$

where $\mathbf{L}_2 \in \mathrm{N}^{K\times L_p}$, $S = \mathrm{mod}_K(L_p)$[1], and $\mathbf{A}_K$ is an identity matrix of a form to be further defined later for each specific modulation and stacking type. The impulse response for the kth analysis subband filter is therefore given by

$$h_k[n] = \tilde{\mathbf{t}}_k \mathbf{L}_2 \mathbf{P} \tag{4.5}$$

Recalling the definition of the analysis polyphase transfer matrix $\mathbf{E}(z)$ derived in section 3.2, note that each row of $\mathbf{E}(z)$ contains the polyphase components of the respective subband filter transfer function, i.e., the kth row of $\mathbf{E}(z)$ contains the polyphase components of the kth analysis subband filter transfer function. Each row of $\mathbf{E}(z)$ can therefore be factorized as

$$\begin{aligned} \mathbf{e}_k(z) &= \mathbf{p}\begin{bmatrix} \mathbf{I}_N & z^{-1}\mathbf{I}_N & \cdots & z^{-\lfloor L_p/N \rfloor+1}\mathbf{I}_N & z^{-\lfloor L_p/N \rfloor}\mathbf{I}_R \\ & & & & \mathbf{0}_{(N-R)\times R} \end{bmatrix}^T \\ &= \mathbf{p}\mathbf{L}_1(z) \end{aligned} \tag{4.6}$$

where $\mathbf{L}_1(z)$ has dimensions $L_p \times N$, $R = \mathrm{mod}_N(L_p)$, and $\mathbf{p}$ is a $1 \times L_p$ vector consisting of the prototype filter impulse response coefficients. $\mathbf{L}_1(z)$ is referred to as the *polyphase delay matrix* since it consists of identity matrices multiplied by elements of the form z^{-k} with $k = 0, 1, \ldots, \lfloor L_p/N \rfloor$, and where k is appropriately chosen to reflect the delay attributed to the impulse response coefficients in each of the polyphase components. For example, consider the polyphase transfer functions illustrated in equation (2.19). In this case, $\mathbf{L}_1(z)$ multiplies the impulse response coefficients $p[l]$, for $l = 0, 1, \ldots, 11$, by the

[1] Note that $\mathrm{mod}_a(b) = \mathrm{modulus}(b / a)$

appropriate elements z^{-k}, for $k = 0, 1, \ldots, 3$, in order to generate the polyphase filter transfer functions $E_0(z)$, $E_1(z)$, and $E_2(z)$.

Combining equations (4.5) and (4.6) results in a generalized factorization of the polyphase analysis transfer matrix for O-MFBs that exploits redundancies in the modulation. This factorization is given by

$$\begin{aligned} \mathbf{H}(z) &= \mathbf{T}\mathbf{L}_2\mathbf{P}\mathbf{L}_1(z) \\ &= \mathbf{T}\mathbf{E}(z) \end{aligned} \tag{4.7}$$

where $\mathbf{T}$ is the $M \times K$ *modulation matrix* defined as $\mathbf{T} = [\tilde{\mathbf{t}}_0 \quad \tilde{\mathbf{t}}_1 \quad \cdots \quad \tilde{\mathbf{t}}_{K-1}]^T$, $\mathbf{L}_2$ is the $K \times L_p$ redundancy matrix, $\mathbf{P}$ is the L_p x L_p prototype filter coefficient matrix, and $\mathbf{L}_1(z)$ is the $L_p \times N$ polyphase delay matrix. Furthermore, if it is further necessary to multiply any of the subband filter transfer functions $H_k(z)$ in $\mathbf{H}(z)$ by an additional element z^{-k}, then a *subband filter delay matrix* $\mathbf{D}(z)$ can be applied, which would result in the factorization

$$\mathbf{H}(z) = \mathbf{D}(z)\mathbf{T}\mathbf{E}(z) \tag{4.8}$$

where $\mathbf{D}(z)$ is a diagonal matrix with elements z^{-k} located on the diagonal and where $k \geq 0$.

To illustrate this factorization, consider an odd-stacked oversampled DFT-MFB with $M = 4$, $N = 2$, and $L_p = 8$. The prototype filter coefficient matrix is given by

$$\mathbf{P} = \begin{bmatrix} p[0] & & & \\ & p[1] & & \\ & & \ddots & \\ & & & p[7] \end{bmatrix}$$

where $p[l]$ are the coefficients of the prototype filter impulse response for $l = 0, 1, \ldots, 7$. The kth analysis subband filter impulse response is derived by multiplying a modulation vector $\mathbf{t}_k$ by $\mathbf{P}$. For the odd-stacked DFT-M case, the coefficients of the kth modulation vector are given by

$$t_k[l] = e^{j2\pi(k-0.5)l/M}$$

for $l = 0, 1, \ldots, 7$. However, this transform has only M unique modulation coefficients for each channel k, resulting in the efficient modulation vector $\tilde{\mathbf{t}}_k$ with elements $\tilde{t}_k[l] = t_k[l]$ for $l = 0, 1, \ldots, 3$. In order to exploit this redundancy, $\tilde{\mathbf{t}}_k$ must be multiplied by the redundancy matrix

$$\mathbf{L}_2 = [\mathbf{I}_4 \quad \mathbf{I}_4]$$

which would result in the factorization

$$h_k[n] = [\tilde{t}_k[0] \quad \tilde{t}_k[1] \quad \tilde{t}_k[2] \quad \tilde{t}_k[3]][\mathbf{I}_4 \quad \mathbf{I}_4] \begin{bmatrix} p[0] & & & \\ & p[1] & & \\ & & \ddots & \\ & & & p[7] \end{bmatrix}$$

Finally, the polyphase delay matrix is given by

$$\mathbf{L}_1(z) = \begin{bmatrix} 1 & z^{-1} & z^{-2} & z^{-3} \\ 1 & z^{-1} & z^{-2} & z^{-3} \end{bmatrix}^T$$

and the modulation matrix is

$$\mathbf{T} = \begin{bmatrix} \tilde{\mathbf{t}}_0 \\ \tilde{\mathbf{t}}_1 \\ \tilde{\mathbf{t}}_2 \\ \tilde{\mathbf{t}}_3 \end{bmatrix} = \begin{bmatrix} \tilde{t}_0[0] & \tilde{t}_0[1] & \tilde{t}_0[2] & \tilde{t}_0[3] \\ \tilde{t}_1[0] & \tilde{t}_1[1] & \tilde{t}_1[2] & \tilde{t}_1[3] \\ \tilde{t}_2[0] & \tilde{t}_2[1] & \tilde{t}_2[2] & \tilde{t}_2[3] \\ \tilde{t}_3[0] & \tilde{t}_3[1] & \tilde{t}_3[2] & \tilde{t}_3[3] \end{bmatrix}$$

where $\tilde{t}_k[j]$ represents the jth coefficient of the kth efficient transformation vector. This results in the efficient analysis polyphase transfer matrix factorization

$$\begin{aligned} \mathbf{H}(z) &= \begin{bmatrix} \tilde{t}_0[0] & \tilde{t}_0[1] & \tilde{t}_0[2] & \tilde{t}_0[3] \\ \tilde{t}_1[0] & \tilde{t}_1[1] & \tilde{t}_1[2] & \tilde{t}_1[3] \\ \tilde{t}_2[0] & \tilde{t}_2[1] & \tilde{t}_2[2] & \tilde{t}_2[3] \\ \tilde{t}_3[0] & \tilde{t}_3[1] & \tilde{t}_3[2] & \tilde{t}_3[3] \end{bmatrix} [\mathbf{I}_4 \quad \mathbf{I}_4] \begin{bmatrix} p[0] & & & \\ & p[1] & & \\ & & \ddots & \\ & & & p[7] \end{bmatrix} \begin{bmatrix} 1 & & & \\ & 1 & & \\ z^{-1} & & & \\ & z^{-1} & & \\ & & z^{-2} & \\ & & & z^{-2} \\ z^{-3} & & & \\ & z^{-3} & & \end{bmatrix} \\ &= \begin{bmatrix} \tilde{t}_0[0] & \tilde{t}_0[1] & \tilde{t}_0[2] & \tilde{t}_0[3] \\ \tilde{t}_1[0] & \tilde{t}_1[1] & \tilde{t}_1[2] & \tilde{t}_1[3] \\ \tilde{t}_2[0] & \tilde{t}_2[1] & \tilde{t}_2[2] & \tilde{t}_2[3] \\ \tilde{t}_3[0] & \tilde{t}_3[1] & \tilde{t}_3[2] & \tilde{t}_3[3] \end{bmatrix} \begin{bmatrix} p[0] - z^{-2}p[4] & 0 \\ 0 & p[1] - z^{-2}p[5] \\ z^{-1}p[2] - z^{-3}p[6] & 0 \\ 0 & z^{-1}p[3] - z^{-3}p[7] \end{bmatrix} \\ &= \mathbf{TE}(z) \end{aligned}$$

It is not necessary to further multiply any of the k channels by additional elements z^{-k}, hence, $\mathbf{D}(z)$ is simply an $M \times M$ identity matrix, resulting in the factorization

$$\mathbf{H}(z) = \mathbf{D}(z)\mathbf{TE}(z)$$

where $\mathbf{D}(z) = \mathbf{I}_M$.

The analysis polyphase transfer matrix $\mathbf{E}(z)$ consists of the Z-transforms of the elements $e_{i,j}[n]$, for $i = 0, 1, \ldots, M-1$ and $j = 0, 1, \ldots, K-1$. Each element $\mathbf{E}_{i,j}(z)$ is the jth K-spaced polyphase filter transfer function of the ith analysis subband filter and can be labeled $z^{-k}E_i(z^l)$ for $i = 0, 1, \ldots, K-1$. Depending on M and N, matrix $\mathbf{E}(z)$ resulting from the factorization of equation (4.7) assumes one of three possible forms as shown in [44]:

Form 1. *M is a multiple of N*:

If M is a multiple of N, $\mathbf{E}(z)$ tends to be sparse, with only one element in each row. These elements tend to form vertically stacked diagonal matrices. For example, if $M = 6$, $N = 3$, and $K = 6$, $\mathbf{E}(z)$ assumes the form

$$\mathbf{E}(z) = \begin{bmatrix} E_0(z^2) & 0 & 0 \\ 0 & E_1(z^2) & 0 \\ 0 & 0 & E_2(z^2) \\ z^{-1}E_3(z^2) & 0 & 0 \\ 0 & z^{-1}E_4(z^2) & 0 \\ 0 & 0 & z^{-1}E_5(z^2) \end{bmatrix}$$

Form 2. *M and N are coprime*:

If M and N are coprime, $\mathbf{E}(z)$ is dense. For example, if $M = 3$, $N = 2$, and $K = 6$, $\mathbf{E}(z)$ assumes the form

$$\mathbf{E}(z) = \begin{bmatrix} E_0(z^3) & z^{-1}E_3(z^3) \\ z^{-2}E_4(z^3) & E_1(z^3) \\ z^{-1}E_2(z^3) & z^{-2}E_5(z^3) \end{bmatrix}$$

Form 3. *Neither Form 1 nor Form 2*:

For any other relation between M and N, $\mathbf{E}(z)$ has diagonal rows. For example, if $M = 6$, $N = 4$, and $K = 12$, $\mathbf{E}(z)$ assumes the form

$$\mathbf{E}(z)=\begin{bmatrix} E_0(z^3) & 0 & z^{-1}E_6(z^3) & 0 \\ 0 & E_1(z^3) & 0 & z^{-1}E_7(z^3) \\ z^{-2}E_8(z^3) & 0 & E_2(z^3) & 0 \\ 0 & z^{-2}E_9(z^3) & 0 & E_3(z^3) \\ z^{-1}E_4(z^3) & 0 & z^{-2}E_{10}(z^3) & 0 \\ 0 & z^{-1}E_5(z^3) & 0 & z^{-2}E_{11}(z^3) \end{bmatrix}$$

The allowable length of $p[n]$ is influenced by the form of $\mathbf{E}(z)$ since all of the polyphase filter impulse responses $e_i[n]$ must be of equal length. Slight changes to the allowable lengths of $p[n]$ may be obtained for arbitrary modulation and stacking types by following the procedure outlined in [70] for the odd-stacked DFT-M case. Forms 1 and 3 of $\mathbf{E}(z)$ are sparse; however, by pre- and post-multiplication with appropriate permutation matrices $\mathbf{P}$ and $\mathbf{Q}$ a block diagonal matrix $\mathbf{S}(z)$ is generated consisting of g rectangular matrices, i.e.,

$$\mathbf{S}(z)=\mathbf{P}\mathbf{E}(z)\mathbf{Q}=\begin{bmatrix} \mathbf{S}_0(z) & & 0 \\ & \ddots & \\ 0 & & \mathbf{S}_{g-1}(z) \end{bmatrix} \tag{4.9}$$

where $\mathbf{S}_i(z)$ are $S \times T$ polynomial matrices and $g = \gcd(M, N)$. For example, in the Form 3 case with $M = 6$ and $N = 4$, applying the permutation matrices

$$\mathbf{P}=\begin{bmatrix} 1 & 0 & 0 & 0 & 0 & 0 \\ 0 & 0 & 0 & 0 & 1 & 0 \\ 0 & 0 & 1 & 0 & 0 & 0 \\ 0 & 1 & 0 & 0 & 0 & 0 \\ 0 & 0 & 0 & 0 & 0 & 1 \\ 0 & 0 & 0 & 1 & 0 & 0 \end{bmatrix}$$

and

$$\mathbf{Q}=\begin{bmatrix} 1 & 0 & 0 & 0 \\ 0 & 0 & 1 & 0 \\ 0 & 1 & 0 & 0 \\ 0 & 0 & 0 & 1 \end{bmatrix}$$

results in the factorization

$$\mathbf{S}(z)=\begin{bmatrix} E_0(z^3) & z^{-1}E_6(z^3) & 0 & 0 \\ z^{-1}E_4(z^3) & z^{-2}E_{10}(z^3) & 0 & 0 \\ z^{-2}E_8(z^3) & E_2(z^3) & 0 & 0 \\ 0 & 0 & E_1(z^3) & z^{-1}E_7(z^3) \\ 0 & 0 & z^{-1}E_5(z^3) & z^{-2}E_{11}(z^3) \\ 0 & 0 & z^{-2}E_9(z^3) & E_3(z^3) \end{bmatrix}$$

The rectangular matrices $\mathbf{S}_i(z)$ for $i = 0$ and $i = 1$ are subsequently given by

$$\mathbf{S}_0(z)=\begin{bmatrix} E_0(z^3) & z^{-1}E_6(z^3) \\ z^{-1}E_4(z^3) & z^{-2}E_{10}(z^3) \\ z^{-2}E_8(z^3) & E_2(z^3) \end{bmatrix}$$

and

$$\mathbf{S}_1(z)=\begin{bmatrix} E_1(z^3) & z^{-1}E_7(z^3) \\ z^{-1}E_5(z^3) & z^{-2}E_{11}(z^3) \\ z^{-2}E_9(z^3) & E_3(z^3) \end{bmatrix}$$

Each $\mathbf{S}_i(z)$ contains elements $z^{-k}E_i(z^l)$ where each k is not an integer factor of L. When relating the polyphase components in $\mathbf{S}_i(z)$ to the prototype filter coefficients it is necessary to ensure that each polyphase filter transfer function $z^{-k}E_i(z^l)$ includes elements z^{-k} where k is an integer multiple of L. In order to do this, each $\mathbf{S}_i(z)$ may need to be pre- and post-multiplied by appropriate diagonal delay/advance matrices, wherein an advance matrix $\mathbf{M}(z)$ consists of an identity matrix with appropriate elements z^k on the diagonal, and a delay matrix $\mathbf{N}(z)$ consists of an identity matrix with appropriate elements z^{-k} on the diagonal. Pre- and post-multiplying each $\mathbf{S}_i(z)$ by appropriate delay/advance matrices results in a factorization of the form

$$\hat{\mathbf{S}}_i(z) = \mathbf{M}_i(z)\mathbf{S}_i(z)\mathbf{N}_i(z) \tag{4.10}$$

where $\hat{\mathbf{S}}_i(z)$ is of size $S \times T$ and $\mathbf{M}_i(z)$ and $\mathbf{N}_i(z)$ are $S \times S$ and $T \times T$ diagonal matrices, respectively, with appropriate powers of z located on the diagonal. For the example outlined above, the appropriate matrices $\mathbf{M}_i(z)$ and $\mathbf{N}_i(z)$ are given by

$$\mathbf{M}_i(z) = \begin{bmatrix} z & 0 & 0 \\ 0 & z^2 & 0 \\ 0 & 0 & 1 \end{bmatrix}$$

and

$$\mathbf{N}_i(z) = \begin{bmatrix} z^{-1} & 0 \\ 0 & 1 \end{bmatrix}$$

which results in

$$\hat{\mathbf{S}}_0(z) = \begin{bmatrix} E_0(z^3) & E_6(z^3) \\ E_4(z^3) & E_{10}(z^3) \\ z^{-3}E_8(z^3) & E_2(z^3) \end{bmatrix}$$

and

$$\hat{\mathbf{S}}_1(z) = \begin{bmatrix} E_1(z^3) & E_7(z^3) \\ E_5(z^3) & E_{11}(z^3) \\ z^{-3}E_9(z^3) & E_3(z^3) \end{bmatrix}$$

Paraunitary Factorization

As discussed in Section 3.5, a PUFB is generated if the analysis bank transfer matrix $\mathbf{H}(z)$ satisfies the property

$$\tilde{\mathbf{H}}(z)\mathbf{H}(z) = cz^{-n_0}\mathbf{I}_M \tag{4.11}$$

and the synthesis bank transfer matrix $\mathbf{R}(z)$ is subsequently chosen as

$$\mathbf{R}(z) = cz^{-n_0}\tilde{\mathbf{H}}(z) \tag{4.12}$$

Considering the factorization of an O-MFB transfer matrix $\mathbf{E}(z)$ derived above, if an $S \times T$ rectangular matrix $\hat{\mathbf{S}}_i(z)$ is PU then $\mathbf{S}_i(z)$ is also PU since the diagonal matrices $\mathbf{M}_i(z)$ and $\mathbf{N}_i(z)$ are PU by definition. Furthermore, if a square matrix $\mathbf{S}(z)$ is PU then a subset of the columns of $\mathbf{S}(z)$ is also PU. This implies that if a square block diagonal matrix $\mathbf{S}(z)$ is generated with rectangular PU submatrices $\mathbf{S}_i(z)$, then $\mathbf{S}(z)$ is also PU [71]. If $\mathbf{S}(z)$ is PU then $\mathbf{E}(z)$ will also be PU since the permutation matrices $\mathbf{P}$ and $\mathbf{Q}$ are PU by

definition. Finally, if $\mathbf{E}(z)$ is PU then for DFT-MFBs, since $\mathbf{T}$ is PU (see, for example [20]), then $\mathbf{H}(z)$ is also PU. For DCT-MFBs, subject to the conditions of $\mathbf{E}(z)$ to be discussed in section 4.3, $\mathbf{H}(z)$ is also PU. Hence, in order to generate a PU matrix $\mathbf{H}(z)$ what remains is to find PU matrices $\hat{\mathbf{S}}_i(z)$.

As further discussed in section 3.5, it is well known that a square matrix $\mathbf{G}(z)$ of degree-C has the PU factorization

$$\mathbf{G}(z) = \mathbf{V}_C(z)\mathbf{V}_{C-1}(z)\ldots\mathbf{V}_1(z)\mathbf{R} \tag{4.13}$$

where each $\mathbf{V}_i(z)$ is a degree-1 PU building block and $\mathbf{R}$ is a unitary matrix that can be further factorized as a product of Householder matrices, i.e.,

$$\mathbf{R} = \mathbf{H}_S\mathbf{H}_{S-1}\mathbf{H}_1$$

Since a subset of the columns in a PU matrix are also PU, then an $S \times T$ ($S > T$) PU matrix can be extracted from an $S \times S$ PU matrix. In practice, an $S \times T$ PU matrix $\hat{\mathbf{S}}_i(z)$ can be extracted from an $S \times S$ PU matrix $\mathbf{G}(z)$. Furthermore, $\mathbf{G}(z)$ can be generated by forming a product of degree-1 PU matrices $\mathbf{V}_i(z)$ and Householder matrices $\mathbf{H}_i$, respectively. The generalized factorization of a PU transfer matrix $\mathbf{E}(z)$ derived from an O-MFB is therefore given by

$$\mathbf{E}(z) = \mathbf{P}^T \operatorname{diag}\left(\mathbf{M}_i^T(z)\mathbf{S}_i(z)\mathbf{N}_i^T\right)\mathbf{Q}^T \tag{4.14}$$

for $i = 1, 2, \ldots, g-1$ where each $\mathbf{S}_i(z)$ is extracted from $\mathbf{G}(z)$, i.e.,

$$[\mathbf{G}(z)]_{S\times S} = \left[\mathbf{S}_i(z)_{S\times T} \quad \mathbf{0}_{S\times(S-T)}\right] \tag{4.15}$$

4.2 DFT Modulation

DFT-MFBs derive the analysis and synthesis subband filter impulse responses by multiplying an analysis and synthesis prototype filter impulse response by the DFT. Since DFT modulation is basically a multiplication with an exponential function, imaginary signal representations are typically encountered even for real-valued input signals. If certain conditions are imposed on the number of channels M, then a very fast implementation of the DFT, such as the FFT, can be employed. Two classes of DFT modulation have been proposed in the literature, namely even- and odd-stacked DFT modulations. In either case, it is not possible to obtain subband filters with linear phase.

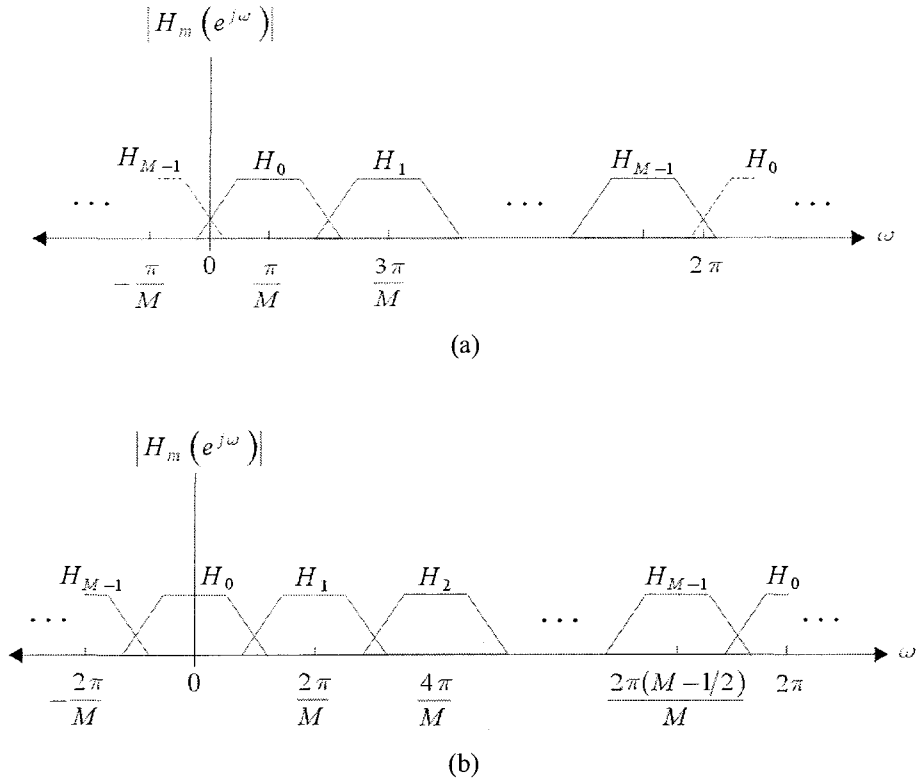

Figure 18. *Amplitude response of the subband filters in an M-channel DFT-modulated filter bank. (a) Odd-stacked case. (b) Even-stacked case.*

In an M-channel DFT-MFB the subbands are centered about the frequencies $\omega_k = \pm 2\pi(k+1/2)/M$ for the odd-stacked case and $\omega_k = \pm 2\pi k/M$ for the even-stacked case, with $k = 0, 1, \ldots, M-1$. The amplitude response of the subband filters in both an odd-stacked DFT-MFB and an even-stacked DFT-MFB are illustrated in figure 18. The subband filter impulse responses are generated by multiplying the analysis and synthesis prototype filter impulse responses with the appropriate exponential function. In the odd-stacked case the analysis and synthesis subband filter impulse responses are given by

$$h_k[n] = p[n] W_M^{-(k+1/2)n} \tag{4.16}$$

and

$$f_k[n] = q[n] W_M^{-(k+1/2)n} \tag{4.17}$$

respectively. In the even-stacked case the analysis and synthesis subband filter impulse responses are given by

$$h_k[n] = p[n]W_M^{-kn} \tag{4.18}$$

and

$$f_k[n] = q[n]W_M^{-kn} \tag{4.19}$$

respectively. In both cases, $k = 0, 1, \ldots, M-1$, $W_M = e^{j2\pi/M}$ and $p[n]$ and $q[n]$ are the analysis and synthesis prototype filter impulse responses of length L_p and L_q, respectively. The analysis bank transfer matrix can be factorized as $\mathbf{H}(z) = \mathbf{D}(z)\mathbf{T}\mathbf{L}_2\mathbf{P}\mathbf{L}_1(z) = \mathbf{D}(z)\mathbf{T}\mathbf{E}(z)$ as outlined in section 4.1. The modulation matrix $\mathbf{T}$ for an odd- or even-stacked oversampled DFT-MFB consists of a $M \times M$ DFT matrix with elements derived from the modulation sequences in equations (4.16) and (4.18), respectively. Exploiting redundancies in the modulation matrix results in $\mathbf{L}_2$ consisting of the identity matrices $\mathbf{A}_K = \mathbf{I}_M$ in the odd-stacked case and $\mathbf{A}_K = [\mathbf{I}_M \ -\mathbf{I}_M]$ in the even-stacked case. In either case, no additional multiplication by z^{-k} on the subband filter transfer functions is necessary, resulting in $\mathbf{D}(z) = \mathbf{I}_M$.

The analysis bank polyphase transfer matrix $\mathbf{E}(z)$ assumes three possible forms as described in section 4.1. If L_p is an integer factor of M, $\mathbf{E}(z)$ assumes Form 1. If L_p is an integer factor of MN or MN/g, $\mathbf{E}(z)$ assumes either Forms 2 or 3, respectively, where $g = \gcd(M,N)$.

Paraunitary Solution

In OFBs, multiple left-inverses of the analysis bank transfer matrix $\mathbf{H}(z)$ exist for the generation of a synthesis bank transfer matrix $\mathbf{F}(z)$. One elegant solution can be derived from the Smith form decomposition of $\mathbf{H}(z)$. Considering the Smith form decomposition of the left inverse of $\mathbf{H}(z)$, shown in equation (3.23), we see that if the arbitrary polynomial matrix $\mathbf{X}(z)$ is vacuous then the left-inverses of $\mathbf{H}(z)$ are given by $\mathbf{F}(z) = \mathbf{Q}^{-1}(z)\mathbf{D}^{-1}(z)\mathbf{P}^{-1}(z) = \mathbf{H}^{-1}(z)$. Furthermore, imposing $\mathbf{Q}(z) = \mathbf{D}_1(z) = \mathbf{I}_N$ and $\mathbf{P}^{-1}(z) = \tilde{\mathbf{P}}(z)$ results in $\mathbf{H}^{-1}(z) = \mathbf{F}(z) = \mathbf{P}^{-1}(z) = \tilde{\mathbf{P}}(z)$, which implies that $\mathbf{H}(z)$ is PU.

The efficient factorization of $\mathbf{H}(z)$ for O-MFBs as derived in section 4.1 is given by $\mathbf{H}(z) = \mathbf{T}\mathbf{E}(z)$. If the PU property is imposed on $\mathbf{H}(z)$, then the inverse of $\mathbf{H}(z)$ is expressed as $\mathbf{F}(z) = \tilde{\mathbf{H}}(z) = \tilde{\mathbf{E}}(z)\tilde{\mathbf{T}}$. Noting that $\tilde{\mathbf{T}} = \mathbf{T}^{-1}$, the synthesis bank transfer matrix factorization is then expressed as $\mathbf{F}(z) = \tilde{\mathbf{E}}(z)\mathbf{T}^{-1}$. This implies that the inverse DFT (IDFT) can be applied in the synthesis bank, the synthesis prototype filter impulse response is equal to the analysis prototype filter impulse response, i.e.,

$q[n] = p[n]$, and the synthesis subband filter impulse responses are paraconjugates of the analysis subband filter impulse responses, i.e., $f_k[n] = h_k^*[L_p - n]$.

4.3 Cosine Modulation

CMFBs derive the analysis and synthesis subband filter impulse responses by multiplying an analysis and synthesis prototype filter impulse response by the DCT. Since DFT modulation is essentially a multiplication with an exponential function, imaginary signal representations are typically encountered even for real-valued input signals. With the DCT modulation, however, appropriate pairs of exponential functions are combined, resulting in a real-value modulation transform. If certain conditions are imposed on the number of subbands and the length of the subband filters, very fast implementations of the DCT can be employed. Two classes of CMFBs have been proposed in the literature, namely even- and odd-stacked CMFBs. Odd-stacked CMFBs are similar to DFT-MFBs in that it is not possible to generate subband filters with linear phase. Even-stacked CMFBs, on the other hand, are unique in that they are defined using two FBs, resulting in a total of $2M$ bands, and can generate subband filters with linear phase.

4.3.1 Odd-Stacked Cosine-Modulated Filter Banks

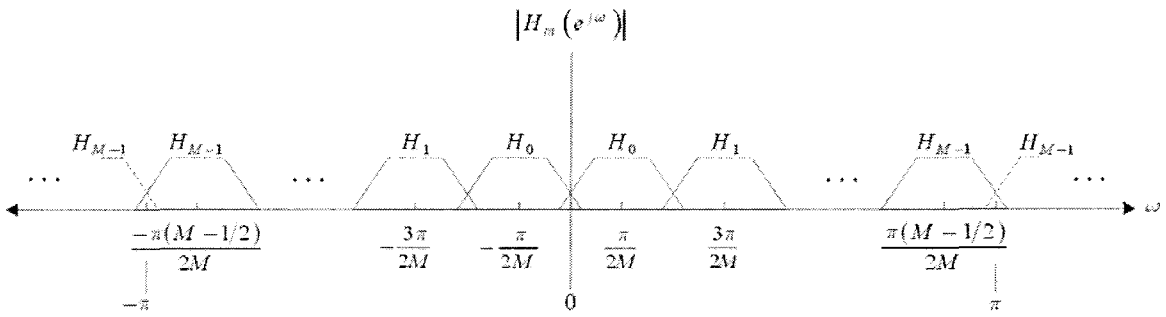

Figure 19. *Amplitude response of the subband filters in an M-channel odd-stacked cosine-modulated filter bank.*

In M-channel odd-stacked CMFBs, the subbands are centered about the frequencies $\omega_k = \pm\pi(k+1/2)/M$, as illustrated in figure 19. The subband filter impulse responses are generated by multiplying the analysis and synthesis prototype filter impulse responses with the appropriate modulation sequence, and are given by

$$h_k[n] = 2p[n]\cos\left[\frac{\pi}{M}\left(k+\frac{1}{2}\right)\left(n-\frac{L_p-1}{2}\right)+(-1)^k\left(\frac{\pi}{4}\right)\right] \tag{4.20}$$

and

$$f_k[n] = 2q[n]\cos\left[\frac{\pi}{M}\left(k+\frac{1}{2}\right)\left(n-\frac{L_p-1}{2}\right)-(-1)^k\left(\frac{\pi}{4}\right)\right] \tag{4.21}$$

respectively. In this case, $k = 0, 1, \ldots, M-1$ and $p[n]$ and $q[n]$ are the analysis and synthesis prototype filter impulse responses of length L_p and L_q, respectively. The analysis bank transfer matrix can be factorized as $\mathbf{H}(z) = \mathbf{D}(z)\mathbf{T}\mathbf{L}_2\mathbf{P}\mathbf{L}_1(z) = \mathbf{D}(z)\mathbf{T}\mathbf{E}(z)$, as outlined in section 4.1. The modulation matrix $\mathbf{T}$ consists of an $M \times 2M$ DCT matrix with elements derived from the modulation sequence in equation (4.20). Exploiting redundancies in the modulation matrix results in $\mathbf{L}_2$ consisting of the identity matrices $\mathbf{A}_K = [\mathbf{I}_{2M} \ -\mathbf{I}_{2M}]$. No additional multiplication by z^{-k} on the subband filter transfer functions is necessary, resulting in $\mathbf{D}(z) = \mathbf{I}_M$.

Paraunitary Solution

In OFBs, multiple left-inverses of the analysis bank transfer matrix $\mathbf{H}(z)$ exist for the generation of a synthesis bank transfer matrix $\mathbf{F}(z)$. One possible solution to finding an $\mathbf{F}(z)$ that results in PR is to impose the PU property on $\mathbf{H}(z)$. Contrary to the PU solution of oversampled DFT-MFBs which relies on the existence of the IDFT, the DCT is singular, hence non-invertible. It is therefore necessary to perform further analysis in order to determine the conditions $H_k(z)$ and $F_k(z)$ must meet in order to achieve PR. One such analysis is performed through the factorization of the analysis and synthesis polyphase transfer matrices as described in [47]. This analysis shows that in order to obtain PU PR CMFBs the following conditions on $P(z)$ must be met:

PR Condition #1:

$$\sum_{l=0}^{2L-1} P_{k+lN}(z)\tilde{P}_{k+lN}(z) = \frac{1}{2N}$$

for $k = 0, 1, \ldots, \lfloor N/2 \rfloor - 1$.

PR Condition #2:

$$P_{k+lN}(z)\tilde{P}_{k+lN+M}(z) - P_{k+lN+M}(z)\tilde{P}_{k+lN}(z) = 0$$

for $k = 0, 1, \ldots, N-1$ and $l = 0, 1, \ldots, L-1$. In both PR conditions, $P_i(z)$ is the ith $2M$-spaced Type-1 polyphase component of the analysis prototype filter. PR Condition #2 can be satisfied by imposing linear phase on the analysis prototype filter and assigning $q[n] = p^*[L_p - n]$. PR Condition #1 can be satisfied by restricting $\mathbf{E}(z)$ to assume Form 1. For a Form 1 factorization the columns of $\mathbf{E}(z)$ form the polyphase components given by $P_{k+lN}(z)$ in PR Condition #1. If $\mathbf{E}(z)$ is PU then the columns of $\mathbf{E}(z)$ will also be PU, ensuring that the requirements of PR Condition #1 are satisfied. Restricting $\mathbf{E}(z)$ to assume Form 1 further restricts L_p to be an integer multiple of $2M$.

4.3.2 Even-Stacked Cosine-Modulated Filter Banks

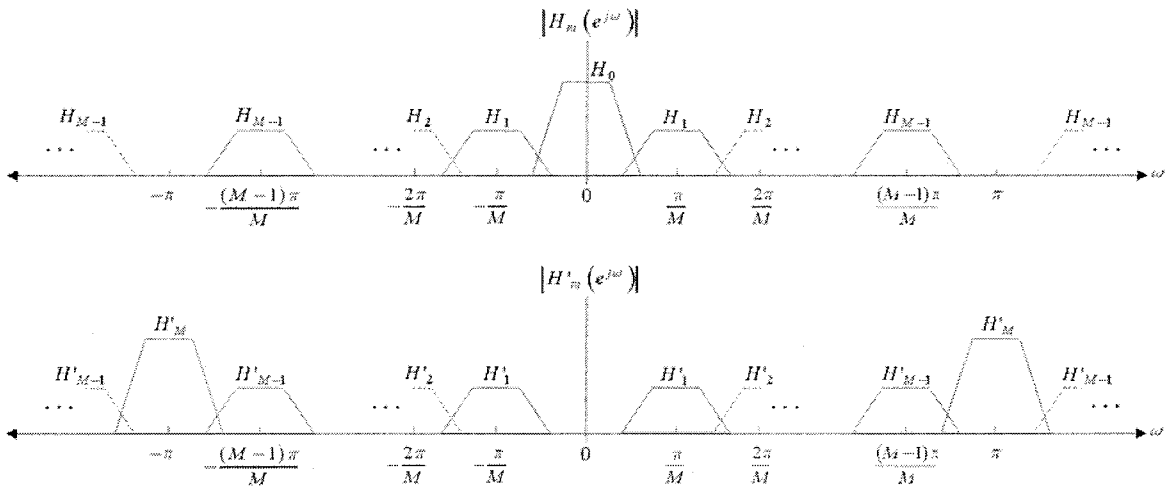

Figure 20. *Amplitude response of the two banks of subband filters in a 2M-channel even-stacked cosine-modulated filter bank.*

Unlike DFT-MFBs and odd-stacked CMFBs, the $2M$-channel even-stacked CMFB consists of two FBs containing M subband filters each. In the first FB the subbands are centered about the frequencies $\omega_k = \pm\pi k/M$ with an additional band at $\omega_k = 0$. The second FB consists of subbands centered about the frequencies $\omega_k = \pm\pi k/M$ with an additional band at $\omega_k = \pi$. The amplitude response of these two banks is illustrated in figure 20. The subband filter impulse responses are generated by multiplying the analysis and

synthesis prototype filter impulse responses with the appropriate modulation sequence. The analysis and synthesis subband filter impulse responses for the first bank are given by

$$h_k[n] = \rho_k p[n] \cos\left[\frac{\pi}{M} k\left(n - \frac{L_p - 1 + M}{2}\right)\right] \tag{4.22}$$

and

$$f_k[n] = \rho_k q[n - M] \cos\left[\frac{\pi}{M} k\left(n - M - \frac{L_p - 1 - M}{2}\right)\right] \tag{4.23}$$

respectively, for $k = 0, 1, \ldots, M-1$. Those for the second bank are given by

$$h_k'[n] = \rho_k p[n - M] \sin\left[\frac{\pi}{M} k\left(n - M - \frac{L_p - 1 + M}{2}\right)\right] \tag{4.24}$$

and

$$f_k'[n] = -\rho_k q[n] \sin\left[\frac{\pi}{M} k\left(n - \frac{L_p - 1 - M}{2}\right)\right] \tag{4.25}$$

respectively, for $k = 1, 2, \ldots, M$. In both banks, $p[n]$ and $q[n]$ are the analysis and synthesis prototype filter impulse responses of length L_p and L_q, respectively, $\rho_k = \sqrt{2}$ if $k = 0$ or M, and $\rho_k = 2$ for all other k. The analysis bank transfer matrix can be factorized as $\mathbf{H}(z) = \mathbf{D}(z)\mathbf{T}\mathbf{L}_2\mathbf{P}\mathbf{L}_1(z) = \mathbf{D}(z)\mathbf{T}\mathbf{E}(z)$ as outlined in section 4.1. The modulation matrix $\mathbf{T}$ is given by $\mathbf{T} = [\mathbf{C} \quad \mathbf{S}]^T$, where $\mathbf{C}$ is an $M \times 2M$ DCT matrix with elements derived from the modulation sequence in equation (4.22) and $\mathbf{S}$ is an $M \times 2M$ discrete sine transform (DST) matrix with elements derived from the modulation sequence in equation (4.24). Exploiting redundancies in the modulation matrix results in $\mathbf{L}_2$ consisting of the identity matrices $\mathbf{A}_K = \mathbf{I}_{2M}$. In even-stacked CMFBs it is necessary to multiply the second bank of subband filter transfer functions by z^{-M}, resulting in

$$\mathbf{D}(z) = \begin{bmatrix} \mathbf{I}_M & \\ & z^{-M}\mathbf{I}_M \end{bmatrix} \tag{4.26}$$

Paraunitary Solution

The derivation of the conditions that $H_k(z)$ and $F_k(z)$ must meet in order to achieve PR in even-stacked O-CMFBs is similar to the derivation for odd-stacked O-CMFBs. An analysis on the factorization of the $2M$-

channel analysis and synthesis polyphase transfer matrices is given in Appendix A.2. This analysis shows that in order to attain PR, the PR conditions for odd-stacked O-CMFB must be satisfied. For the even-stacked case, PR condition #2 can be satisfied by imposing linear phase on the prototype filter and assigning $q[n] = p^*[L_p - n]$. PR Condition #1 can be satisfied by ensuring an odd oversampling ratio L and restricting $\mathbf{E}(z)$ to assume Form 1. Forcing $\mathbf{E}(z)$ to assume Form 1 further restricts L_p to be an integer multiple of $2M$.

4.4 Summary and Conclusions

O-MFBs were studied. In section 4.1, a generalized factorization for O-MFB transfer matrices with arbitrary modulation was reviewed. This factorization is particularly efficient since it directly relates the prototype filter coefficients to the modulation transform while exploiting redundancies in the modulation matrix. The matrix $\mathbf{E}(z)$ resulting from this factorization was shown to assume three possible forms. Based on the form of $\mathbf{E}(z)$, a method for manipulating $\mathbf{E}(z)$ into a block diagonal matrix $\mathbf{S}_i(z)$ with submatrices denoted by $\hat{\mathbf{S}}_i(z)$ was then proposed. Following manipulation of $\mathbf{E}(z)$ into submatrices $\hat{\mathbf{S}}_i(z)$, it was then shown that if each $\hat{\mathbf{S}}_i(z)$ is PU then $\mathbf{E}(z)$ is also PU.

In section 4.2, DFT-MFBs were taken into consideration. The specific form that $\mathbf{D}(z)$, $\mathbf{T}$, and $\mathbf{L}_2$ must assume for the transfer matrix factorization of both odd and even-stacked DFT-MFBs was presented. By analyzing the PU factorization of $\mathbf{H}(z)$, the conditions on $\mathbf{H}(z)$, $q[n]$, and $f_k[n]$ were derived in order for PU factorizations of $\mathbf{H}(z)$ to be obtained.

In section 4.3, CMFBs were taken into consideration. The specific form that $\mathbf{D}(z)$, $\mathbf{T}$, and $\mathbf{L}_2$ must assume for the transfer matrix factorization of both odd- and even-stacked CMFBs was presented. By analyzing $\mathbf{E}(z)$ the conditions on $P(z)$ required for PR were derived. Finally, the conditions on $\mathbf{E}(z)$, $p[n]$, and $q[n]$ were derived in order for PU factorizations of $\mathbf{H}(z)$ to be obtained.

Chapter 5

Lifting-Based Implementation

PR in an FB is classically defined as reconstructing an input signal at the output of the FB such that it is free of linear distortion such as aliasing, amplitude, and phase distortion in the absence of subband processing. Conditions that must necessarily be imposed on the subband filters in order to eliminate these types of distortion in multirate FBs have been derived in section 3.4. Non-linear distortion, however, such as that due to quantization of the subband filter coefficients, the truncation of intermediate results, and the processing of overflows in intermediate operations, has yet to be taken into consideration. Direct implementations of multirate FBs tend to be susceptible to non-linear distortion, which results in a loss of the PR property when considering practical implementations of FBs. Thus, implementations that are resilient to non-linear distortion are highly desirable.

Lifting-based structures, also known as ladder structures, constitute a particular form of the well-known lattice structure. Single-rate lattice structures are known to have low sensitivity to coefficient quantization for digital filter implementations. In multirate systems, lattice structures have more recently been used in FB implementations that are resilient to distortion caused by quantization of the subband filter coefficients. Lattice structures also ease the design of multirate FBs by reducing the number of parameters required for optimization thereby facilitating the application of unconstrained optimization algorithms. In addition to this, they also offer a modular structure wherein the order of the FB can be incremented by simply cascading low-order lattice building blocks. Since lifting-based implementations are a particular form of lattice structures, they share all of the properties of lattice structures in addition to providing some of their own desirable properties such as resilience to non-linear distortion caused by intermediate processing.

Lifting-based structures are a special type of lattice-structure wherein the low-order building blocks are generated using only Type-3 elementary matrix operations. In addition to being resilient to the distortion caused by quantization of the subband filter coefficients, this structure is also resilient to the distortion

caused by the truncation of intermediate results and the processing of overflows during intermediate operations. This results in an implementation that provides PR in the sense of eliminating both linear *and* non-linear distortion. Since PR is structurally-inherent in spite of coefficient quantization, the design of integer- or dyadic-coefficient FBs is facilitated. By quantizing the filter coefficients to integer or dyadic values, implementations on microprocessors using fast integer arithmetic or multiplierless hardware is made possible.

In section 5.1, the fundamental structure of a lifting-based implementation is provided. Included is a mathematical analysis on the factorization of rectangular and square PU matrices as well as an FB analysis for understanding the relationship between the lifting-based factorization and the lifting-based structure used in FB implementations. In section 5.2, the lifting-based factorization is applied to derive a lifting-based structure for oversampled PU MFBs. Oversampled DFT-MFBs and CMFBs of both even- and odd-stacking types are taken into consideration, followed by a discussion on the insertion of zeros resulting from particular cases of the proposed factorization.

5.1 Fundamental Structure

The fundamental structure of lifting-based implementations is derived by performing a Smith form decomposition on polynomial matrices. This factorization is first performed for arbitrary square polynomial matrices followed by a generalization to arbitrary rectangular polynomial matrices. The square matrix factorization leads to a PU factorization that can be applied to both square and rectangular PU matrices. Section 5.1 concludes with a discussion regarding the relation between lifting-based factorizations of polynomial matrices and lifting-based structures for FB implementations.

5.1.1 Analysis of Lifting-based Structures

A mathematical analysis of lifting-based structures provides a framework for the generation of such structures and is essential in order to derive factorizations and design methods for lifting-based FB implementations. An existing algorithm for deriving lifting-based factorizations of square polynomial matrices proposed in [30] is reviewed, followed by a presentation of the PU lifting-based factorization of square polynomial matrices. A similar factorization is then derived for rectangular polynomial matrices, followed by a factorization of PU rectangular polynomial matrices.

Square Matrix Factorization

Consider an $M \times M$ polynomial matrix $\mathbf{H}(z)$ with $\det(\mathbf{H}(z)) = z^{-k}$ where k is a positive integer and each element $\mathbf{H}_{i,j}(z)$ is a Laurent polynomial. Applying the Smith form decomposition outlined in section 3.3 results in the factorization

$$\mathbf{H}(z) = \mathbf{P}(z)\mathbf{D}(z)\mathbf{Q}(z) \tag{5.1}$$

where $\mathbf{P}(z)$ and $\mathbf{Q}(z)$ are unimodular polynomial matrices of dimensions $M \times M$ and $N \times N$, respectively, and $\mathbf{D}(z)$ is an $M \times M$ polynomial matrix referred to as the Smith form of $\mathbf{H}(z)$. Recall that $\mathbf{P}(z)$ and $\mathbf{Q}(z)$ take on one of three types of elementary matrix operations; Type-1, the interchanging of rows or columns, Type-2, the multiplication of a row or column by a nonzero constant, or Type-3, the addition of a row or column to another row or column multiplied by an arbitrary Laurent polynomial.

The lifting-based factorization of $\mathbf{H}(z)$ is given by

$$\mathbf{H}(z) = \mathbf{L}(z)\mathbf{D}(z)\mathbf{U}(z) \tag{5.2}$$

where $\mathbf{D}(z)$ is a diagonal matrix with polynomials on the diagonal and $\mathbf{L}(z)$ and $\mathbf{U}(z)$ are products of $M \times M$ Type-3 elementary matrix operations, i.e.,

$$\mathbf{L}(z) = \prod_{k=0}^{p} \mathbf{L}_k(z)$$

and

$$\mathbf{U}(z) = \prod_{k=0}^{q} \mathbf{U}_k(z)$$

where p and q have integer values greater than or equal to zero. Furthermore,

$$\mathbf{L}_k(z) = \begin{bmatrix} 1 & & & \\ & 1 & & A_k(z) \\ & & \ddots & \\ & & & 1 \\ & & & & 1 \end{bmatrix}$$

and

$$\mathbf{U}_k(z) = \begin{bmatrix} 1 & & & \\ & 1 & & \\ & & \ddots & \\ & B_k(z) & & 1 \\ & & & & 1 \end{bmatrix}$$

where $A_k(z)$ and $B_k(z)$ are arbitrary Laurent polynomials. By restricting the factorization to consist of only Type-3 elementary operations, $\mathbf{L}(z)$ and $\mathbf{U}(z)$ result in $M \times M$ and $N \times N$ lower and upper triangular polynomial matrices, respectively, where $\mathbf{L}_k(z)$ correspond to Gaussian eliminations and $\mathbf{U}_k(z)$ correspond to lifting steps. Furthermore, an algorithm referred to as the *Monic Euclidean Algorithm* has been developed in [30] which shows that by careful choice of $\mathbf{L}_k(z)$ and $\mathbf{U}_k(z)$ the factorization of $\mathbf{E}(z)$ can result in ones being located on the diagonal of $\mathbf{D}(z)$ with the exception of $\mathbf{D}_{M,M}(z)$, which assumes the form z^{-K}, where K is an integer greater than or equal to zero, i.e.,

$$\mathbf{D}(z) = \begin{bmatrix} 1 & 0 & 0 & \cdots & 0 \\ 0 & 1 & & & 0 \\ 0 & & \ddots & & \vdots \\ \vdots & & & 1 & 0 \\ 0 & 0 & \cdots & 0 & z^{-K} \end{bmatrix}$$

One of the key properties of the Type-3 elementary matrix operation is that it is easily invertible. The inverses of $\mathbf{L}_k(z)$ and $\mathbf{U}_k(z)$ are given by similar matrices but with the off-diagonal element replaced by a negated version of the original element, i.e.,

$$\mathbf{L}_k^{-1}(z) = \begin{bmatrix} 1 & & & \\ & 1 & -A_k(z) & \\ & & \ddots & \\ & & & 1 \\ & & & & 1 \end{bmatrix}$$

and

$$\mathbf{U}_k^{-1}(z) = \begin{bmatrix} 1 & & & \\ & 1 & & \\ & & \ddots & \\ & -B_k(z) & & 1 \\ & & & & 1 \end{bmatrix}$$

The inverse of the lifting-based factorization of $\mathbf{H}(z)$ is therefore given by

$$\mathbf{F}(z) = \mathbf{H}^{-1}(z) = \mathbf{U}^{-1}(z)\mathbf{D}^{-1}(z)\mathbf{L}^{-1}(z) \tag{5.3}$$

where

$$\mathbf{D}^{-1}(z) = \begin{bmatrix} 1 & 0 & 0 & \cdots & 0 \\ 0 & 1 & & & 0 \\ 0 & & \ddots & & \vdots \\ \vdots & & & 1 & 0 \\ 0 & 0 & \cdots & 0 & z^{K} \end{bmatrix}$$

and $\mathbf{L}^{-1}(z)$ and $\mathbf{U}^{-1}(z)$ are products of $\mathbf{L}_k^{-1}(z)$ and $\mathbf{U}_k^{-1}(z)$, for $k = 0, 1, \ldots, p$ and $k = 0, 1, \ldots, q$, respectively.

Paraunitary Factorization

The polynomial matrix $\mathbf{H}(z)$ is PU if $\tilde{\mathbf{H}}(z)\mathbf{H}(z) = cz^{-K}\mathbf{I}$, or equivalently, $\mathbf{H}^{-1}(z) = cz^{-K}\tilde{\mathbf{H}}(z)$. We recall that the factorization of a PU $M \times M$ polynomial matrix $\mathbf{H}(z)$ with elements that are Laurent polynomials is given by

$$\mathbf{H}(z) = \prod_{i=C}^{1} \mathbf{V}_i(z)\mathbf{R}$$

for a degree-C $\mathbf{H}(z)$. Each $\mathbf{V}_i(z)$ is the degree-1 PU building block and $\mathbf{R}$ is a unitary matrix that can further be factorized as a product of Householder matrices, i.e.,

$$\mathbf{R} = \prod_{i=S}^{1} \mathbf{H}_i$$

It has been shown in [30] that it is possible to factor each $\mathbf{V}_i(z)$ and $\mathbf{H}_i$ using only Type-3 elementary matrix operations, which results in a lifting-based factorization of the PU building blocks. These factorizations are shown in equations (5.5) and (5.6), respectively, where the x_i are independent lifting coefficients and the y_i are given by

$$y_i = \frac{x_i}{1 + \sum_{k=1, k \neq r}^{S} |x_k|^2} \tag{5.4}$$

$$\mathbf{V}_i(z)=\begin{bmatrix}1 & & x_1 & & \\ & \ddots & \vdots & & \\ & 1 & x_{r-1} & & \\ & & 1 & & \\ & & x_{r+1} & 1 & \\ & & \vdots & & \ddots \\ & & x_S & & 1\end{bmatrix}\begin{bmatrix}1 & & & & & & \\ & \ddots & & & & & \\ & & 1 & & & & \\ -y_1 & \cdots & -y_{r-1} & z^{-1} & -y_{r+1} & \cdots & -y_S \\ & & & & 1 & & \\ & & & & & \ddots & \\ & & & & & & 1\end{bmatrix}$$
$$\cdot\begin{bmatrix}1 & & & & & & \\ & \ddots & & & & & \\ & & 1 & & & & \\ y_1 & \cdots & y_{r-1} & 1 & y_{r+1} & \cdots & y_S \\ & & & & 1 & & \\ & & & & & \ddots & \\ & & & & & & 1\end{bmatrix}\begin{bmatrix}1 & & & -x_1 & & \\ & \ddots & & \vdots & & \\ & & 1 & -x_{r-1} & & \\ & & & 1 & & \\ & & & -x_{r+1} & 1 & \\ & & & \vdots & & \ddots \\ & & & -x_S & & 1\end{bmatrix} \tag{5.5}$$

$$\mathbf{H}_i=\begin{bmatrix}1 & & x_1 & & \\ & \ddots & \vdots & & \\ & 1 & x_{r-1} & & \\ & & 1 & & \\ & & x_{r+1} & 1 & \\ & & \vdots & & \ddots \\ & & x_S & & 1\end{bmatrix}\begin{bmatrix}1 & & & & & & \\ & \ddots & & & & & \\ & & 1 & & & & \\ -2y_1 & \cdots & -2y_{r-1} & -1 & -2y_{r+1} & \cdots & -2y_S \\ & & & & 1 & & \\ & & & & & \ddots & \\ & & & & & & 1\end{bmatrix}$$
$$\cdot\begin{bmatrix}1 & & -x_1 & & \\ & \ddots & \vdots & & \\ & 1 & -x_{r-1} & & \\ & & 1 & & \\ & & -x_{r+1} & 1 & \\ & & \vdots & & \ddots \\ & & -x_S & & 1\end{bmatrix} \tag{5.6}$$

Rectangular Matrix Factorization

Consider an $M \times N$ $(M > N)$ polynomial matrix $\mathbf{H}(z)$ with full rank **N** such that $\det(\mathbf{H}(z)) = z^{-k}$, where k is a positive integer and each element $\mathbf{H}_{i,j}(z)$ is a Laurent polynomial. Applying the Smith form decomposition results in the factorization

$$\mathbf{H}(z) = \mathbf{P}(z)\mathbf{D}(z)\mathbf{Q}(z)$$

where $\mathbf{P}(z)$ and $\mathbf{Q}(z)$ are unimodular polynomial matrices of dimensions $M \times M$ and $N \times N$, respectively, and $\mathbf{D}(z)$ is an $M \times N$ polynomial matrix which is the Smith form of $\mathbf{H}(z)$.

The lifting-based factorization of $\mathbf{H}(z)$ is given by

$$\mathbf{H}(z) = \mathbf{L}(z)\mathbf{D}(z)\mathbf{U}(z) \tag{5.7}$$

where $\mathbf{D}(z)$ is given by equation (3.18) and $\mathbf{L}(z)$ and $\mathbf{U}(z)$ are products of $M \times M$ and $N \times N$ Type-3 elementary matrix operations, respectively, i.e.,

$$\mathbf{L}(z) = \prod_{k=0}^{p} \mathbf{L}_k(z)$$

and

$$\mathbf{U}(z) = \prod_{k=0}^{q} \mathbf{U}_k(z)$$

where p and q are integers greater than or equal to zero. Recalling the left-inverse of a Smith form decomposition for rectangular polynomial matrices presented in equation (3.23), the inverse of the lifting-based factorization of $\mathbf{H}(z)$ is therefore given by

$$\mathbf{F}(z) = \mathbf{U}^{-1}(z)\left(\left[\mathbf{D}_1^{-1}(z) \quad \mathbf{0}_{N\times(M-N)}\right] + \left[\mathbf{0}_{N\times N} \quad \mathbf{X}(z)\right]\right)\mathbf{L}^{-1}(z) \tag{5.8}$$

where $\mathbf{U}^{-1}(z)$ is the product of matrices $\mathbf{U}_k(z)$ for $k = 0, 1, \ldots, q$ with negated elements $A_k(z)$, $\mathbf{L}^{-1}(z)$ is the product of matrices $\mathbf{L}_k(z)$ for $k = 0, 1, \ldots, p$ with negated elements $B_k(z)$, and $\mathbf{X}(z)$ is an arbitrary $N \times (M - N)$ polynomial matrix.

Paraunitary Factorization

In the case of a rectangular $\mathbf{H}(z)$, multiple left inverses exist for the inversion matrix $\mathbf{F}(z)$. A lifting-based factorization of $\mathbf{H}(z)$ results following a factorization into Type-3 elementary matrix operations. However,

the factorization of $\mathbf{F}(z)$ includes an arbitrary matrix $\mathbf{X}(z)$. Since the structure of $\mathbf{X}(z)$ will affect the structure of $\mathbf{F}(z)$, a lifting-based factorization of $\mathbf{F}(z)$ may not exist for arbitrary $\mathbf{X}(z)$. In order to maintain the lifting-based structure in both $\mathbf{H}(z)$ and $\mathbf{F}(z)$, it is therefore necessary to force this structure onto $\mathbf{F}(z)$. This can be done by making $\mathbf{X}(z)$ vacuous, $\mathbf{Q}(z) = \mathbf{D}_1(z) = \mathbf{I}_N$, and $\mathbf{P}^{-1}(z) = \tilde{\mathbf{P}}(z)$, resulting in $\mathbf{H}(z)$ being PU.

One method of forcing $\mathbf{H}(z)$ to be PU is as follows. Consider an $M \times M$ PU matrix $\hat{\mathbf{H}}(z)$. Since subsets of the columns in $\hat{\mathbf{H}}(z)$ are also PU, an $M \times N$ $(M > N)$ PU matrix $\mathbf{H}(z)$ can be extracted from $\hat{\mathbf{H}}(z)$. In practice, this can easily be performed by generating a PU matrix $\hat{\mathbf{H}}(z)$ and simply using only the columns of $\hat{\mathbf{H}}(z)$ necessary to define $\mathbf{H}(z)$. The unused elements of $\hat{\mathbf{H}}(z)$ can be taken to be 0's, i.e.

$$\left[\hat{\mathbf{H}}(z)\right]_{M\times M} = \left[\mathbf{H}(z)_{M\times N} \quad \mathbf{0}_{M\times(M-N)}\right] \tag{5.9}$$

The PU inverse of $\hat{\mathbf{H}}(z)$ is then given by

$$\left[\hat{\mathbf{F}}(z)\right]_{M\times M} = \left[\tilde{\hat{\mathbf{H}}}(z)\right]_{M\times M} = \begin{bmatrix} \tilde{\mathbf{H}}(z)_{N\times M} \\ \mathbf{0}_{(M-N)\times M} \end{bmatrix} = \begin{bmatrix} \mathbf{F}(z)_{N\times M} \\ \mathbf{0}_{(M-N)\times M} \end{bmatrix} \tag{5.10}$$

The PU inverse of $\mathbf{H}(z)$, i.e., $\mathbf{F}(z)$, is therefore obtained by extracting the $N \times M$ matrix $\mathbf{F}(z)$ from the $M \times M$ matrix $\hat{\mathbf{F}}(z)$. It easily follows that a lifting-based factorization of a rectangular PU matrix of dimensions $M \times N$ can be derived by determining a lifting-based factorization for a square PU matrix of dimensions $M \times M$.

5.1.2 Filter Bank Analysis

The analysis and synthesis bank polyphase transfer matrices of an OFB and a critically-sampled FB can be directly related to the Smith form decomposition with Type-3 elementary matrix operations. As discussed in section 3.2, each row k in the matrix $\mathbf{E}(z)$ contains the K-spaced polyphase filter transfer functions of the kth analysis subband filter transfer function $H_k(z)$. Since a Type-3 elementary matrix operation adds one row in a matrix to another row (with possible multiplication by a polynomial), each subband filter is essentially a multiple of or a filtered version of another subband filter, as illustrated in figure 21(a).

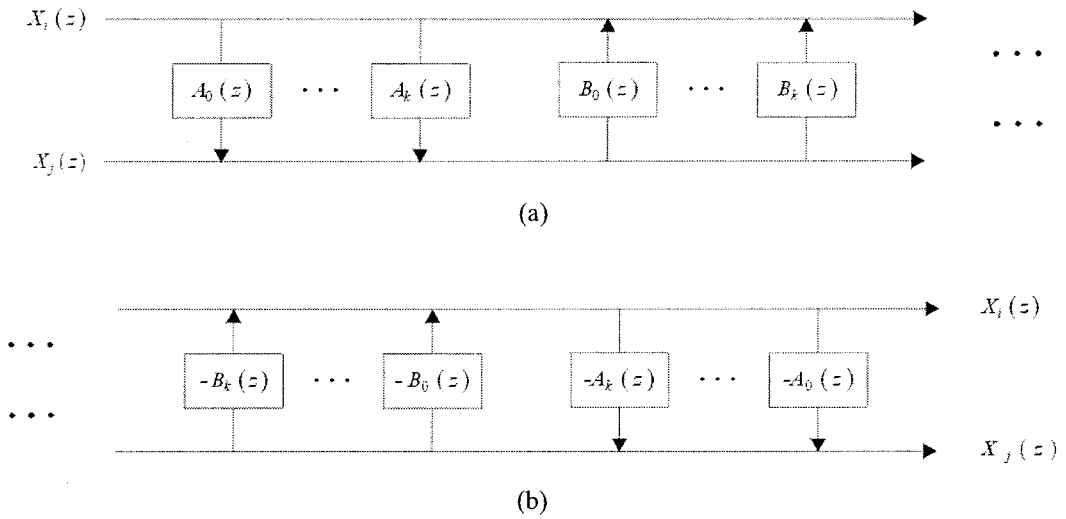

Figure 21. *Lifting-based implementation applying filtering operations between channels i and j. (a) Analysis bank. (b) Synthesis bank.*

A lifting-based factorization of $\mathbf{E}(z)$ is generated by multiplying Type-3 elementary matrix operations while the inverse is generated by multiplying inverse Type-3 elementary matrix operations. The attractive property of the inverse Type-3 elementary matrix operation is that the polynomial coefficient found in the inverse matrix is identical to the negative of the polynomial coefficient found in the Type-3 elementary matrix prior to inversion. When considering this factorization as the structure of an FB, the synthesis bank essentially performs the exact opposite operations as the analysis bank. For each channel in the analysis bank that is summed with a possibly filtered version of another channel, the synthesis bank performs a difference using the respective filtering operation, as illustrated in figure 21(b). This results in an FB structure wherein the synthesis bank is generated using the exact same coefficients as the analysis bank.

The benefit of this relationship, as discussed by Chen and Amaratunga in [30], is that if the lifting coefficients are quantized during implementation, as long as identical quantization algorithms are applied to both the analysis and synthesis banks, the PR property will hold since the quantized values of the lifting coefficients in each bank will be identical. In addition to this, intermediate operations such as the multiplication of quantized lifting-coefficients with an input signal, truncation of these results, and overflows due to the summation of these results, may occur. However, as long as similar truncation and overflow condition algorithms are applied to the both the analysis and synthesis banks, similar results following multiplication, truncation and overflow will occur in each bank. This results in a structure that is resilient to non-linear distortion typically found in direct and lattice structures.

5.2 Factorization of Modulated Filter Bank Transfer Matrices

MFBs are an important class of FBs since they can often be efficiently implemented using well-known fast transforms. In an effort to exploit the advantages offered by both modulation and lifting-based implementations, it is desirable to derive a lifting-based structure for MFBs. Recalling the generalized factorization of the PU analysis bank polyphase transfer matrix $\mathbf{E}(z)$ given by equation (4.14) in section 4.1, we obtain the factorization

$$\mathbf{E}(z) = \mathbf{P}^T \operatorname{diag}\left(\mathbf{M}_i^T(z)\mathbf{S}_i(z)\mathbf{N}_i^T\right)\mathbf{Q}^T$$

for $i = 0, 1, \ldots, g-1$, where $g = \gcd(M,N)$, $\mathbf{S}_i(z)$ is an $S \times T$ polynomial matrix, $\mathbf{P}$ and $\mathbf{Q}$ are $M \times M$ and $N \times N$ permutation matrices, respectively, and $\mathbf{M}_i(z)$ and $\mathbf{N}_i(z)$ are $S \times S$ and $T \times T$ diagonal matrices, respectively, with appropriate powers of z located on the diagonal. Furthermore, recall that a PU matrix $\mathbf{S}_i(z)$ is generated by extracting T columns from the matrix $\mathbf{G}(z)$, where $\mathbf{G}(z)$ is a PU matrix defined as the product of degree-one PU building blocks $\mathbf{V}_i(z)$ and Householder matrices $\mathbf{H}_i$. Now, if $\mathbf{V}_i(z)$ and $\mathbf{H}_i$ are further factorized using only Type-3 elementary matrix operations as shown in equations (5.5) and (5.6), respectively, then a lifting-based factorization for oversampled PU MFB transfer matrices results.

5.2.1 DFT- and Cosine-Modulation

The lifting-based factorization of a PU matrix $\mathbf{E}(z)$ derived by DFT-M or CM follows directly from the PU factorizations of DFT-MFB and CMFB transfer matrices presented in sections 4.2 and 4.3, respectively, and the generalized PU lifting-based factorization described above. Odd- and even-stacked DFT-MFBs with arbitrary M and N, and odd- and even-stacked CMFBs with odd L and M being an integer multiple of N, can be generated. The resulting modulation parameters such as $\mathbf{A}_K$, $\mathbf{T}$, and $\mathbf{D}(z)$, and the necessary filter prototype filter lengths L_p for DFT-MFBs and CMFBs are presented in tables 1 and 2, respectively. Note that L_p is defined as JM, JMN, JMN/g, or $2JM$, where J is a positive integer greater than zero. The number of rectangular matrices $\hat{\mathbf{S}}_i(z)$ that need to be parameterized for each modulation type and stacking type is also included, in addition to the dimensions and order (**O**) of $\hat{\mathbf{S}}_i(z)$. Finally, the total number of parameters required for optimization is included. For Form 3 modulations, the order of each $\hat{\mathbf{S}}_i(z)$ do not need to be made equal. In this case, the maximum order of $\hat{\mathbf{S}}_i(z)$ for a given L_p is denoted by Max. **O**, whereas the order that results if the order of each $\hat{\mathbf{S}}_i(z)$ is equal is denoted by Avg. **O**. The total number

of parameters required for optimization is based on all $\hat{\mathbf{S}}_i(z)$ having identical orders. In the DFT-M case, the conditions on the synthesis bank subband filter impulse responses for generating PU analysis bank transfer matrices are included. In the CM case, the conditions on the analysis and synthesis bank prototype filter impulse responses for generating PU analysis bank transfer matrices are included.

Table 1. *Lifting-based factorization parameters for oversampled DFT-modulated filter banks.*

Form	1		2		3	
Stack	Odd	Even	Odd	Even	Odd	Even
$\mathbf{A}_K$	$[\mathbf{I}_M \; -\mathbf{I}_M]$	$\mathbf{I}_M$	$[\mathbf{I}_M \; -\mathbf{I}_M]$	$\mathbf{I}_M$	$[\mathbf{I}_M \; -\mathbf{I}_M]$	$\mathbf{I}_M$
$\mathbf{T}$	$[M \times M \text{ DFT}]$					
$\mathbf{D}(z)$	$\mathbf{I}_M$					
L_p	JM		JMN		JMN/g^2	
$f_k[n]$	$f_k[n] = h_k[L_p - n]$					
# of $\hat{\mathbf{S}}_i(z)$	g		1		g	
$\hat{\mathbf{S}}_i(z)$ dimensions	$L \times 1$		$M \times N$		$M/g \times N/g$	
$\mathbf{O}\left(\hat{\mathbf{S}}_i(z)\right)$	$J = L_p / M$		$J = L_p / MN$		*Max:* $J = L_p g^2 / MN$ *Avg:* $J = L_p / MN$	
# Parameters	$\frac{g}{2}(2(J+\rho)+L)(L-1)$		$\frac{1}{2}(2(J+\rho)+M)(M-1)$		$\frac{1}{2}\left(2(J+\rho)+\frac{M}{g}\right)\left(\frac{M}{g}-1\right)$	
Note: $\rho = 0$ for $J = 1$, $\rho = -1$ otherwise						

Table 2. *Lifting-based factorization parameters for oversampled cosine-modulated filter banks.*

Form	1	
Stack	Odd	Even
$\mathbf{A}_K$	$[\,\mathbf{I}_{2M}\ -\mathbf{I}_{2M}\,]$	$\mathbf{I}_{2M}$
$\mathbf{T}$	$[\,M \times 2M\ \text{DCT}\,]$	$\begin{bmatrix} M \times 2M\ \text{DCT} \\ M \times 2M\ \text{DST} \end{bmatrix}$
$\mathbf{D}(z)$	$\mathbf{I}_{2M}$	$\begin{bmatrix} \mathbf{I}_M & \\ & z^{-M}\mathbf{I}_M \end{bmatrix}$
L_p	$2JM$	
$p[n]$	Linear phase	
$q[n]$	$q[n] = p[L_p - n]$	
# of $\hat{\mathbf{S}}_i(z)$	N	
$\hat{\mathbf{S}}_i(z)$ dimensions	$2L$ x 1	
$\mathbf{O}\left(\hat{\mathbf{S}}_i(z)\right)$	$J = L_p / 2M$	
# Parameters	$\frac{N}{2}(J + L + \rho)(2L - 1)$	
Note: $\rho = 0$ for $J = 1$, $\rho = -1$ otherwise		

5.2.2 Insertion of Zeros

In Form 2 and Form 3 factorizations, the matrix $\hat{\mathbf{S}}_i(z)$ may contain elements $z^{-k}E_i(z^l)$ where $k \geq 0$. In order to properly relate the polyphase components $E_i(z^l)$ which are multiplied by z^{-k} to the prototype filter coefficients $p[n]$, each $E_i(z^l)$ must be multiplied by z^k and the prototype filter impulse response must be redefined accordingly. To illustrate this, consider the example in section 4.1 where Form 2 matrices $\hat{\mathbf{S}}_i(z)$ are derived from the factorization of a Form 3 matrix $\mathbf{E}(z)$ with $M = 6$ and $N = 4$. In this example, $L_p = 2JM = 24$. Therefore, a $2M$-spaced polyphase decomposition of $p[n]$ is applied. The transfer function of the prototype filter can be expressed as

$$P(z) = E_0(z) + z^{-1}E_1(z) + z^{-2}E_2(z) + \ldots + z^{-11}E_{11}(z)$$

where $E_0(z) = p[0] + z^{-1}p[12]$, $E_1(z) = p[1] + z^{-1}p[13]$, $E_2(z) = p[2] + z^{-1}p[14]$, ..., $E_{11}(z) = p[11] + z^{-1}p[23]$. This $2M$-spaced Type-1 polyphase decomposition of $p[n]$ is illustrated in figure 22.

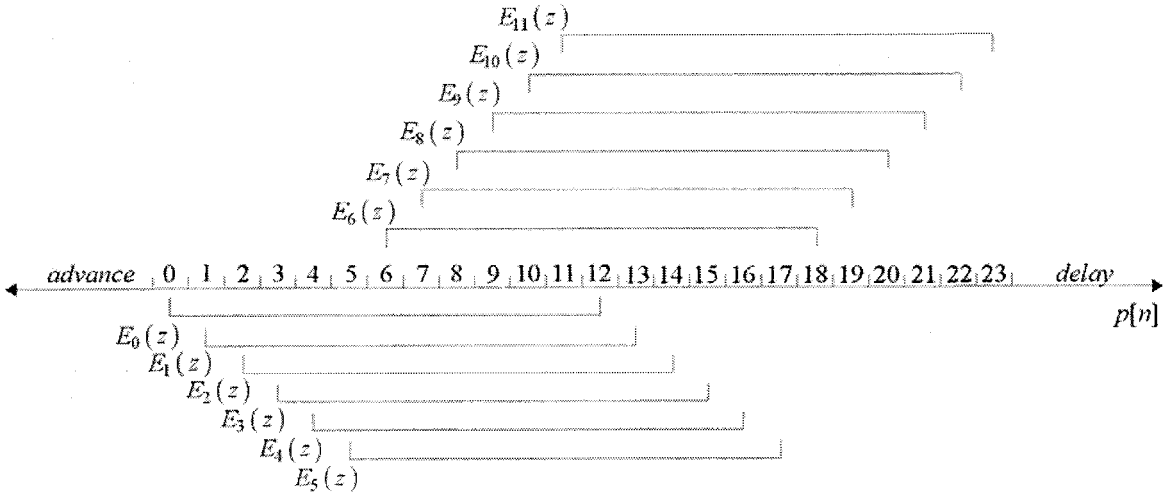

Figure 22. *Association of $E_i(z)$ to $p[n]$ for a 2M-spaced polyphase decomposition of $p[n]$ with $L_p = 24$ and $M = 6$.*

To relate the polyphase filters $E_0(z^3)$, $E_1(z^3)$, etc. to the polyphase filters $E_0(z)$, $E_1(z)$, etc., each polyphase filter must be downsampled by a factor of 3. Since the element $E_8(z^3)$ was manipulated to be multiplied by z^{-3}, downsampling the polyphase filters results in $z^{-1}E_8(z^3)$ and $z^{-1}E_9(z^3)$. The element z^{-1} must be accounted for when relating the polyphase components to the prototype filter impulse response. As illustrated in

figure 23, the multiplication of $E_8(z)$ and $E_9(z)$ by z^{-1} relates to an advance in the time domain of those polyphase components with respect to the prototype filter impulse response $p[n]$.

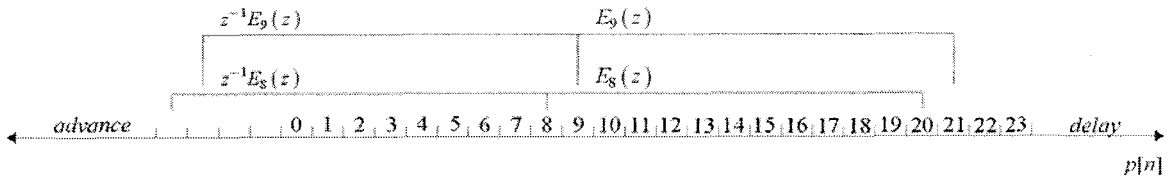

Figure 23. *Effect of multiplying $E_8(z)$ and $E_9(z)$ by z^{-1}.*

Once the polyphase components $z^{-1}E_8(z)$ and $z^{-1}E_9(z)$ are properly related to $p[n]$, the prototype filter transfer function is given by

$$P(z) = E_8(z) + z^{-1}E_9(z) + z^{-4}E_0(z) + z^{-5}E_1(z) + z^{-6}E_2(z) + \ldots + z^{-15}E_{11}(z) \tag{5.11}$$

Figure 24 illustrates how the prototype filter impulse response is properly redefined following redistribution of the polyphase components. It is noticed that this redistribution causes the length of $p[n]$ to be increased by 4 and zeros (illustrated with **x**'s) to be imposed. Although these zeros do not add to the computational complexity of the prototype filter design optimization algorithm to follow, the increased length does result in an increased amount of storage required in a hardware implementation.

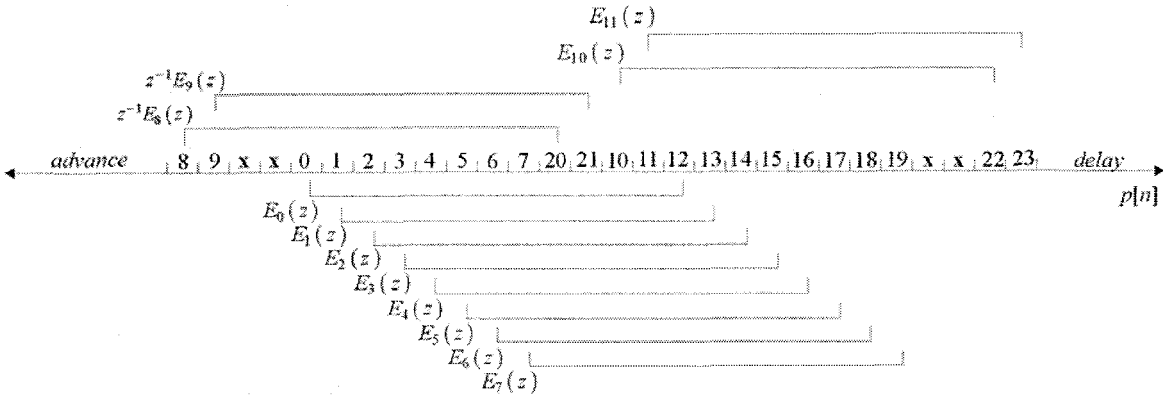

Figure 24. *Association of $E_i(z)$ with $p[n]$ following multiplication of $E_8(z)$ and $E_9(z)$ by z^{-1}.*

5.3 Summary and Conclusions

Lifting-based factorizations were studied. In section 5.1, the fundamental structure of lifting-based implementations was derived by performing a Smith form decomposition on polynomial matrices. A mathematical framework provided a lifting-based factorization for square and rectangular polynomial matrices as well as for square and rectangular PU polynomial matrices. It was shown that a lifting-based factorization for rectangular PU matrices can be derived from lifting-based factorizations of square PU matrices. Section 5.1 concluded with a discussion regarding the relationship between lifting-based factorizations and FB implementations.

In section 5.2, the parameters for lifting-based factorizations of PU O-MFB transfer matrices were summarized. For DFT-MFBs these parameters include the structure of $\mathbf{A}_K$, $\mathbf{T}$, and $\mathbf{D}(z)$, the constraints on L_p and $f_k[n]$, the number of matrices $\hat{\mathbf{S}}_i(z)$ required to represent a given $\mathbf{E}(z)$, the dimensions of each matrix $\hat{\mathbf{S}}_i(z)$, the order of z in each $\hat{\mathbf{S}}_i(z)$, and the number of parameters required for optimization. For CMFBs these parameters include the structure of $\mathbf{A}_K$, $\mathbf{T}$, and $\mathbf{D}(z)$, the constraints on L_p, $p[n]$, and $q[n]$, the number of matrices $\hat{\mathbf{S}}_i(z)$ required to represent a given $\mathbf{E}(z)$, the dimensions of each matrix $\hat{\mathbf{S}}_i(z)$, the order of z in each $\hat{\mathbf{S}}_i(z)$, and the number of parameters required for optimization. Section 5.2 concluded with a discussion on the insertion of zeros into $p[n]$ based on the factorization of $\mathbf{E}(z)$. It was shown that certain factorizations may result in zeros being inserted into $p[n]$ resulting in an increased L_p, and an increased amount of storage required for hardware implementation.

Chapter 6

Filter Bank Design

There are three methods that are typically used for the design of multirate FBs. The choice of method depends on how closely the PR conditions must be met, whether or not there are any restrictions on the computational complexity of the design algorithm, and the sensitivity of the intended application to non-linear distortion. The three primary methods of designing an FB consist of:

- applying constrained optimization algorithms to the design of the subband filters in multirate FBs or the design of a prototype filter in MFBs,
- applying unconstrained optimization algorithms to FB structures, and
- applying spectral factorization techniques to directly design the subband filters in multirate FBs.

FB design methods that employ constrained optimization algorithms formulate the objective function so that the filter coefficients are optimized to minimize the stopband energy of the subband filters, while the constraints are given by the PR constraints on the subband filters' impulse responses. Similarly, in MFBs the stopband energy of the prototype filter is defined as the objective function while the constraints are given by the PR constraints on the prototype filter impulse response. Formulating the PR constraints as a quadratic function and minimizing the least squared error of the stopband energy results in the quadratically-constrained least squares (QCLS) FB design method derived by Nguyen in [72]. In this method, the subband filter impulse responses are directly optimized. By formulating the PR constraints as a quadratic function it is typically necessary to apply linear approximations to this function in order to solve the optimization problem. However, applying linear approximations to the PR constraints results in FBs wherein PR is not exactly achieved.

FB design methods that apply unconstrained optimization algorithms typically factorize the polyphase transfer matrices $\mathbf{E}(z)$ and $\mathbf{R}(z)$ into a product of elementary matrices that have desirable properties, such as PR, linear phase and/or paraunitariness. These properties tend to propagate through the product of

elementary matrices to the realization of $\mathbf{E}(z)$ and $\mathbf{R}(z)$, as described in [20]. The simpler matrices can then be parameterized and the matrix coefficients can be related to the impulse response of the prototype filter or subband filters in modulated and non-modulated FB formulations, respectively. In lattice factorizations, the coefficients in the parameterized matrices are referred to as the *lattice coefficients*, whereas in ladder factorizations, the coefficients in the parameterized matrices are referred to as the *ladder coefficients*. In either case, the elementary matrix coefficients are referred to as the *structural coefficients*. FB design methods that employ unconstrained optimization algorithms formulate the objective function so that the structural coefficients are optimized to minimize the stopband energy of the subband filters or the stopband energy of the prototype filter. The PR property is typically induced in the elementary matrices used to factorize $\mathbf{E}(z)$ and $\mathbf{R}(z)$, and hence further constraints for PR need not be imposed in the optimization algorithm. Structural factorizations tend to result in PRFBs while requiring a relatively small number of coefficients to optimize. However, the objective function tends to be very non-linear and hence good starting points to the optimization algorithm are necessary in order to avoid local minimas and obtain good frequency selectivity.

Spectral factorization techniques consist of determining a prototype filter impulse response by extracting an Mth band spectral factor from an all-pass transfer function. The prototype filter transfer function is then multiplied with a modulation matrix (i.e., DFT or DCT) in order to obtain the analysis and synthesis subband transfer functions. Filter design methods employing spectral factorization techniques are much less computationally complex than methods that require the application of constrained or unconstrained optimization algorithms since spectral factorization techniques typically offer closed-form solutions. However, since optimization algorithms are not applied, prototype filters with suboptimal frequency responses result. An example of an FB design method applying spectral factorization techniques is presented in [73].

A lifting-based factorization provides a modular structure wherein PR is structurally imposed and unconstrained optimization algorithms can be employed. In section 6.1, a lifting-based design method is proposed for designing and implementing PU O-MFBs including DFT-MFBs and CMFBs of either odd- or even-stacked types. In section 6.2, a lifting-based design example is presented for both an odd-stacked oversampled PU DFT-MFB and an even-stacked oversampled PU CMFB.

6.1 Lifting-Based Design Method

A method for designing PU O-MFBs implemented using a lifting-structure is generated by deriving an objective function for an unconstrained optimization algorithm based on the lifting-based factorization of PU O-MFB transfer matrices. The design method is as follows:

1. Select the FB properties consisting of the integers M, N, L_p, the modulation type, and the stacking type.

   Note: Following selection of the desired modulation and stacking types, the remaining FB properties are subject to the constraints outlined in tables 1 and 2 for DFT-MFBs and CMFBs, respectively.

2. Derive the analysis polyphase transfer matrix $\mathbf{E}(z)$ by applying the factorization presented in section 4.2 for DFT-MFBs and section 4.3 for CMFBs.

3. Manipulate $\mathbf{E}(z)$ into a block diagonal matrix $\mathbf{S}(z)$ by applying the method presented in section 4.1. Generate submatrices $\hat{\mathbf{S}}_i(z)$ by pre- and post-multiplying $\mathbf{S}(z)$ with appropriate permutation matrices $\mathbf{P}$ and $\mathbf{Q}$, and matrices $\mathbf{M}_i(z)$ and $\mathbf{N}_i(z)$ with appropriate powers of z on the diagonal.

4. Determine the size and number of PU matrices $\mathbf{G}(z)$ required to generate each $\hat{\mathbf{S}}_i(z)$.

   Note: Less restrictive prototype filter lengths as defined in step #1 may be derived by appropriately redefining the dimensions and order of submatrices $\hat{\mathbf{S}}_i(z)$, as outlined in [70] for the odd-stacked DFT-M case.

5. Factorize each matrix $\mathbf{G}(z)$ into lifting matrices by applying the PU factorization presented in equation (4.13) followed by the lifting factorization presented in equations (5.5) and (5.6).

6. Associate the resulting lifting coefficients found in the lifting matrices with the prototype filter coefficients generated from the polyphase components contained in $\hat{\mathbf{S}}_i(z)$.

   Note: This association must be performed carefully since zeros may be inserted due to the polyphase components $E_i(z^l)$ in the matrices $\hat{\mathbf{S}}_i(z)$ being multiplied by z^{-k}. The number of inserted zeros can, however, be minimized by appropriately redefining the dimensions and order of each $\hat{\mathbf{S}}_i(z)$, as outlined in [70] for the odd-stacked DFT-M case.

7. Employ an unconstrained optimization algorithm to optimize the lifting coefficients to minimize the stopband energy of the prototype filter.

   Note: Standard unconstrained optimization algorithms can be applied. In order to reduce the computational complexity of the optimization algorithm, the stopband energy of the prototype filter can be defined as a quadratic function as outlined in [74].

8. If FB implementations are desired where the lifting-based coefficients are quantized to either integer or dyadic values, quantization methods such as those presented in [40] or [43] can be employed.

6.2 Lifting-Based Design Examples

6.2.1 Oversampled Odd-Stacked DFT-Modulated Filter Bank

An odd-stacked oversampled PU DFT-MFB with $M = 6$, $N = 4$, and $L_p = 24$ was designed. An analysis bank polyphase transfer matrix $\mathbf{E}(z)$ of Form 3 resulted and was transformed into two $M/g \times N/g = 3 \times 2$ matrices, denoted by $\mathbf{S}_0(z)$ and $\mathbf{S}_1(z)$, where $g = \gcd(M,N) = 2$. The order of each $\hat{\mathbf{S}}_i(z)$ was chosen to be identical, resulting in a filter length definition of $L_p = JMN$. The analysis and synthesis subband filters were therefore represented by MN-spaced Type-1 and Type-2 polyphase filters, respectively. The order of each $\hat{\mathbf{S}}_i(z)$ is given by $L_p/MN = 1$ and therefore the PU factorization of each matrix $\hat{\mathbf{S}}_i(z)$ consisted of one $M/g \times M/g = 3 \times 3$ degree-1 PU matrix $\mathbf{V}_1(z)$ and a product of $M/g - 1 = 2$ Householder matrices $\mathbf{H}_i$. The total number of independent variables required for the lifting optimization is given by

$$\#Parameters = \frac{1}{2}\left(2(J+\rho)+\frac{M}{g}\right)\left(\frac{M}{g}-1\right) = \frac{1}{2}(2(1+0)+3)\left(\frac{6}{2}-1\right) = 5$$

where $J = L_p/MN = 24/(6 \times 4) = 1$ and $\rho = 0$. Since $\mathbf{S}_0(z)$ and $\mathbf{S}_1(z)$ contain the polyphase filter transfer functions $E_8(z)$ and $E_9(z)$ multiplied by z^{-1}, it was necessary to introduce four zeros into the prototype filter impulse response $p[n]$ at $n = 2$, 3, 24, and 25, resulting in a prototype filter with length $L_p = 28$. An unconstrained optimization algorithm was employed which had an objective function that minimized the stopband energy of the prototype filter by optimization of the lifting coefficients. The prototype filter was designed to have passband and stopband edges at $\omega_p = \pi/2M = \pi/12$ and $\omega_s = \pi/M = \pi/6$, respectively. The amplitude response of the resulting FB is illustrated in figure 25.

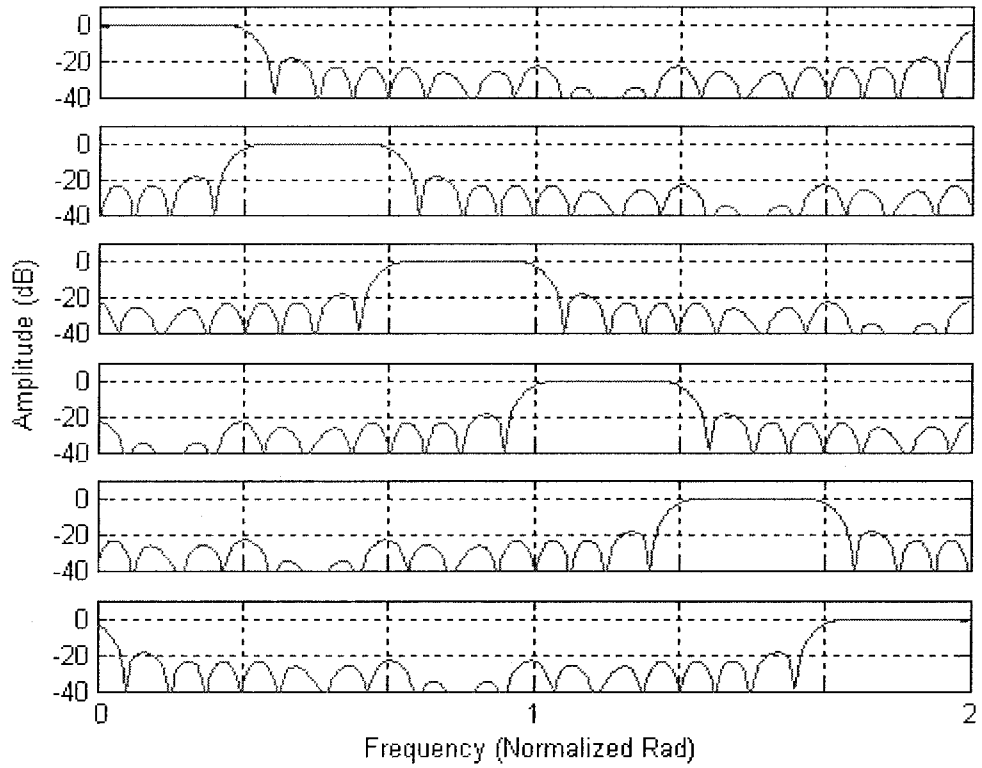

Figure 25. *Amplitude response of the subband filters in an odd-stacked oversampled DFT-modulated filter bank with $M = 6$, $N = 4$, and $L_p = 28$.*

6.2.2 Oversampled Even-Stacked Cosine-Modulated Filter Bank

An even-stacked oversampled PU CMFB with $2M = 12$, $2N = 4$, and $L_p = 24$ was designed. An analysis bank polyphase transfer matrix $\mathbf{E}(z)$ of Form 1 resulted and was transformed into two $2L \times 1 = 6 \times 1$ matrices, denoted by $\mathbf{S}_0(z)$ and $\mathbf{S}_1(z)$, where $L = M / N = 3$. The prototype filter length is defined by $L_p = 2JM$, hence the analysis and synthesis subband filters were represented by $2M$-spaced Type-1 and Type- 2 polyphase filters, respectively. The order of each $\hat{\mathbf{S}}_i(z)$ is given by $L_p/2M = 1$ and therefore the PU factorization of each matrix $\hat{\mathbf{S}}_i(z)$ consisted of one $2L \times 2L = 6 \times 6$ degree-1 PU matrix $\mathbf{V}_1(z)$, and a product of $2L - 1 = 5$ Householder matrices $\mathbf{H}_i$. The total number of independent variables required for the lifting optimization is given by

$$\#Parameters = \frac{N}{2}(J+L+\rho)(2L-1) = \frac{2}{2}(1+3+0)(6-1) = 20$$

where $J = L_p/MN = 24/(6 \times 4) = 1$ and $\rho = 0$. Since the prototype filter was chosen to have linear phase, the polyphase components in $\mathbf{S}_1(z)$ were derived from $\mathbf{S}_0(z)$. Therefore it was not necessary to include the polyphase components in $\mathbf{S}_1(z)$ as independent variables in the following optimization procedure. An unconstrained optimization algorithm was employed which had an objective function that minimized the stopband energy of the prototype filter by optimization of the lifting coefficients. The prototype filter was designed to have passband and stopband edges at $\omega_p = \pi/2M = \pi/12$ and $\omega_s = \pi/M = \pi/6$, respectively. The amplitude response of the resulting FB is illustrated in figure 26.

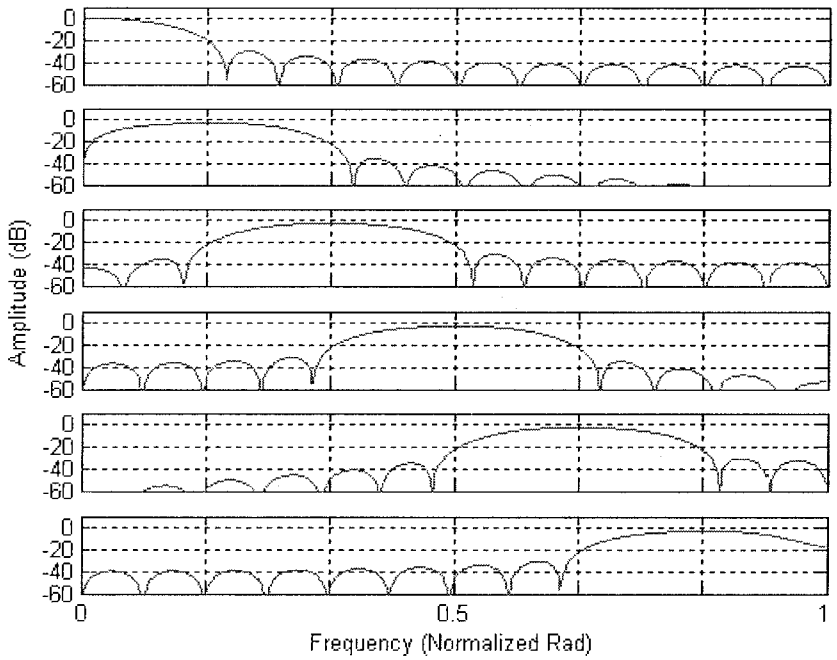

(a)

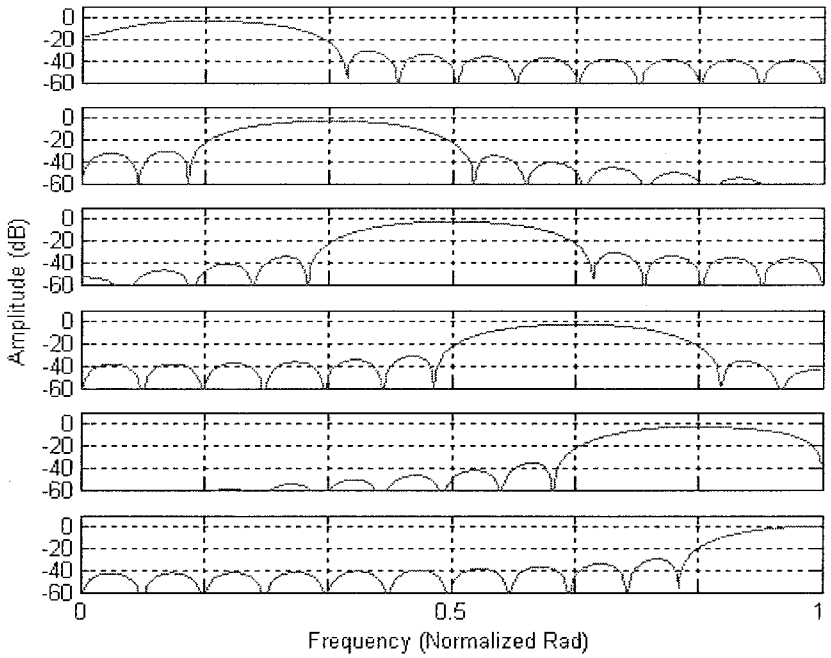

(b)

Figure 26. *Amplitude response of the subband filters in an even-stacked oversampled cosine-modulated filter bank with 2M = 12, 2N = 4, and L_p = 24. (a) First bank. (b) Second bank.*

6.3 Summary and Conclusions

A design method employing an unconstrained optimization algorithm was presented. In section 6.1, a design method was specifically outlined that employs unconstrained optimization algorithms for the design of PU O-MFBs that are realized using lifting-based structures. Oversampled DFT-MFBs and O-CMFBs of either odd- or even-stacked types with an arbitrary number of channels and subsampling factor can be designed using this method, subject to the limitations in tables 1 and 2.

In section 6.2, examples were given for the design of an odd-stacked oversampled DFT-MFB and an even-stacked O-CMFB.

Chapter 7

Conclusions and Future Research

The design and implementation of PR OFBs has been investigated. A design method employing unconstrained optimization algorithms has been derived based on the factorization of transfer matrices generated by O-MFBs. A particular factorization that results in PRFBs was derived through the application of the PU property. By applying lifting-based factorizations of PU matrices, a lifting-based factorization of PU O-MFB transfer matrices was derived. This factorization leads to a structural design method where unconstrained optimization algorithms could be employed.

7.1 Lifting-Based Factorization

OFBs have transfer functions that are characterized by rectangular transfer matrices. It was shown by application of the Smith form decomposition that multiple left-inverses exist for a given rectangular matrix. Analogously, a plurality of synthesis banks exist that result in PR for a particular analysis bank. In order to maintain a lifting-based structure in both the analysis and synthesis banks, the PU property was applied to the transfer matrices. Although this facilitates the employment of lifting-based factorizations, it also restricts the scope of the left-inverse that corresponds to the synthesis bank to contain only a subset of all possible left-inverse matrices which result in PRFBs. The factorization of the polyphase transfer matrix $\mathbf{E}(z)$ into PU matrices $\hat{\mathbf{S}}_i(z)$ tends to be fairly complicated. As the order of the subband filters increases, so does the complexity of the factorization. Methods for performing this factorization for matrices $\mathbf{E}(z)$ with a high order are not obvious and could be quite difficult to automate.

For the lifting-based factorization presented, each rectangular matrix $\hat{\mathbf{S}}_i(z)$ with dimensions $S \times T$ is embedded into a square matrix $\mathbf{G}_i(z)$ with dimensions $S \times S$. Since columns of $\mathbf{G}_i(z)$ are inevitably ignored, all of the parameters used to characterize $\mathbf{G}_i(z)$ are unnecessary. This is particularly evident in

factorizations using only Type-1 elementary matrix operations wherein the polyphase components of $p[n]$ are defined using only a single column of $\mathbf{G}_i(z)$.

The factorization of $\hat{\mathbf{S}}_i(z)$ often results in elements $z^{-k}E_i(z^l)$, where $k > 0$. In this case, some of the coefficients of the prototype filter impulse response are forced to be zero. Compared to prototype filter impulse responses that do not have coefficients forced to be zero, this factorization is particularly inefficient since the achievable stopband attenuation of the prototype filter and resulting subband filters will be less for the case where the prototype filter impulse coefficients are forced to be zero. Furthermore, the factorization of matrix $\mathbf{E}(z)$ into matrices $\hat{\mathbf{S}}_i(z)$ results in restrictions on L_p based on the form of the factorization. These restrictions are undesirable since the freedom to choose L_p is lost, as is most evident in Form 3 factorizations.

7.2 Design Method

The proposed method facilitates the design of oversampled PU DFT-MFBs and oversampled PU CMFBs with arbitrary stacking. DFT-MFBs and odd-stacked CMFBs cannot generate subband filters with linear phase; on the other hand, this is possible if the prototype filter has linear phase. The design method also facilitates the implementation of FBs using a lifting-based structure that is resilient to both linear and non-linear distortion. Furthermore, the resilience of this structure to non-linear distortion such as that caused by the coefficient quantization facilitates the design of integer- and dyadic-valued FBs that allow for particularly efficient realizations.

FB design methods that derive structural factorizations and apply unconstrained optimization algorithms typically tend to have objective functions that are very non-linear. The application of unconstrained optimization algorithms to these non-linear objective functions typically results in sub-optimal solutions unless a 'good' starting point is used. Experimental results have shown that unconstrained optimization of structural coefficients derived through transfer matrix factorizations using the proposed factorization method tends to result in similar solutions regardless of the optimization starting point. This suggests that the objective function is convex with a global minimum; however, this remains to be proven.

7.3 Future Research

This research has provided insight into the derivation of lifting-based structures for a particular class of OFBs; however, there are still many areas that could potentially benefit from further research. Some of these areas include:

- Lifting-based factorizations for the transfer matrices of arbitrary OFBs, classified as pseudo-biorthogonal FBs, could be explored. Specifically, under consideration in this thesis has been lifting-based factorizations for PU O-MFBs. The generalized case of lifting-based factorizations could be applied to biorthogonal OFBs wherein the limitation on the analysis transfer matrices, i.e., $\tilde{\mathbf{H}}(z)\mathbf{H}(z) = cz^{-n_0}\mathbf{I}_N$, is not imposed. Removing this limitation would result in a larger solution space being searched when applying constrained or unconstrained optimization algorithms, perhaps facilitating the design of filter banks with better subband channel separation for a given number of subband filter coefficients. In addition to this, removing this limitation may also give a filter bank designer greater freedom in choosing the overall filter bank delay. These factorizations would include O-MFBs, PU OFBs, and PU O-MFBs as specific cases.

- Lifting-based factorizations for the transfer matrices of O-MFBs using modulation schemes other than those proposed in this thesis, i.e., other than cosine and DFT-modulation, could be explored. Specifically, recent work has been performed on a modulation scheme referred to as modified DFT (M-DFT) modulation [75]. M-DFT modulation is essentially similar to DFT modulation; however, M-DFT modulation facilitates the design of filter banks with all analysis and synthesis subband filters having linear phase and structurally-inherent alias-free implementations. It may be possible to realize oversampled M-DFT filter banks using lifting structures by simply determining the PR conditions using M-DFT modulation and multiplying the analysis and synthesis prototype filter impulse responses with appropriate exponential functions corresponding to M-DFT modulation rather than DFT modulation. In the case of M-DFT modulated FBs, the constraints necessary to generate PR and LP in the presently discussed LP even-stacked CMFBs may be relaxed since LP and alias-free signal reconstruction is inherent in the M-DFT modulation.

- Lifting-based factorizations for the transfer matrices of OFBs could be explored with the restrictions imposed by the PR property relaxed. In this thesis, lifting-based factorizations for PRFBs have been considered and shown. It has been shown that relaxing the PR constraints in FB design allows for increased separation between subbands while inducing only minimal

amounts of noise [70]. In the case of relaxing the PR constraints, it may be desirable to apply lifting-based factorizations to non-PR filter banks in order to realize the benefits of both lifting-based structures and increased separation between subbands.

Bibliography

[1] A. CROISIER, D. ESTEBAN, AND C. GALAND, "Perfect channel splitting by use of interpolation/decimation/tree decomposition techniques," in *Proc. IEEE Int. Symp. on Info., Circuits and Systems*, 1976.

[2] J. MASSON AND Z. PICEL, "Flexible design of computationaly efficient nearly perfect QMF filter banks," in *Proc. IEEE ICASSP*, vol. 10, pp. 541-544, Apr. 1985.

[3] J. NUSSBAUMER AND M. BETTERLI, "Computationally efficient QMF filter banks," in *Proc. IEEE ICASSP*, vol. 9, pp. 437-440, Mar. 1984.

[4] J. H. ROTHWEILER, "Polyphase quadrature filters – a new subband coding technique," in *Proc. IEEE ICASSP*, vol. 8, pp. 1280-1283, Apr. 1983.

[5] M. J. T. SMITH AND T. P. BARNWELL III, "A procedure for designing exact reconstruction filter banks for tree structured subband coders," in *Proc. IEEE ICASSP*, vol. 9, pp. 421-424, Mar. 1984.

[6] M. VETTERLI, "Splitting a signal into subsampled channels allowing perfect reconstruction," in *Proc. IASTED Conf. Appl. Signal Proc., and Digital Filtering*, Jun. 1985.

[7] P. P. VAIDYANATHAN, "Theory and design of M-channel maximally decimated quadrature mirror filters with arbitrary M, having perfect reconstruction property," *IEEE Trans. on Acoustics, Speech and Signal Processing*, vol. 35, no. 4, pp. 476-492, Apr. 1987.

[8] T. A. RAMSTAD AND J. P. TANEM, "Cosine-modulated analysis-synthesis filterbank with critical sampling and perfect reconstruction," in *Proc. IEEE ICASSP*, vol. 3, pp. 1789-1792, Apr. 1991.

[9] R. D. KOILPILLAI AND P. P. VAIDYANATHAN, "Cosine-modulated FIR filter banks satisfying perfect reconstruction," *IEEE Trans. Signal Processing*, vol. 40, no. 4, pp. 770-783, Apr. 1992.

[10] H. S. MALVAR, "Modulated QMF filter banks with perfect reconstruction," *IEEE Electronics Letters*, vol. 26, no. 13, pp. 906-907, Jun. 1990.

[11] K. NAYEBI, T. P. BARNWELL, III, AND M. J. T. SMITH, "Time-domain filter bank analysis: a new design theory," *IEEE Trans. Signal Processing*, vol. 40, no. 6, pp. 1412-1429, Jun. 1992.

[12] K. NAYEBI, T. P. BARNWELL, III, AND M. J. T. SMITH, "Low delay FIR filter banks: design and evaluation," *IEEE Trans. Signal Processing*, vol. 42, no. 1, pp. 24-31, Jan. 1994.

[13] T. Q. NGUYEN, "A class of generalized cosine modulated filter bank," in *Proc. IEEE ISCAS*, vol. 2, pp. 943-946, May 1992.

[14] G. SCHULLER AND M. J. T. SMITH, "New framework for modulated perfect reconstruction filter banks," *IEEE Trans. Signal Processing*, vol. 44, no. 8, pp. 1941-1954, Aug. 1996.

[15] Y.-P. LIN AND P. P. VAIDYANATHAN, "Linear-phase cosine modulated maximally decimated filter banks with perfect reconstruction," *IEEE Trans. Signal Processing*, vol. 43, no. 11, pp. 2525-2539, Nov. 1995.

[16] P. N. HELLER, T. KARP, T. Q. NGUYEN, "A general formulation of modulated filter banks," *IEEE Trans. Signal Processing*, vol. 47, no. 4, pp. 986-1002, Apr. 1999.

[17] R. A. GOPINATH, "Modulated filter banks and wavelets – a general unified theory," in *Proc. IEEE ICASSP*, vol. 3, pp. 1585-1588, May 1996.

[18] R. GOPINATH AND C. BURRUS, "Theory of modulated filter banks and modulated wavelet tight frames," in *Proc. IEEE ICASSP*, vol. 3, pp. 169-172, Apr. 1993.

[19] P. P. VAIDYANATHAN, "Quadrature mirror filter banks, M-band extensions and perfect-reconstruction techniques," *IEEE ASSP magazine*, vol. 4, no. 3, pp. 4-20, Jul. 1987.

[20] P. P. VAIDYANATHAN, *Multirate Systems and Filter Banks*. Englewood Cliffs, NJ: Prentice-Hall, 1992.

[21] H. MALVAR, *Signal Processing with Lapped Transforms*. Norwood, MO: Artech House, 1992.

[22] M. VETTERLI AND J. KOVAČEVIĆ, *Wavelets and Subband Coding*. Englewood Cliffs, NJ: Prentice-Hall, 1995.

[23] G. STRANG AND T. Q. NGUYEN, *Wavelets and Filter Banks*. Wellesley, U.K.: Cambridge Univ. Press, 1996.

[24] P. P. VAIDYANATHAN AND P.-Q. HOANG, "Lattice structures for optimal design and robust implementation of two-channel perfect reconstruction QMF banks," *IEEE Trans. on Acoustics, Speech and Signal Processing*, vol. 36, no. 1, pp. 81-94, Jan. 1988.

[25] P. P. VAIDYANATHAN, T. Q. NGUYEN, Z. DOGANATA, AND T. SARAMAKI, "Improved technique for design of perfect reconstruction FIR QMF banks with lossless polyphase matrices," *IEEE Trans. on Acoustics, Speech and Signal Proc.*, vol. 37, no. 7, pp. 1042-1056, Jul. 1989.

[26] A. K. SOMAN, P. P. VAIDYANATHAN, AND T. Q. NGUYEN, "Linear phase paraunitary filter banks: theory, factorizations and designs," *IEEE Trans. Signal Processing*, vol. 41, no. 12, pp. 3480-3496, Dec. 1993.

[27] T. D. TRAN, R. L. DE QUEIROZ, AND T. Q. NGUYEN, "Linear-phase perfect reconstruction filter bank: Lattice structure, design, and application in image coding," *IEEE Trans. Signal Processing*, vol. 48, no. 1, pp. 133-147, Jan. 2000.

[28] F. A. M. L. BRUEKERS AND A. W. M. VAN DEN ENDEN, "New networks for perfect inversion and perfect reconstruction," *IEEE J. Selected Areas in Comms.*, vol. 10, no. 1, pp. 129-137, Jan. 1992.

[29] J. LIANG AND T. D. TRAN, "Fast multiplierless approximations of the DCT with the lifting scheme," *IEEE Trans. Signal Processing*, vol. 49, no. 12, pp. 3032-3044, Dec. 2001.

[30] Y.–J. CHEN AND K. AMARATUNGA, "M-channel lifting factorization of perfect reconstruction filter banks and reversible M-band wavelet transforms," *IEEE Trans. Circuits Syst. II*, vol. 50, no. 12, pp. 963 – 976, Dec. 2003.

[31] I. DAUBECHIES AND W. SWELDENS, "Factoring wavelet transforms into lifting steps," *J. Fourier Anal. Appl.*, vol. 4, no. 3, pp. 247 – 269, 1998.

[32] W. SWELDENS, "The lifting scheme: A custom-design construction of biorthogonal wavelets," *Appl. Comput. Harmon. Anal.*, vol. 3, no. 2, pp. 186-200, 1996.

[33] T. G. MARSHALL, "U-L block-triangular matrix and ladder realizations of subband coders," in *Proc. IEEE ICASSP*, vol. 3, pp. 177-180, Apr. 1993.

[34] M. GHARBI, *ET AL.* "Factorization of perfect reconstruction modulated filter banks with variable global delay," *Signal Processing*, vol. 80, no. 7, pp. 1299-1306, July 2000.

[35] T. KARP, A. MERTINS, AND G. SCHULLER, "Efficient biorthogonal cosine-modulated filter banks," *Signal Processing*, vol. 81, no. 5, pp. 997-1016, May 2001.

[36] T. A. C. M. KALKER AND I. SHAH, "Ladder structures for multidimensional linear phase perfect reconstruction filter banks," in *Proc. SPIE Conf. on Visual Comms. and Image Proc.*, pp. 12-20, 1992.

[37] I. SHAH AND T. A. C. M. KALKER, "On ladder structures and linear phase conditions for bi-orthogonal filter banks," in *Proc. IEEE ICASSP*, vol. 3, pp. 181-184, Apr. 1994.

[38] M. ANTONINI, M. BARLAUD, P. MATHIEU, AND I. DAUBECHIES, "Image coding using wavelet transform," *IEEE Trans. Image Processing*, vol. 1, no. 2, pp. 205-220, Apr. 1992.

[39] B. R. HORNG, H. SAMUELI, AND A. N. WILSON, JR., "The design of two-channel lattice-structure perfect-reconstruction filter banks using powers-of-two coefficients," *IEEE Trans. Circuits Syst. I.*, vol. 40, no. 7, pp. 497-499, July 1993.

[40] T. KARP, A. MERTINS, AND T. Q. NGUYEN, "Efficiently VLSI-realizable prototype filters for modulated filter banks," in *Proc. IEEE ICAASP*, vol. 3, pp. 2445-2448, Apr. 1997.

[41] S. C. CHAN, W. LIU, AND K. L. HO, "Perfect reconstruction modulated filter banks with sum of powers-of-two coefficients," in *Proc. IEEE ISCAS*, vol. 2, pp. 73-76, May 2000.

[42] M. BI, S. H. ONG, AND Y. H. ANG, "Integer-modulated FIR filter banks for image compression," *IEEE Trans. Circuits Syst. Video Technol.*, vol. 8, no. 8, pp. 923-927, Dec. 1998.

[43] A. MERTINS AND T. KARP, "Modulated, perfect reconstruction filterbanks with integer coefficients," *IEEE. Trans. Signal Processing*, vol. 50, no. 6, June 2002, pp. 1398-1408.

[44] Z. CVETKOVIĆ, "Oversampled modulated filter banks and tight Gabor frames in $l^2(Z)$," in *Proc. IEEE ICASSP*, vol. 2, pp. 1456-1459, May 1995.

[45] R. E. CROCHIERE AND L. R. RABINER, *Multirate Digital Signal Processing.* Englewood Cliffs, NJ: Prentice-Hall, 1983.

[46] J. KLIEWER AND A. MERTINS, "Design of paraunitary oversampled cosine-modulated filter banks," in *Proc. IEEE ICASSP*, vol. 3, pp. 2073-2076, Apr. 1997.

[47] J. KLIEWER AND A. MERTINS, "Oversampled cosine-modulated filter banks with arbitrary system delay," *IEEE Trans. Signal Processing*, vol. 46, no. 4, pp. 941-955, Apr. 1998.

[48] H. BÖLCSKEI AND F. HLAWATSCH, "Oversampled Wilson-type cosine modulated filter banks with linear phase," in *Proc. 27th Asilomar Conf. Signals, Syst., Comput.*, vol. 2, pp. 998-1002, Nov. 1996.

[49] H. BÖLCSKEI AND F. KLAWATSCH, "Oversampled cosine modulated filter banks with perfect reconstruction," *IEEE Trans. Circuits Syst. II*, vol. 45, no. 8, pp. 1057-1071, Aug. 1998.

[50] H. BÖLCSKEI, "Oversampled filter banks and predictive subband coders," Ph.D. dissertation, Vienna Univ. Technol., Vienna, Austria, Nov. 1997.

[51] Z. CVETKOVIĆ, "Overcomplete expansions for digital signal processing," Ph.D. dissertation, Univ. California, Berkeley, Dec. 1995.

[52] F. LABEAU, L. VANDENDORPE, AND B. MACQ, "Structures, factorizations, and design criteria for oversampled paraunitary filterbanks yielding linear-phase filters," *IEEE Trans. Signal Processing*, vol. 48, no. 11, pp. 3062-3071, Nov. 2000.

[53] L. GAN AND K.–K. MA, "Oversampled linear-phase perfect reconstruction filterbanks: Theory, lattice structure, and parameterization," *IEEE Trans. Signal Processing*, vol. 51, no. 3, pp. 744 – 759, Mar. 2003.

[54] B. RIEL, D. J. SHPAK, AND A. ANTONIOU, "Oversampled biorthogonal cosine-modulated filter bank realization using a critically constrained lifting scheme," in *Proc. IEEE NEWCAS*, pp. 285 – 288, June 2004.

[55] B. RIEL, D. J. SHPAK, AND A. ANTONIOU, "Lifting-based design and implementation of oversampled paraunitary modulated filter banks," in *Proc. IEEE MWSCAS*, vol. 2, pp. 97 – 100, July 2004.

[56] W. B. PENNEBAKER AND J. L. MITCHELL, *JPEG: Still Image Compression Standard.* New York: Van Nostrand Reinhold, 1993.

[57] J. L. MITCHELL, D. LEGALL, AND C. FOGG, *MPEG Video Compression Standard.* New York: Chapman & Hall, 1996.

[58] COX *ET AL.*, "The analog voice privacy system," *AT&T Tech. J.*, vol. 66, pp. 119-131, Jan. 1987.

[59] M. VETTERLI, "Perfect transmultiplexers," in *Proc. IEEE ICASSP*, vol. 11, pp. 2567-2570, Apr. 1986.

[60] M. HARTENECK, S. WEISS, AND R. W. STEWART, "Design of near perfect reconstruction oversampled filter banks for subband adaptive filters," *IEEE Trans. Circuits Syst. II*, vol. 46, no. 8, pp. 1081-1085, Aug. 1999.

[61] Q.-G. LIU, B. CHAMPAGNE, AND D. K. C. HO, "Simple design of oversampled uniform DFT filter banks with applications to subband acoustic echo cancellation," *Signal Processing*, vol. 80, pp. 831-847, May 2000.

[62] M. HARTENECK, J. M. PAEZ-BORRALLO, AND R. W. STEWART, "An oversampled subband adaptive filter without cross adaptive filters," *Signal Processing*, vol. 64, no. 1, pp. 93-101, Jan. 1998.

[63] V. S. SOMAYAZULU, S. K. MITRA, AND J. J. SHYNK, "Adaptive line enhancement using multirate techniques," in *Proc. IEEE ICASSP*, vol. 2, pp. 928-931, May 1989.

[64] G. CHERUBINI, E. ELEFTHERIOU, S. OLCER, AND J. M. CIOFFI, "Filter bank modulation techniques for very high-speed digital subscriber lines," *IEEE Comm. Magazine*, vol. 38, no. 5, pp. 98-104, May 2000.

[65] P. L. DRAGOTTI, J. KOVAČEVIĆ, V. K. GOYAL, "Quantized oversampled filter banks with erasures," in *Proc. Data Compression Conf.*, pp. 173-182, Mar. 2001.

[66] L. DUVAL AND T. TANAKA, "Denoising of seismic signals with oversampled filter banks," in *Proc. IEEE ICASSP*, vol. 6, pp. VI_189-VI_192, Apr. 2003.

[67] V. K. GOYAL, J. KOVAČEVIĆ, AND M. VETTERLI, "Multiple description transform coding: Robustness to erasures using tight frame expansions," in *Proc. Int. Sympo. Inform. Theory*, pp. 408-410, Aug. 1998.

[68] H.-M. PARK, S.-H. OH, AND S.-Y. LEE, "A uniform oversampled filter bank approach to independent component analysis," in *Proc. IEEE ICASSP*, vol. 5, pp. 249-252, 2003.

[69] S. WEISS AND R. W. STEWART, "Fast implementation of oversampled modulated filter banks," *Electronics Letters*, vol. 36, no. 17,pp. 1502-1503, Aug. 2000.

[70] K. ENEMAN AND M. MOONEN, "DFT modulated filter bank design for oversampled subband systems," *Signal Processing*, vol. 81, no. 9, pp. 1947-1973, Sept. 2001.

[71] H. PARK, T. KALKER, AND M. VETTERLI, *Parahermitian Modules and Lossless Systems,* preprint, Univ. Calif., Berkeley, CA, Dec. 1994.

[72] T. Q. NGUYEN, "Digital filter bank design quadratic-constrained formulation," *IEEE Trans. Signal Processing*, vol. 43, no. 9, pp. 1128-1139, Sept. 1995.

[73] R. D. KOILPILLAI AND P. P. VAIDYANATHAN, "A spectral factorization approach to pseudo-QMF design," *IEEE ISCAS*, vol. 1, pp. 160-163, Jun. 1991.

[74] T. Q. NGUYEN, "The design of arbitrary FIR digital filters using the eigenfilter method," *IEEE Trans. Signal Processing*, vol. 41, no. 3, pp. 1128-1139, Mar. 1993.

[75] T. KARP AND N.J. FLIEGE, "Modified DFT filter banks with perfect reconstruction," *IEEE Trans. Analog and Digital Signal Processing*, vol. 46, issue 11, pp. 1404-1414, Nov. 1999.

Appendix A

Proofs

A.1 General Conditions for PR

Following the logic outlined in [20] for the critically sampled case, if we consider figure 15, the transfer function at the output of each downsampler, we have

$$U_k(z) = \frac{1}{N}\sum_{l=0}^{N-1}\left(z^{1/N}W_N^l\right)^{-k} X\left(z^{1/N}W_N^l\right)$$

for $k = 0, 1, \ldots, M-1$ where $W_N = e^{-j2\pi/N}$. Further, if we consider the matrix $\mathbf{P}(z) = \mathbf{R}(z)\mathbf{E}(z)$, the output at each of the synthesis filters is given by

$$W_k(z) = \sum_{l=0}^{N-1} P_{k,l}(z)U_k(z)$$

The overall input-output transfer function may therefore be derived as

$$\begin{aligned}
Y(z) &= \sum_{m=0}^{N-1} z^{-(N-1-m)} W_m\left(z^N\right) \\
&= \sum_{m=0}^{N-1} z^{-(N-1-m)} \sum_{k=0}^{N-1} P_{m,k}\left(z^N\right) U_k\left(z^N\right) \\
&= \sum_{m=0}^{N-1} z^{-(N-1-m)} \sum_{k=0}^{N-1} P_{m,k}\left(z^N\right) \frac{1}{N}\sum_{l=0}^{N-1}\left(zW^l\right)^{-k} X\left(zW^l\right) \\
&= \frac{1}{N}\sum_{l=0}^{N-1} X\left(zW^l\right) \sum_{k=0}^{N-1} W^{-kl} \sum_{m=0}^{N-1} z^{-k} z^{-(N-1-m)} P_{m,k}\left(z^N\right)
\end{aligned} \tag{A.1}$$

The terms of $X(zW^l)$ for $l > 0$ represent aliasing. In order to obtain an alias-free filter bank, these terms must be set to zero. Specifically,

$$\sum_{k=0}^{N-1} W^{-kl} \sum_{m=0}^{N-1} z^{-k} z^{-(N-1-m)} P_{m,k}\left(z^N\right) \doteq 0 \tag{A.2}$$

for $l > 0$, which can be written using matrix notation as

$$\mathbf{W}^{\dagger} \begin{bmatrix} V_0(z) \\ V_1(z) \\ \vdots \\ V_{N-1}(z) \end{bmatrix} = \begin{bmatrix} \times \\ 0 \\ \vdots \\ 0 \end{bmatrix} \tag{A.3}$$

where $\mathbf{W}$ is the $N \times N$ DFT matrix and $\times$ indicates a possibly non-zero entry. Knowing that $\mathbf{W}\mathbf{W}^{\dagger} = N\mathbf{I}$, we can rewrite equation (A.3) as

$$\begin{bmatrix} V_0(z) \\ V_1(z) \\ \vdots \\ V_{N-1}(z) \end{bmatrix} = \mathbf{W} \begin{bmatrix} \times \\ 0 \\ \vdots \\ 0 \end{bmatrix}$$

which implies that $V_k(z) = V(z)$ for $k = 0, 1, \ldots, M-1$ since the 0th column of $\mathbf{W}$ has all entries equal to one. Looking closely at $\mathbf{P}(z)$, we see that forcing $V_k(z) = V(z)$ results in $\mathbf{P}(z)$ necessarily being a right-pseudo-circulant matrix, i.e., each row l is derived from the row $l-1$ by a right shift operation and imposing a delay on the newly shifted component. For example, if we consider a $\mathbf{P}(z)$ of dimensions 4×4, $\mathbf{P}(z)$ is right-pseudo-circulant if

$$\mathbf{P}(z) = \begin{bmatrix} P_0(z) & P_1(z) & P_2(z) & P_3(z) \\ z^{-1}P_3(z) & P_0(z) & P_1(z) & P_2(z) \\ z^{-1}P_2(z) & z^{-1}P_3(z) & P_0(z) & P_1(z) \\ z^{-1}P_1(z) & z^{-1}P_2(z) & z^{-1}P_3(z) & P_0(z) \end{bmatrix}$$

In order to induce PR, all elements $P_k(z)$ on the 0th row of $\mathbf{P}(z)$ must be equal to 0 except for one, which must have the form cz^{-n_0}. This is only assured if $\mathbf{P}(z)$ has the form

$$\mathbf{R}(z)\mathbf{E}(z) = cz^{-n_0} \begin{bmatrix} \mathbf{0}_{(N-r)\times r} & \mathbf{I}_{N-r} \\ z^{-1}\mathbf{I}_r & \mathbf{0}_{r\times(N-r)} \end{bmatrix} \tag{A.4}$$

for some $r = 0, 1, \ldots, N-1$.

A.2 PR Conditions for Oversampled Even-Stacked Cosine-Modulated Filter Banks

The analysis polyphase transfer matrix $\mathbf{E}(z^L)$ for an even-stacked O-CMFB with $2M$ channels, a subsampling factor of $2N$, and an oversampling factor of L can be expressed as

$$\begin{aligned}\mathbf{E}(z^L) &= \begin{bmatrix}\mathbf{C}_1 & \mathbf{0}\\ \mathbf{0} & \mathbf{S}_1\end{bmatrix}\begin{bmatrix}\mathbf{p}(z^L)\\ \hat{\mathbf{p}}(z^L)\end{bmatrix}\mathbf{S}^{(L)}(z)\\ &= \begin{bmatrix}\mathbf{C}_1 & \mathbf{0}\\ \mathbf{0} & \mathbf{S}_1\end{bmatrix}\begin{bmatrix}\mathbf{p}_0(z^L) & \mathbf{0}\\ \mathbf{0} & \mathbf{p}_1(z^L)\\ z^{-L}\mathbf{p}_1(z^L) & \mathbf{0}\\ \mathbf{0} & \mathbf{p}_0(z^L)\end{bmatrix}\left(\frac{1}{\sqrt{L}}\begin{bmatrix}\mathbf{I}_{2N}\\ z^{-1}\mathbf{I}_{2N}\\ \vdots\\ z^{-(L-1)}\mathbf{I}_{2N}\end{bmatrix}\right)\end{aligned} \tag{A.5}$$

Similarly, the synthesis polyphase transfer matrix $\mathbf{R}(z^L)$ can be expressed as

$$\begin{aligned}\mathbf{R}(z^L) &= z^{-(L-1)}\tilde{\mathbf{S}}^{(L)}(z)\begin{bmatrix}\hat{\mathbf{q}}(z^L) & \mathbf{q}(z^L)\end{bmatrix}\begin{bmatrix}\mathbf{C}_2' & \mathbf{0}\\ \mathbf{0} & \mathbf{S}_2'\end{bmatrix}\\ &= \frac{z^{-(L-1)}}{\sqrt{L}}\begin{bmatrix}\mathbf{I}_{2N} & z\mathbf{I}_{2N} & \cdots & z^{(L-1)}\mathbf{I}_{2N}\end{bmatrix}\\ &\quad\cdot\begin{bmatrix}\mathbf{q}_0(z^L) & \mathbf{0} & \mathbf{q}_1(z^L) & \mathbf{0}\\ \mathbf{0} & z^{-L}\mathbf{q}_1(z^L) & \mathbf{0} & \mathbf{q}_0(z^L)\end{bmatrix}\begin{bmatrix}\mathbf{C}_2' & \mathbf{0}\\ \mathbf{0} & \mathbf{S}_2'\end{bmatrix}\end{aligned} \tag{A.6}$$

where $\mathbf{C}_1$ and $\mathbf{C}_2$ are $M \times 2M$ modulation matrices with elements obtained from the modulation sequences given in equations (4.22) and (4.24), respectively. Matrices $\mathbf{S}_1$ and $\mathbf{S}_2$ are $M \times 2M$ modulation matrices with elements obtained from the modulation sequences given in equations (4.23) and (4.25), respectively. Furthermore,

$$\begin{aligned}\mathbf{p}_0(z) &= \mathrm{diag}[P_0(z) \quad P_1(z) \quad \cdots \quad P_{M-1}(z)]\\ \mathbf{p}_1(z) &= \mathrm{diag}[P_M(z) \quad P_{M+1}(z) \quad \cdots \quad P_{2M-1}(z)]\\ \mathbf{q}_0(z) &= \mathrm{diag}[Q_{M-1}(z) \quad Q_{M-2}(z) \quad \cdots \quad Q_0(z)]\\ \mathbf{q}_1(z) &= \mathrm{diag}[Q_{2M-1}(z) \quad Q_{2M-2}(z) \quad \cdots \quad Q_M(z)]\end{aligned}$$

where $P_i(z)$ and $Q_i(z)$ are the $2M$-spaced Type-1 polyphase components of the analysis and synthesis prototype filters, respectively. For PR we need to ensure that

$$\mathbf{P}\left(z^L\right) = \mathbf{R}\left(z^L\right)\mathbf{E}\left(z^L\right) = cz^{-Ln}\begin{bmatrix}\mathbf{0}_{(N-r)\times r} & \mathbf{I}_{N-r} \\ z^{-L}\mathbf{I}_r & \mathbf{0}_{r\times(N-r)}\end{bmatrix} \tag{A.7}$$

Using equations (A.5) and (A.6) we see that

$$\mathbf{P}\left(z^L\right) = z^{-(L-1)}\tilde{\mathbf{S}}^{(L)}(z)\left[\hat{\mathbf{q}}\left(z^L\right)\ \ \mathbf{q}\left(z^L\right)\right]\begin{bmatrix}\mathbf{C}_2'\mathbf{C}_1 & \mathbf{0} \\ \mathbf{0} & \mathbf{S}_2'\mathbf{C}_2'\end{bmatrix}\begin{bmatrix}\mathbf{p}\left(z^L\right) \\ \hat{\mathbf{p}}\left(z^L\right)\end{bmatrix}\mathbf{S}^{(L)}(z) \tag{A.8}$$

This results in the summation of two equations, given by $\mathbf{P}\left(z^L\right) = \mathbf{P}_1\left(z^L\right) + \mathbf{P}_2\left(z^L\right)$, where

$$\mathbf{P}_1\left(z^L\right) = z^{-(L-1)}2M\tilde{\mathbf{S}}^{(L)}(z)\left(\hat{\mathbf{q}}\left(z^L\right)\mathbf{J}_{2M}\mathbf{p}\left(z^L\right) - \mathbf{q}\left(z^L\right)\mathbf{J}_{2M}\hat{\mathbf{p}}\left(z^L\right)\right)\mathbf{S}^{(L)}(z) \tag{A.9}$$

and

$$\begin{aligned}\mathbf{P}_2\left(z^L\right) &= z^{-(L-1)}2M\tilde{\mathbf{S}}^{(L)}(z) \\ &\cdot\left(\hat{\mathbf{q}}\left(z^L\right)\begin{bmatrix}0 & \mathbf{I}_M \\ \mathbf{I}_M & 0\end{bmatrix}\mathbf{p}\left(z^L\right) + \mathbf{q}\left(z^L\right)\begin{bmatrix}0 & \mathbf{I}_M \\ \mathbf{I}_M & 0\end{bmatrix}\hat{\mathbf{p}}\left(z^L\right)\right)\mathbf{S}^{(L)}(z)\end{aligned} \tag{A.10}$$

where

$$\mathbf{J}_i = \begin{bmatrix}0 & \cdots & 0 & 1_{i-1} \\ \vdots & & \iddots & 0 \\ 0 & 1_1 & & \vdots \\ 1_0 & 0 & \cdots & 0\end{bmatrix}$$

When considering $\mathbf{P}_1(z^L)$, we see that

$$\mathbf{P}_1\left(z^L\right) = \tilde{\mathbf{S}}^{(L)}(z)\left(\begin{bmatrix} & \mathbf{D}_1(z) \\ \mathbf{D}_0(z) & \end{bmatrix}\right)\mathbf{S}^{(L)}(z)$$

$\mathbf{D}_0(z)$ is given by

$$\mathbf{D}_0(z) = \begin{bmatrix} & & z^{-L}A(z) \\ & \iddots & \\ z^{-L}B(z) & & \end{bmatrix}$$

where

$$A(z) = Q_{2M-1}(z)P_{M-1}(z) - Q_{M-1}(z)P_{2M-1}(z)$$

and

$$B(z) = Q_M(z)P_0(z) - Q_0(z)P_M(z)$$

$\mathbf{D}_1(z)$ is given by

$$\mathbf{D}_1(z) = \begin{bmatrix} & & C(z) \\ & \iddots & \\ D(z) & & \end{bmatrix}$$

where

$$C(z) = Q_{M-1}(z)P_{2M-1}(z) - Q_{2M-1}(z)P_{M-1}(z)$$

and

$$D(z) = Q_0(z)P_M(z) - Q_M(z)P_0(z)$$

We see that if L is even then

$$\mathbf{P}_1\left(z^L\right) = \mathbf{0}_{2N}$$

and if L is odd then

$$\mathbf{P}_1\left(z^L\right) = \begin{bmatrix} \mathbf{0} & \mathbf{b}(z)\mathbf{J}_N \\ \mathbf{a}(z)\mathbf{J}_N & \mathbf{0} \end{bmatrix}$$

where

$$\mathbf{a}(z) = \operatorname{diag}\left(\left[\sum_{l=0}^{L-1} \operatorname{eqn}(2lN+i) + i \qquad \text{for } i = 0, 1, \ldots, N-1\right]\right)$$

with

$$\operatorname{eqn}(k) = \begin{cases} z^{-2l-1}\left(P_k(z)Q_{k+M}(z) - Q_k(z)P_{k+M}(z)\right) & \text{for } k = 0, 1, \ldots, M-1 \\ z^{-2\left(l-\left\lfloor\frac{L}{2}\right\rfloor+1\right)}\left(P_k(z)Q_{k-M}(z) - Q_k(z)P_{k-M}(z)\right) & \text{for } k = M, M+1, \ldots, 2M-1 \end{cases}$$

and $\mathbf{b}(z) = -z\mathbf{a}(z)$. The non-zero entries of $\mathbf{P}_1(z^L)$ are on the anti-diagonal. In order to assure PR, these elements must be equal to zero. We see that the elements on the anti-diagonal consist of a sum of the equations in eqn(k), with each polyphase pair difference having a unique multiplication by z. Since $\mathbf{b}(z)$ is identical to $\mathbf{a}(z)$ except for a multiplication by -z, we can conclude that to ensure that $\mathbf{P}_1(z^L) = 0$ it is necessary and sufficient to set $\mathbf{a}(z) = 0$. This is achieved if we use linear-phase PU prototype filters.

When considering $\mathbf{P}_2(z^L)$, we notice that for odd L equation (A.10) can be expressed as

$$\mathbf{P}_2\left(z^L\right) = \operatorname{diag}\left(\sum_{l=0}^{2L-1} P_{k+lN}(z) Q_{2M-1-k-lN}(z)\right) \cdot \begin{bmatrix} & \mathbf{I}_N \\ \mathbf{I}_N & \end{bmatrix}$$

for $k = 0, 1, \ldots, N-1$. Noting that the elements of $\mathbf{P}_2(z^L)$ on the upper diagonal are equivalent to those on the lower diagonal, we see that in order for $\mathbf{P}_2(z^L)$ to satisfy equation (A.7) it is necessary and sufficient to ensure that

$$\sum_{l=0}^{2L-1} P_{k+lN}(z) Q_{2M-1-k-lN}(z) = 0 \tag{A.11}$$

for $k = 0, 1, \ldots, N-1$.

These conditions for PR are similar to those derived by Gopinath in [17] for CMFBs with arbitrary system delay.